

AD-A064 680

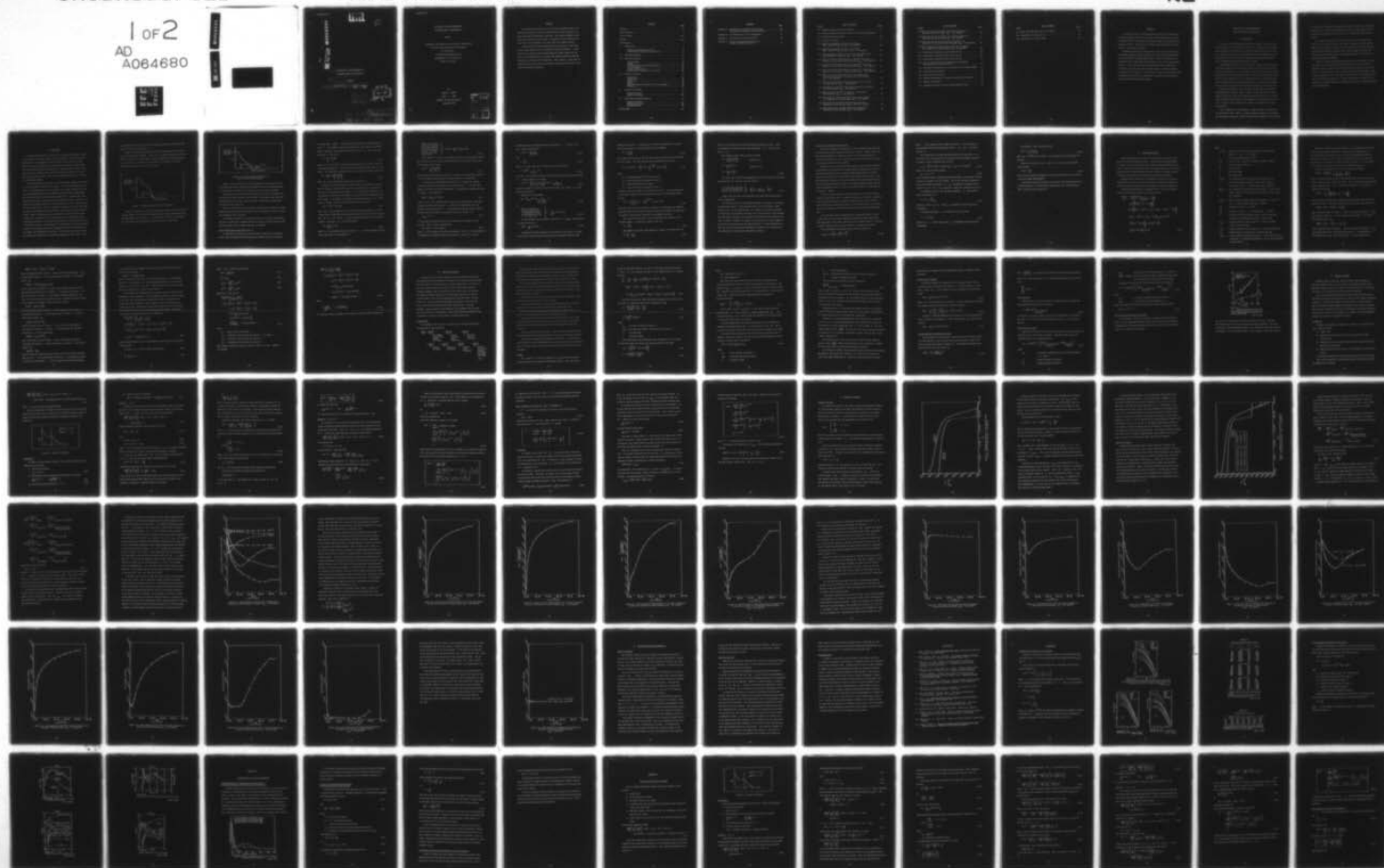
AIR FORCE INST OF TECH WRIGHT-PATTERSON AFB OHIO SCH--ETC F/6 20/8
THE EFFECTS OF BEAM CURRENTS ON ELECTRON ENERGY DISTRIBUTIONS. (U)
DEC 78 E D SEWARD

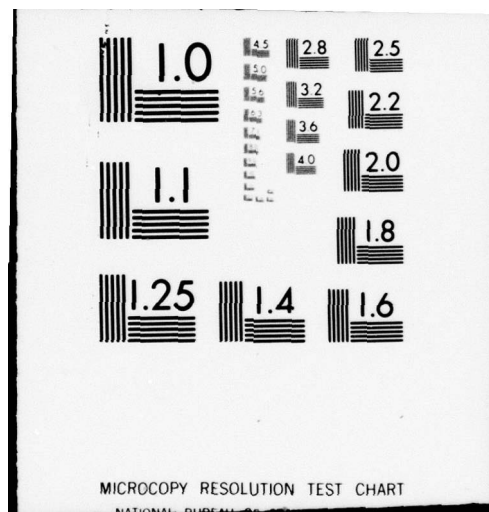
UNCLASSIFIED

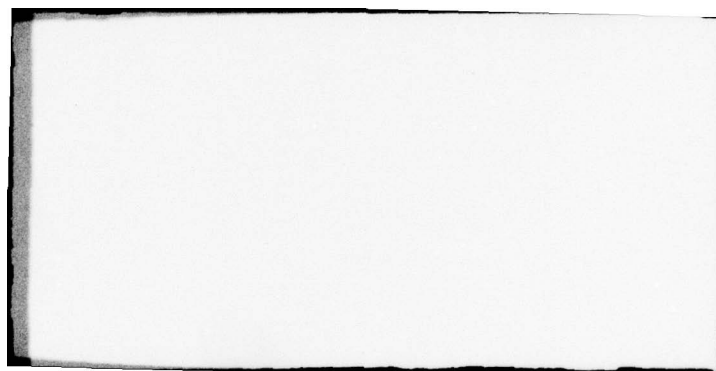
AFIT/GEP/PH/78D-12

NL

1 of 2
AD
A064680







LEVEL

①

ADA064680

DDC FILE COPY

⑥ THE EFFECTS OF BEAM CURRENTS ON
ELECTRON ENERGY DISTRIBUTIONS

⑨ Master's THESIS

⑭ AFIT/GEP/PH/78D-12

⑩ Edwin D. Seward
Capt USAF

⑪ Dec 78

⑫ 109 p.

DDC
RECEIVED
FEB 15 1979
A

DISTRIBUTION STATEMENT A
Approved for public release,
Distribution Unlimited

012 225

79 01 30 125

642

THE EFFECTS OF BEAM CURRENTS ON
ELECTRON ENERGY DISTRIBUTIONS

THESIS

Presented to the Faculty of the School of Engineering
of the Air Force Institute of Technology
Air University
in Partial Fulfillment of the
Requirements for the Degree of
Master of Science

by

Edwin D. Seward

Capt USAF

Graduate Engineering Physics

December 1978

ACCESSION No.	
DTIC	White Section <input checked="" type="checkbox"/>
DOC	Ref Section <input type="checkbox"/>
UNANNOUNCED	<input type="checkbox"/>
JUSTIFICATION	
BY	
DISTRIBUTION/AVAILABILITY CODES	
DIS.	AVAIL. ADD. OR SPECIAL
A	

Preface

Due to the recent interest in electron beam sustained lasers, the effects of the beam on the energy distribution of free electrons in a plasma has gained considerable attention. This thesis attempts to provide some insight into the problem. Although the results obtained are a bit brief, it may provide a starting point for further analysis.

I would like to extend my appreciation to my advisor, Capt Allen Hunter, whose insight into the problem has proved invaluable. I would also like to extend my sincere appreciation to Judy Csizmadi for her help in the preparation of this thesis and whose optimism provided the incentive for its successful completion. And, finally, I would like to thank Bill Ercoline for the time he spent in gathering data used in the various numerical evaluations.

Contents

	Page
Preface	ii
List of Figures	v
List of Tables	vii
Abstract	viii
Introduction	1
I. Background	3
Electron Beam Energy Deposition	5
Differential Ionization Cross Section	11
II. Boltzmann Equation	14
III. Numerical Solution	21
Program Logic	21
Method	22
Energy Absorption and Depletion Rates	26
Drift Velocity	27
Reaction Efficiencies	27
Reliability of NGB Numerical Solution	28
IV. Analytic Solution	30
Assumptions	30
Constraints	31
Region 1	32
Region 2	34
Apply Piecewise Continuity of $f(u)$ to Compute c'''	36
Normalize	36
V. Analysis of Results	39
Analytic Solution	39
Numerical Solution	42
VI. Conclusion and Recommendations	65
Analytic Solution	65
Numerical Solution	66
Recommendations	67
Bibliography	68

Contents

	Page
Appendix A: Differential Ionization Cross Sections	69
Loss Functions and Reaction Efficiencies	72
Appendix B: Justification of Initial Assumptions	75
Appendix C: Derivation of Analytic Solution	79
Appendix D: Analysis of Approximations Used in Analytic Solution Derivation	91

List of Figures

Figure	Page
1-1 Optimum Electron Energy Distribution	4
1-2 Electron Energy Distribution to Meet Ionization Requirements .	5
3-1 Rockwood Drift Velocities	29
4-1 Regions of Solution	31
5-1 Numerical and Analytic Solutions for Argon ($E/N = 10 \times 10^{-17} \text{V-cm}^2$ and $j_{eb} = .001 \text{ amp/cm}^2$)	40
5-2 Numerical and Analytic Solutions for Argon ($E/N = 10 \times 10^{-17} \text{V-cm}^2$ and $j_{eb} = .001, 1, 10 \text{ amp/cm}^2$)	43
5-3 Efficiencies for Energy Loss Processes as a Function of Field Strength for Mercury ($j_{eb} = .001 \text{ amp/cm}^2$)	47
5-4 Ratio of Field to Beam Effects for the Hg** Excitation Process as a Function of Field Strength ($j_{eb} = .001 \text{ amp/cm}^2$) .	49
5-5 Ratio of Field to Beam Effects for the Hg*** Excitation Process as a Function of Field Strength ($j_{eb} = .001 \text{ amp/cm}^2$) .	50
5-6 Ratio of Field to Beam Effects for the Hg**** Excitation Process as a Function of Field Strength ($j_{eb} = .001 \text{ amp/cm}^2$) .	51
5-7 Ratio of Field to Beam Effects for the Ground State Ionization of Mercury as a Function of Field Strength ($j_{eb} = .001 \text{ amp/cm}^2$)	52
5-8 Efficiency for the Hg** Excitation Process as a Function of Field Strength ($j_{eb} = .001 \text{ amp/cm}^2$)	54
5-9 Efficiency for the Hg*** Excitation Process as a Function of Field Strength ($j_{eb} = .001 \text{ amp/cm}^2$)	55
5-10 Efficiency for the Hg**** Process as a Function of Field Strength ($j_{eb} = .001 \text{ amp/cm}^2$)	56
5-11 Efficiency for the Ground State Ionization of Mercury as a Function of Field Strength ($j_{eb} = .001 \text{ amp/cm}^2$)	57
5-12 Efficiency for the Hg**** Excitation Process as a Function of Field Strength ($j_{eb} = .001$ and 1 amp/cm^2)	58
5-13 Rate Constant for the Hg** Excitation Process as a Function of Field Strength ($j_{eb} = .001 \text{ amp/cm}^2$)	59

List of Figures

Figure	Page
5-14 Rate Constant for the Hg*** Excitation Process as a Function of Field Strength ($j_{eb} = .001 \text{ amp/cm}^2$)	60
5-15 Rate Constant for the Hg**** Excitation Process as a Function of Field Strength ($j_{eb} = .001 \text{ amp/cm}^2$)	61
5-16 Rate Constant for the Ground State Ionization of Mercury as a Function of Field Strength ($j_{eb} = .001 \text{ amp/cm}^2$) .	62
5-17 Rate Constant for Ground State Ionization of Mercury as a Function of Field Strength ($j_{eb} = 10 \text{ amp/cm}^2$)	64
A-1 Differential Ionization Cross Section for He	70
A-2 Differential Ionization Cross Section for N_2	70
A-3 Differential Ionization Cross Section for O_2	70
A-4 The Loss Function and Its Contributions as Computed Directly From the Cross Sections	73
A-5 Efficiency of Each State as a Fraction of the Incident Energy.	73
A-6 Loss Function for Mercury	74
A-7 Efficiencies for Mercury	74
B-1 Angular Distributions of Scattered and Ejected Electrons . . .	75
C-1 Regions of Solution	80
D-1 Lorentzian Form of $S(u)$ and its Approximation $S_A(u)$	95

List of Tables

Table	Page
A-1 $A(E)$, $\Gamma(E)$ and $T_O(E)$ for He, N_2 , and O_2	71
A-2 Parameters of He, N_2 and O_2	71
D-1 Parameters for Various Gases	94

Abstract

An attempt is made at determining the effects of an external flux of high energy electrons on the electron energy distribution function. An analytic model is developed for a simple system and compared against numerical results. Normalization problems precluded detailed investigation of the analytic solution.

Numerical solutions were obtained for a more complex system using a Boltzmann computer code developed for this and three related theses. It was found that an electron beam tends to "mask" the effects of an applied dc field in the high energy region of the electron distribution function. This accounts for an uncharacteristic dip in efficiency curves for processes with high threshold energies as the magnitude of the applied field increases. The beam also accounts for an insensitivity of pumping rate constants to variations in applied field strength for processes with high threshold energies.

THE EFFECTS OF BEAM CURRENTS ON ELECTRON ENERGY DISTRIBUTIONS

Introduction

Gas lasers have provided plasma physicists with a variety of interesting problems. One such problem involves the "pumping" of a laser by a mono-energetic electron beam. In order to insure proper laser design, it is essential to determine the distribution of energy among electrons in the laser cavity [referred to as the electron energy distribution $f(\epsilon)$] and how this distribution changes in time.

The Boltzmann equation is one of the most common tools used to describe this process. It relates the time rate of change of the electron energy distribution to: 1) energy losses due to electron collisions with heavy particles (ions and neutral atoms), electron collisions with cavity walls, electron diffusion, etc.; 2) energy gain due to collisions with excited heavy particles, heating mechanisms, etc.; and 3) free electrons being created via field driven ionization and various external sources.

Numerical solutions to the Boltzmann equation have been obtained through Boltzmann computer codes. However, these codes produce only a single solution for each set of physical parameters; hence, it is difficult to determine the effect of each parameter on the distribution function. Because of this problem, laser design is a somewhat trial and error process.

Due to complexity of the problem, a complete analytic solution has not yet been derived. However, by making various assumptions, depending on the physical parameters, terms in the Boltzmann equation can be modified

or neglected in an effort to obtain partial analytic solutions. These partial solutions, although not completely accurate, provide a great deal of insight into parameter effects and serve as a significant asset to laser design.

One design area currently of interest to the Air Force deals with electron beam sustained lasers. This thesis attempts to provide some insight into this problem through numerical solutions and a partial analytic solution to the Boltzmann equation with special emphasis placed on the effects of electron beam current and an applied dc electric field on the electron distribution function.

Chapters I and II provide some background into the problem of energy deposition by an external flux of high energy electrons, introduce the Boltzmann equation, and define most of the terms and symbols used in this thesis. The computer code used to provide the numerical solutions is discussed in Chapter III and a summary of the derivation of the analytic solution is presented in Chapter IV. Chapter V presents the results of the numerical and analytic solutions and Chapter VI contains concluding remarks and recommendations.

I. Background

To induce lasing action in a gas, it is necessary to excite a certain percentage of the atoms serving as the laser medium. One means of accomplishing this is by applying a large dc field across the laser medium. The free electrons in the gas are accelerated, gain energy, collide with the laser medium, and excite the particles. When the proper level of excitation has been reached, lasing action can occur (of course, it is a bit more complicated than this). This type of excitation process is referred to as discharge pumping.

For optimum discharge pumping, a specified number density of electrons in a given energy range must be maintained. If too few electrons are present, not enough particles can be excited; if too many, the free electrons and corresponding positive ions reabsorb the photons being emitted when the excited particles return to their ground state. In either case, the optimum power output of the laser will be severely reduced. Therefore, one problem in discharge pumping is to control the number of electrons in this critical energy range. This is a complicated process since free electrons are prone to recombine with positive ions, and can lose energy via elastic and/or inelastic collisions with heavy particles, other electrons, and cavity walls. Therefore, the dc field must be large enough not only to accelerate electrons to an energy state capable of exciting particles, but to accelerate them to a state capable of ionizing particles, thus creating a source of secondary electrons to compensate for free electrons lost to attachment and recombination reactions. These high energy electrons may be relatively ineffective in exciting the appropriate laser level. While

they provide the necessary source of secondary electrons, the overall efficiency of the laser may decline.

Figure 1 illustrates an optimum electron energy distribution function for exciting the laser medium. In this case, a high percentage of the free electrons in the laser cavity have energies compatible with the excitation cross section, σ_0 , while few are available to provide the necessary ionization to compensate for electron losses.

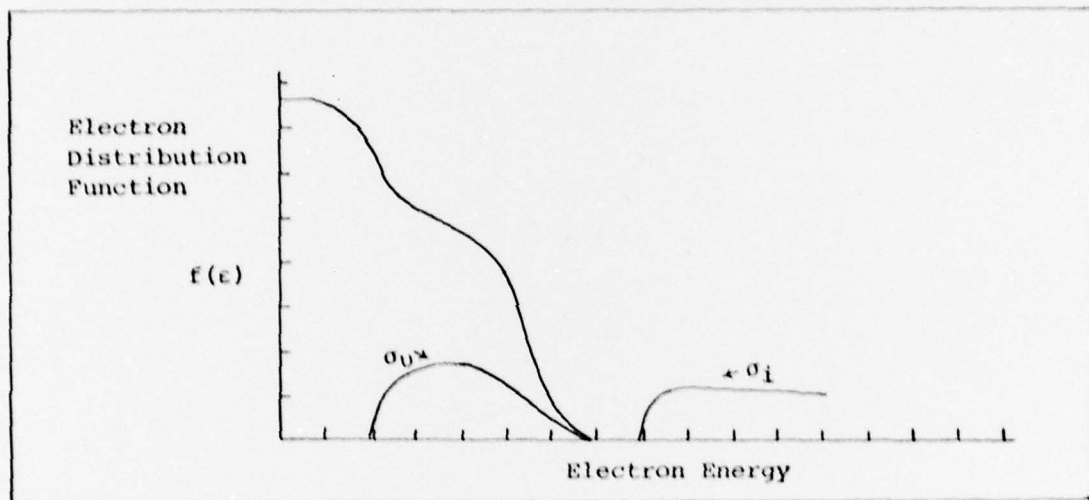


Figure 1 Optimum Electron Energy Distribution

Figure 2 illustrates an electron energy distribution function in which a finite number of electrons are maintained with energies compatible with the ionization cross section, σ_i . Here, fewer electrons are available for excitation thus reducing the overall efficiency of the laser.

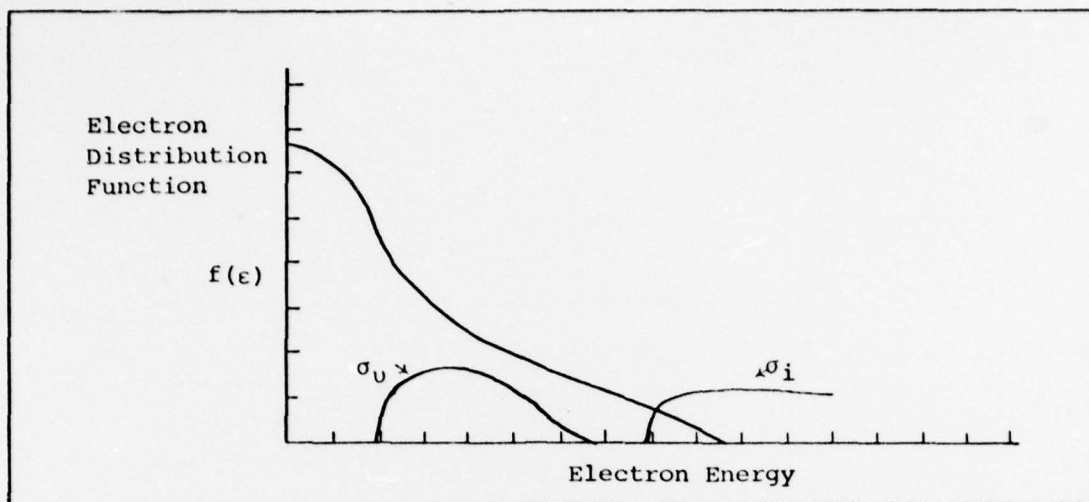


Figure 2 Electron Energy Distribution to Meet Ionization Requirements

Thus, it can be shown that if the secondary electron production can be accomplished without modifying the optimum electron energy distribution for excitation, the efficiency of the laser can be greatly increased.

An alternate means of producing secondary electrons is to bombard the gas tube with a mono-energetic electron beam. These high energy electrons collide with neutral atoms, ionize the atoms, and produce the necessary secondary electron spectrum.

Thus, it can be seen that the manner in which these secondary electrons modify the electron energy distribution is of considerable interest to agencies engaged in laser research.

To analyze the effect of an electron beam on the electron distribution function, a quantitative understanding of the manner in which energy is lost by the injected flux of primary electrons is required.

Electron Beam Energy Deposition (Ref 12)

In examining the energy loss by the primary injection of charged particles, one can experimentally determine the energy lost per unit length

of penetration, $-d\epsilon/dx$. Given this and the effective ionization potential, \bar{I} , the number of ion pairs produced per unit length can be determined. Therefore, the volumetric ionization rate, S_0 , due to the primary beam of particles is

$$S_0 = \frac{j_{eb}}{q} \frac{(-d\epsilon/dx)}{\bar{I}} \quad (1-1)$$

where j_{eb} is the electron beam current density and q is the charge of a primary beam particle. Since different materials have different \bar{I} and $d\epsilon/dx$, the volumetric ionization rate for a mixture of several species is

$$S_0 = \frac{j_{eb}}{q} \sum_s \psi_s \left(\frac{-d\epsilon_s/dx}{\bar{I}_s} \right) \quad (1-2)$$

where ψ_s is the fractional concentration of species s .

Secondary electrons produced in this manner emerge from the reaction with a variety of energies thus creating a secondary source spectrum of electrons which depend on the energy, ϵ , of the primary electrons. If one defines a differential ionization cross section for a primary particle with energy ϵ to produce a secondary electron with energy T as $S(\epsilon, T)$ (units = cm^2/eV) then the total ionization cross section is

$$\sigma_i(\epsilon) = \int_0^{T_m} S(\epsilon, T) dT \quad (1-3)$$

where T_m is the maximum kinetic energy of an ejected electron. If one assumes that the fastest outgoing electron from the reaction is the primary, then $T_m = (\epsilon - I)/2$ where I is the ionization potential of the neutral species. Therefore, S_0 can be rewritten as

$$S_0 = \frac{j_{eb}}{q} \sum_s n_s \sigma_{is} \quad (1-4)$$

where n_s is the number density of species s , and the secondary electron source spectrum can be expressed as

$$\left. \begin{array}{l} \text{Number of electrons} \\ \text{per unit volume per} \\ \text{unit time produced} \\ \text{with energy between} \\ \text{T and T + dt by} \\ \text{primary electrons} \\ \text{with energy } \epsilon \end{array} \right\} = S(T)dt = \frac{j_{eb}}{q} \epsilon n_s S_s(\epsilon, T) dT \quad (1-5)$$

From equation 1-2 and 1-4 one should also note the relationship between the ionization cross section and the energy lost per primary electron per unit length of penetration

$$\sigma_{is}(\epsilon) = \frac{1}{n_s} \left(\frac{-d\epsilon_s/dx}{I_s} \right) \quad (1-6)$$

This formulation has been structured to determine the volumetric production rate of secondary electrons due to a mono-energetic electron beam.

A second way of approaching the problem is to analyze the complete energy degradation of a primary electron with energy ϵ . Let the total number of secondary electrons with energy T produced by a primary electron of energy ϵ be defined as

$$N_e(T) = \int_{\epsilon_{min}}^{\epsilon} f(\epsilon', T) d\epsilon' \quad (1-7)$$

where $f(\epsilon', T)$ is a function that involves the probability of producing a secondary electron with energy T as well as the probability that the primary electron has energy ϵ' . The minimum energy the primary electron may have and still produce a secondary electron of energy T is

$$\epsilon_{min} = 2T + I. \quad (1-8)$$

if the fastest outgoing electron in the reaction is assumed to be the primary. $f(\epsilon', T)$ may be expressed as

$$f(\epsilon', T) d\epsilon' = N P(\epsilon', T) \omega(\epsilon') \quad (1-9)$$

where N is the number of scatters encountered, $P(\epsilon', T)$ is the probability of producing a secondary electron with energy T , and $\omega(\epsilon')$ is the

probability that the primary electron has energy ϵ' . $P(\epsilon', T)$ and $\omega(\epsilon')$ may be expressed as

$$P(\epsilon', T) = \frac{S(\epsilon', T)}{\text{unit area}} \quad (1-10)$$

and

$$\omega = \frac{dx}{R} \quad (1-11)$$

where R is the range of the primary electron expressed as

$$R = \int_{\epsilon}^{\epsilon_{\min}} \frac{1}{d\epsilon'/dx} d\epsilon' \quad (1-12)$$

and dx is the fraction of the range where the primary electron has energy ϵ' . Thus, equation 1-9 becomes

$$f(\epsilon', T) = \left(\begin{array}{c} \# \text{ of scatters} \\ \text{per unit area} \end{array} \right) S(\epsilon', T) \frac{d\epsilon'}{(d\epsilon'/dx)} \frac{1}{R} \quad (1-13)$$

where the number of scatters per unit area equals Rn_s where n_s is the density of scatters.

Equation 1-7 then becomes

$$N_e = \int_{\epsilon_{\min}}^{\epsilon} S(\epsilon', T) \frac{1}{\left(\frac{-1}{n_s} \frac{d\epsilon'}{dx} \right)} d\epsilon' \quad (1-14)$$

or

$$\left. \begin{array}{l} \text{The \# of secondary} \\ \text{electrons with energy} \\ T \text{ produced by a pri-} \\ \text{mary electron of energy} \\ \epsilon' \text{ in length } dx \end{array} \right\} = \frac{dN_e}{dx} = n_s S(\epsilon', T) \quad (1-15)$$

If the incident flux of primary electrons is $F = j_{eb}/q$ then equation 1-5 may be written as

$$S(T) = \frac{j_{eb}}{q} n_s S(\epsilon, T) \quad (1-16)$$

Secondary electrons produced in this manner are then free to collide with neutral species causing electronic and vibrational excitation and

additional ionization. To examine the excitation produced by all generations of electrons, the loss function may be introduced

$$L(\epsilon) = \frac{-1}{n_s} \frac{d\epsilon}{dx} \quad (1-17)$$

which expresses the energy lost per unit length of penetration per particle per unit volume. The loss function may alternately be written as

$$L(\epsilon) = \sum_j \omega_j \sigma_j(\epsilon) + \sum_i \left[I_i \sigma_i(\epsilon) + \int_0^{\frac{(\epsilon-I)}{2}} TS_i(\epsilon, T) dT \right] \quad (1-18)$$

where

ω_j = excitation energy of j^{th} excited state

σ_j = cross section for excitation of state j

I_i = ionization potential for state i

σ_i = cross section for ionization of state i

Therefore, the total number of excitations to state j by all generations of electrons (assuming all excitations take place from the ground state) becomes

$$J_j(\epsilon) = \int_0^\epsilon \frac{\sigma_j(\epsilon')}{\omega_j L(\epsilon')} d\epsilon' + \int_0^{\frac{(\epsilon-I)}{2}} J_j(T) n(\epsilon, T) dT \quad (1-19)$$

where the first term on the right of equation 1-19 expresses the number of excitations due to the primary electron alone and the second term expresses the number of excitations resulting from secondary electrons.

The reaction efficiency can then be defined as the fraction of the incident energy ϵ going into exciting state j as

$$\eta_j = \frac{\omega_j J_j}{\epsilon} \quad (1-20)$$

The number of electron volts required to produce an electron pair is

$$\bar{I} = \frac{\omega_i}{\eta_i} = \frac{\epsilon}{J_j(\epsilon)} \quad (1-21)$$

where \bar{I} is the effective ionization potential discussed earlier. Since all inelastic collisions do not cause ionization, $n_i < 1$ and, in general, $\bar{I} > I_i$.

The various source terms can now be related

$$S_o = \frac{j_{eb}}{q} \left(\frac{-d\epsilon/dx}{\bar{I}} \right) \quad (\text{Equation 1-1})$$

$$S_o = \frac{j_{eb}}{q} n_s \sigma_i(\epsilon) \quad (\text{Equation 1-4})$$

$$S_o = \frac{j_{eb}}{q} n_s \frac{L(\epsilon)}{\bar{I}} \quad (1-22)$$

The total rate of electron production by an electron beam can be found by integrating S_o over the electron range or

$$\left. \begin{array}{l} \# \text{ of electrons produced} \\ \text{per cm}^2 \text{ of beam per unit} \\ \text{time by beam electrons} \end{array} \right\} = \int_{2T+I}^{\epsilon} S_o \frac{d\epsilon'}{(-d\epsilon'/dx)} \approx \frac{j_{eb}}{q} \frac{\epsilon}{\bar{I}} \quad (1-23)$$

Sample loss functions and efficiencies for argon and mercury may be found in Appendix A.

One should note that in performing Boltzmann calculations to determine the excitation rate of a given species due to an electron beam, either equation 1-16 or 1-19 could be used. If, however, a dc field is applied to the plasma, the secondary electrons are accelerated after being produced and thus may be capable of more excitation than predicted by equation 1-19. Thus, in order to compute the amount of excitation due to energy supplied by both the electron beam and the applied field, it is more appropriate to make use of the secondary source spectrum of equation 1-16 to monitor the time evolution of the electron distribution function.

Differential Ionization Cross Section

In the last section, the importance of the secondary source spectrum in electron beam related plasma analysis was stressed. However, while the fate of the primary or incident electrons in the collision process is fairly well understood, a great deal of uncertainty surrounds the dynamics of secondary electrons being produced.

Through the use of scattering theory and some standard approximations for many-particle wavefunctions, matrix elements, generalized oscillator strengths and Bethe surfaces, various people have attempted to develop analytic approximations for differential ionization cross sections. "The difficulty here, however, is that the results often depend sensitively on the scattering approximations made, the assumed coupling schemes, and the atomic wavefunctions and it is not at all obvious what the reliability is in general." (Ref 6)

For this reason, and due to the availability of an ever-increasing amount of experimental data, a number of people have turned to a phenomenological approach in which an analytic representation of the secondary source spectrum is developed by using a little insight and a lot of trial and error to develop a function which agrees with available experimental data.

One functional form, developed by Green and Sawada (Ref 3), shows a great deal of promise when compared to experimental data obtained by Opal et al (Ref 7) and later used by Peterson and Allen (Ref 6) in analysis of argon, and Bass, Berg, and Green (Ref 4) in analysis of mercury.

This differential ionization cross section is defined as

$$S(\epsilon, T) = A(\epsilon) \left[\frac{\Gamma^2}{(T - T_0)^2 + \Gamma^2} \right]^k \quad (1-24)$$

where ϵ is the energy of the incident electron; T is the energy of the secondary electron being produced; and A , T_0 , and Γ are functions of ϵ .

One strong point in using this Lorentzian form is that when $\kappa = 1$, it can be easily integrated over all energies of the secondary electrons to obtain a total ionization cross section

$$\sigma_i(\epsilon) = \int_0^{T_m} s(\epsilon, T) dT = A\Gamma [\tan^{-1}(T_m - T_0)/\Gamma + \tan^{-1}(T_0/\Gamma)] \quad (1-25)$$

where, as in the previous section,

$$T_m = 1/2(\epsilon - I) \quad (1-26)$$

is the maximum energy a secondary electron may have if the fastest outgoing electron is assumed to be the primary. Due to the confusion between primary and secondary electrons at $T > T_m$, attempting to examine the behavior of $s(\epsilon, T)$ for $T > T_m$ should be viewed with considerable caution.

A reasonable form for the resonance parameter, T_0 , was found by Green and Sawada to be

$$T_0 = T_s - \frac{T_a}{\epsilon + T_b} \quad (1-27)$$

where $T_a = 1000$, $T_b = 2I$, and T_s is adjusted to fit the gas being considered.

The width parameter, Γ , was chosen to be of the form

$$\Gamma = \Gamma_s \frac{\epsilon}{\epsilon + \Gamma_b} \quad (1-28)$$

where $\Gamma_b = I$, in most cases, and Γ_s is dependent on the gas being considered.

The form for $A(\epsilon)$ was found to be

$$A(\epsilon) = \sigma_0 \frac{K}{\epsilon} \ln \left(\frac{\epsilon}{J} \right) \quad (1-29)$$

where $\sigma_0 = 10^{-16} \text{ cm}^2$ and K and J are dependent on the gas being considered.

With those forms for T_0 , Γ , and A , it is easy to see that for large energies

$$\sigma_i(\epsilon) \propto \frac{\ln \epsilon}{\epsilon} \quad (1-30)$$

which is the traditional asymptotic form for the ionization cross section in the Born Bethe approximation

Comparisons between differential ionization cross section points projected by equation 1-24 and selected experimental data from Opal et al (Ref 7) may be found in Appendix A.

II. Boltzmann Equation

The Boltzmann equation is one of the principle tools used in the study of collision dominated systems. In the case of plasma analysis, it attempts to relate changes in the electron energy distribution functions to collisions between electrons and heavy particles, the effects of applied fields, changes induced by external sources of highly energetic electrons, and the effects of various electron loss mechanisms.

Although the derivation of the Boltzmann equation will not be performed here, it will be necessary to define the various variables and terms to be used in development of the analytic solution of Chapter IV.

Following the guidelines of Rockwood (Ref 5), the flux divergent form of the Boltzmann equation can be expressed as

$$\begin{aligned}
 \frac{\partial n(\epsilon, t)}{\partial t} = & \frac{-2N_e^2 (E/N)^2}{3m} \frac{\partial}{\partial \epsilon} \left[\frac{\epsilon}{v/N} \left(\frac{n}{2\epsilon} - \frac{\partial n}{\partial \epsilon} \right) \right] \\
 & - \frac{\partial}{\partial \epsilon} \left\{ \nabla \left[n \left(\frac{KT}{2} - \epsilon \right) - KT\epsilon \frac{\partial n}{\partial \epsilon} \right] \right\} \\
 & + \sum_{s,j} \sum_s^{N_s^0} \left[R_{sj}(\epsilon + \epsilon_{sj}^*) n(\epsilon + \epsilon_{sj}^*) + \bar{R}_{sj}(\epsilon - \epsilon_{sj}^*) n(\epsilon - \epsilon_{sj}^*) \frac{N_s^j}{N_s^0} \right. \\
 & + R_{si}(\epsilon + \epsilon_{si}^*) n(\epsilon + \epsilon_{si}^*) + \delta(\epsilon) \int_{\epsilon_{si}^*}^{\infty} R_{si}(\epsilon) n(\epsilon) d\epsilon \\
 & \left. - \left(R_{sj}(\epsilon) + \bar{R}_{sj}(\epsilon) \frac{N_s^j}{N_s^0} + R_{si}(\epsilon) \right) n(\epsilon) \right] \\
 & + \sum_s S_s(\epsilon) - \delta(\epsilon) N_a R_a(\epsilon) n(\epsilon)
 \end{aligned} \tag{2-1}$$

where

- $n(\epsilon, t)d\epsilon$ = the number of electrons per unit volume with energies between ϵ and $\epsilon + d\epsilon$ ($1/\text{cm}^3$)
- N = total gas number density ($1/\text{cm}^3$)
- v/N = reaction rate constant for momentum transfer (cm^3/sec)
- q_s = mole fraction of species s
- m = electron mass
- e = electron charge
- T = gas temperature
- $R_{sj}(\epsilon)$ = rate constant at which electrons with velocity $v(\epsilon)$ produce excitation from the ground state of species s to excited state j , losing energy ϵ_{sj}^* (cm^3/sec)
- $\bar{R}_{sj}(\epsilon)$ = rate constant at which electrons at energy ϵ suffer super-elastic collisions with atoms in state N_s^j and gain energy ϵ_{sj}^* (cm^3/sec)
- $R_{si}(\epsilon)$ = rate constant at which electrons of energy ϵ ionize species s while losing energy ϵ_{si}^* (cm^3/sec)
- N_s^0 = density of species s ($1/\text{cm}^3$)
- N_s^j = density of species s in excited state j ($1/\text{cm}^3$)
- \bar{v} = average collision frequency between electrons and heavy particles for transferring energy ($\bar{v} = \frac{m}{M} v$) ($1/\text{sec}$)
- ϵ_{sj}^* = energy required to excite species s from the ground state to excited state j
- ϵ_{si}^* = energy required to ionize species s from the ground state
- N_a = number density of dissociative attachment species
- $R_a(\epsilon)$ = rate at which electrons with energy ϵ react with species a , dissociate a , and attach themselves to one of the by-products of the reaction

Equation 2-1 expresses only ground state to excited state and excited state to ground state transitions. Extrapolations of equation 2-1 to excited-excited state transitions is relatively straightforward but the notation is cumbersome; hence, they were omitted for reasons of clarity. Equation 2-1 also assumes the number density of species s in the ground state approximately equals the total gas density for species s .

A further explanation of the various terms may be helpful.

$$\text{Term 1: } \frac{-2N_e^2 (E/N)^2}{3} \frac{\partial}{\partial \epsilon} \left[\frac{\epsilon}{v/N} \left(\frac{n}{2\epsilon} - \frac{\partial n}{\partial \epsilon} \right) \right]$$

Term 1 describes changes in the distribution function due to the acceleration of electrons by an applied dc field. $n/2\epsilon$ controls the electron flux up the energy axis and $\partial n/\partial \epsilon$ controls the diffusion of electrons as they move up the axis.

$$\text{Term 2: } - \frac{\partial}{\partial \epsilon} \left\{ v \left[n \left(\frac{KT}{2} - \epsilon \right) - KT\epsilon \frac{\partial n}{\partial \epsilon} \right] \right\}$$

Term 2 describes changes due to momentum transfer occurring when electrons experience elastic collisions with heavy particles whose temperature is T .

$$\text{Term 3: } R_{sj} (\epsilon + \epsilon_{sj}^*) n(\epsilon + \epsilon_{sj}^*) N_s^0$$

Term 3 describes gains at energy ϵ due to electrons with energy $\epsilon + \epsilon_{sj}^*$ colliding with species s in the ground state, exciting s to state j while losing energy ϵ_{sj}^* .

$$\text{Term 4: } \bar{R}_{sj} (\epsilon - \epsilon_{sj}^*) n(\epsilon - \epsilon_{sj}^*) N_s^j$$

Term 4 describes gains at energy ϵ due to electrons with energy $\epsilon - \epsilon_{sj}^*$ undergoing superelastic collisions with species s in excited state j and gaining energy ϵ_{sj}^* while de-exciting s to the ground state.

$$\text{Term 5: } R_{si}(\epsilon + \epsilon_{si}^*) n(\epsilon + \epsilon_{si}^*) N_s^0$$

Term 5 describes gains at energy ϵ due to electrons with energy $\epsilon + \epsilon_{si}^*$ colliding with species s in the ground state, ionizing s and losing energy ϵ_{si}^* .

$$\text{Term 6: } \delta(\epsilon) N_s^0 \int_{\epsilon_{si}^*}^{\infty} R_{si}(\epsilon) n(\epsilon) d\epsilon$$

Term 6 represents gains due to electrons with energies greater than the ionization threshold energy for species s colliding with species s in the ground state, ionizing s , and creating secondary electrons. The $\delta(\epsilon)$ in front of this term signifies that all secondary electrons created in this manner are assumed to emerge with zero energy.

$$\text{Term 7: } R_{sj}(\epsilon) n(\epsilon) N_s^0$$

Term 7 describes losses at energy ϵ due to electrons with energy ϵ colliding with species s in the ground state, exciting s to state j while losing energy ϵ_{sj}^* .

$$\text{Term 8: } \bar{R}_{sj}(\epsilon) n(\epsilon) N_s^j$$

Term 8 describes losses at energy ϵ due to electrons with energy ϵ colliding with species s in state j and gaining energy ϵ_{sj}^* while de-exciting s to the ground state.

$$\text{Term 9: } R_{si}(\epsilon) n(\epsilon) N_s^0$$

Term 9 describes losses at energy ϵ due to electrons with energy ϵ colliding with species s in the ground state, ionizing s , and losing energy ϵ_{si}^* .

$$\text{Term 10: } S_s(\epsilon)$$

Term 10 represents gains due to an external flux of electrons colliding with species s in the ground state, ionizing s , and producing secondary electrons with energy ϵ . If the energy of the incident electrons

is sufficiently large ($.3M_e V$), the change in energy of the incident electrons can be neglected.

$$\text{Term 11: } \delta(\epsilon) N_a R_a(\epsilon) n(\epsilon)$$

Term 11 represents losses due to electrons with energy ϵ reacting with species a , dissociating a , and attaching themselves to one of the by-products of the reaction. The $\delta(\epsilon)$ symbol signifies that only electrons with zero energy may be attached in this manner.

If one limits his investigation to a quasi steady state system, time dependence can be eliminated. If one assumes the density of excited atoms is much less than the density of ground state atoms, superelastic collisions may also be ignored. And, finally, if one can assume that the effects of elastic collisions are much smaller than the effects of inelastic collisions, ~~the elastic collisions may also be ignored.~~ With these restrictions, Rockwood's equation (2-1) reduces to

$$\begin{aligned} & \frac{-2N_e^2 (E/N)^2}{3m} \frac{\partial}{\partial \epsilon} \left[\frac{\epsilon}{v/N} \left(\frac{n}{2\epsilon} - \frac{\partial}{\partial \epsilon} \right) \right] \\ & + \sum_{s,j} N_s^0 \left[R_{sj}(\epsilon + \epsilon_{sj}^*) n(\epsilon + \epsilon_{sj}^*) + R_{si}(\epsilon + \epsilon_{si}^*) n(\epsilon + \epsilon_{si}^*) \right. \\ & \left. - \delta(\epsilon) \int_{\epsilon_{si}^*}^{\infty} R_{si}(\epsilon) n(\epsilon) d\epsilon - R_{sj}(\epsilon) n(\epsilon) - R_{si}(\epsilon) n(\epsilon) \right] \\ & + \sum_s S_s(\epsilon) - \delta(\epsilon) N_a R_a(\epsilon) n(\epsilon) = 0 \end{aligned} \quad (2-2)$$

Further simplification can be accomplished by redefining the distribution function from

$$\int_0^{\infty} n(\epsilon) d\epsilon = n_e = \text{total electron number density} \quad (2-3)$$

to

$$\int_0^{\infty} \epsilon^{\frac{1}{2}} f(\epsilon) d\epsilon = 1 \quad (2-4)$$

where $n(\epsilon) = n_e \epsilon^{1/2} f(\epsilon)$ and defining

$$Q(\epsilon) = \sum_s q_s \sigma_s(\epsilon) \quad (2-5)$$

$$N^0_s = N q_s \quad (2-6)$$

$$R_{sj}(\epsilon) = \left(\frac{2}{m}\right)^{1/2} \sigma_{sj}(\epsilon) \epsilon^{1/2} \quad (2-7)$$

$$R_{si}(\epsilon) = \left(\frac{2}{m}\right)^{1/2} \sigma_{si}(\epsilon) \epsilon^{1/2} \quad (2-8)$$

Equation 2-2 then becomes

$$\begin{aligned} & \frac{e^2 (E/N)^2}{3} \frac{\partial}{\partial \epsilon} \left[\frac{\epsilon}{Q(\epsilon)} \frac{\partial f(\epsilon)}{\partial \epsilon} \right] \\ & + \sum_{s,j} q_s \left[\sigma_{sj}(\epsilon + \epsilon_{sj}^*) (\epsilon + \epsilon_{sj}^*) f(\epsilon + \epsilon_{sj}^*) \right. \\ & \quad \left. + \sigma_{si}(\epsilon + \epsilon_{si}^*) (\epsilon + \epsilon_{si}^*) f(\epsilon + \epsilon_{si}^*) \right. \\ & \quad \left. + \delta(\epsilon) \int_{\epsilon_{si}^*}^{\infty} \sigma_{si}(\epsilon) \epsilon f(\epsilon) d\epsilon \right. \\ & \quad \left. - \sigma_{sj}(\epsilon) \epsilon f(\epsilon) - \sigma_{si}(\epsilon) \epsilon f(\epsilon) \right] \\ & + \frac{\sum_s S_s(\epsilon)}{(2/m)^{1/2} N n_e} - \delta(\epsilon) \psi_a \sigma_a(u) u f(u) = 0 \end{aligned} \quad (2-9)$$

where

ψ_a = mole fraction of species a

σ_{sj} = excitation cross section for species s to state j

σ_{si} = ionization cross section for species s

σ_a = attachment cross section for species a

And, finally, converting energy to electron volts ($u = \epsilon/e$), equation

2-9 becomes

$$\begin{aligned}
& \frac{(E/N)^2}{3} \frac{\partial}{\partial u} \left[\frac{u}{Q(u)} \frac{\partial f(u)}{\partial u} \right] \\
& + \sum_{s,j} q_s \left[\sigma_{sj}(u + u_{sj}^*)(u + u_{sj}^*) f(u + u_{sj}^*) \right. \\
& \quad + \sigma_{si}(u + u_{si}^*)(u + u_{si}^*) f(u + u_{si}^*) \\
& \quad + \delta(u) \int_{u_{si}^*}^{\infty} \sigma_{si}(u)(u) f(u) du \\
& \quad \left. - \sigma_{sj}(u)(u) f(u) - \sigma_{si}(u)(u) f(u) \right] \\
& + c \sum_s S_s(u) - \delta(u) \Psi_a \sigma_a(u)(u) f(u) = 0
\end{aligned} \tag{2-10}$$

where

$$c = \frac{1}{\left(\frac{2}{m}\right)^{1/2} N n_e} \approx \frac{1}{(5.93 \times 10^7) N n_e} \tag{2-11}$$

This equation forms the basis for the analytic work performed in Chapter IV.

III. Numerical Solution

In analysis of all but the simplest collision dominated phenomena, the Boltzmann equation adequately expresses the various processes involved, but proves much too complicated to be solved analytically. For this reason, most groups involved in plasma related research have turned to Boltzmann computer codes to analyze the time evolution of the electron distribution function and how it is affected by variations in species concentrations, cross section approximations, applied fields, electron beams, etc. One such code was developed in conjunction with this and three related theses by William Ercoline, Thomas Gist, and Harold Hastings. Various aspects of the Numerical Gas Breakdown (NGB) program will be discussed in this chapter. Details and program documentation may be found in a Technical Report (Ref 11) pending publication.

Program Logic

NGB considers the time rate of change of the electron distribution function due to seven processes

$$\begin{aligned} \frac{dn(\epsilon)}{dt} = & \left(\frac{dn(\epsilon)}{dt} \right)_{\text{Non E-Beam and Indirect E-Beam Ionization}} + \left(\frac{dn(\epsilon)}{dt} \right)_{\text{Direct Electron Beam Ionization}} + \left(\frac{dn(\epsilon)}{dt} \right)_{\text{Electron-Electron Collisions}} \\ & + \left(\frac{dn(\epsilon)}{dt} \right)_{\text{Applied dc Field}} + \left(\frac{dn(\epsilon)}{dt} \right)_{\text{Inelastic Excitation}} + \left(\frac{dn(\epsilon)}{dt} \right)_{\text{Dissociative Attachment}} + \left(\frac{dn(\epsilon)}{dt} \right)_{\text{Elastic Collisions Between Electrons and Heavy Particles}} \end{aligned}$$

(3-1)

The first term represents an electron source due to free electrons with energy greater than the ionization threshold energy colliding with heavy particles and producing secondary electrons. All secondary electrons produced in this manner are assumed to emerge with zero energy.

The second term represents an electron source due to electrons from mono-energetic electron beam colliding with heavy particles and producing secondary electrons. Secondary electrons produced in this manner emerge with a variety of energies.

Term three represents dispersions in the electron distribution function due to collisions between free electrons.

Term four describes changes in the distribution function resulting from the acceleration of free electrons by an applied dc field.

~~Term five describes changes in the distribution function due to in-~~
elastic collisions between electrons and heavy particles.

Term six describes electron losses due to electrons of zero energy reacting with a small concentration of a quenching species resulting in the dissociation of the heavy particle and the attachment of the free electron.

The final term represents changes in the electron distribution function due to elastic collisions between free electrons and heavy particles.

Each term is computed independently of the others. In this manner, it is possible for any combination of the seven processes to be considered, and the relative effect of each term on the distribution function can be monitored.

Method

As in Chapter II, the basic approach for solving the dc Boltzmann equation follows the formulation of Rockwood (Ref 5). The time rate of

change of the number density $n(\epsilon, t)d\epsilon$ of electrons with energy between ϵ and $\epsilon + d\epsilon$ in a mixture of gases of total number density N is determined by

$$\begin{aligned} \frac{\partial n}{\partial t} = & - \frac{\partial J_f}{\partial \epsilon} - \frac{\partial J_{el}}{\partial \epsilon} + \sum_{s,j} N_s^0 \left(R_{sj}(\epsilon + \epsilon_{sj}^*) n(\epsilon + \epsilon_{sj}^*) \right. \\ & + \bar{R}_{sj}(\epsilon - \epsilon_{sj}^*) n(\epsilon - \epsilon_{sj}^*) \frac{N_s^j}{N_s} + R_{si}(\epsilon + \epsilon_{si}^*) n(\epsilon + \epsilon_{si}^*) \\ & \left. + \delta(\epsilon) \int_{\epsilon_{si}^*}^{\infty} R_{si}(\epsilon) n(\epsilon) d\epsilon - [R_{sj}(\epsilon) + \bar{R}_{sj}(\epsilon) + R_{si}(\epsilon)] n(\epsilon) \right) \end{aligned} \quad (3-2)$$

The first term on the right hand side of equation 3-2 is the flux of electrons in energy space driven by an applied dc field

$$J_f = \frac{2N_e^2 (E/N)^2}{3m(v/N)} \epsilon \left(\frac{n}{2\epsilon} - \frac{\partial n}{\partial \epsilon} \right) \quad (3-3)$$

$$\frac{v}{N} = \left(\frac{2\epsilon}{m} \right)^{1/2} \sum_s q_s \sigma_s(\epsilon) \quad (3-4)$$

where

q_s = the mole fraction for species s

$\sigma_s(\epsilon)$ = the momentum transfer cross section for species s

m = electron mass

e = electron charge

The second term on the right hand side of equation 3-2 is the flux of electrons along the energy axis driven by elastic collisions

$$J_{el} = \bar{v} \left[n \left(\frac{KT}{2} - \epsilon \right) - KT\epsilon \frac{\partial n}{\partial \epsilon} \right] \quad (3-5)$$

$$\bar{v} = 2mN \left(\frac{2\epsilon}{m} \right)^{1/2} \sum_s \frac{q_s \sigma_s(\epsilon)}{M_s} \quad (3-6)$$

where

M_s = the mass of species s

T = gas temperature

The final term represents the various inelastic and superelastic collisions which give rise to non-local interactions in energy space. The quantity $R_{sj}(\epsilon) = \sigma_{sj}(\epsilon)v(\epsilon)$ is the rate at which electrons with velocity $v(\epsilon)$ produce excitation from species s to excited state j while losing energy ϵ_{sj}^* . Reverse rates are computed using the principle of microreversibility

$$\bar{R}_{sj}(\epsilon) = \left[\frac{\epsilon + \epsilon_{sj}^*}{\epsilon} \right] \sigma_{sj}(\epsilon + \epsilon_{sj}^*)v(\epsilon) \quad (3-7)$$

The quantity $R_{si}(\epsilon) = \sigma_{si}(\epsilon)v(\epsilon)$ is the rate at which electrons with velocity $v(\epsilon)$ ionize species s while losing energy ϵ_{si}^* . The term multiplied by $\delta(\epsilon)$ indicates that all secondary electrons produced in this manner emerge with zero energy.

Various modifications were made to Rockwood's basic formulation in obtaining the NGB Boltzmann code. An electron source term $S(\epsilon)$ due to an electron beam and a sink term due to dissociative attachment were added.

The source term was computed following the guidelines discussed in Chapter I where the secondary electron source spectrum produced by a mono-energetic electron beam is defined as

$$S(\epsilon) = N \sum_s \psi_s \frac{j_{eb}}{e} S_s(\epsilon, \epsilon_p) \quad (3-8)$$

where

ψ_s = mole fraction of species s

j_{eb} = electron beam current density

e = electron charge

N = total gas density

$S_s(\epsilon, T)$ = differential ionization cross section for species s

ϵ_p = energy of incident electrons

The dissociative attachment term was computed by

$$\left. \frac{dn(\epsilon)}{dt} \right|_{\text{Attachment}} = \delta(\epsilon) N \Psi_a n(\epsilon) R_a(\epsilon) \quad (3-9)$$

where $R_a(\epsilon) = \sigma_a(\epsilon) v(\epsilon)$ is the rate at which electrons react with a molecular species resulting in the dissociation of the molecule and the attachment of a free electron. Ψ_a is the mole fraction of the quenching species. The $\delta(\epsilon)$ indicates that electron attachment only occurs for electrons with zero energy.

Although equation 3-2 represents only ground state to excited state and excited state to ground state transitions, the equation was modified to include excited state to excited state transitions.

Equation 3-2, with the modifications just mentioned, was converted into a set of K coupled ordinary differential equations by finite differencing the electron energy axis into K cells of width $\Delta\epsilon$ and rearranging them such that $\frac{dn(\epsilon)}{dt}$ due to each of the seven processes described in equation 3-1 were isolated. The manner in which this was done is described in Reference 11.

Contributions due to each of the various terms could be summed to obtain a total $\frac{dn(\epsilon)}{dt}$ which could be passed to the integrator to compute the time evolution of the electron distribution function.

The integrator, DVOGER, used by NGB was obtained from the International Mathematical and Statistical Libraries, Inc. (Ref 8) and is based on a sixth order GEAR method (Ref 9). Along with the distribution function,

NGB calculates a number of related parameters useful in analyzing plasma phenomena.

Pumping Rate Constants

Excitation pumping rate constants are the average rates at which electrons produce excitation from species s to excited state j while losing energy ϵ_{sj}^* . These pumping rates are computed in the following manner

$$\langle R_{sj} \rangle = \frac{1}{n_e} \int_0^\infty \sigma_{sj}(\epsilon) v(\epsilon) n(\epsilon) d\epsilon \quad (3-10)$$

where n_e is the average electron density. Reverse pumping rate constants are computed using the principle of microreversibility

$$\langle \bar{R}_{sj} \rangle = \frac{1}{n_e} \int_0^\infty \left[\frac{\epsilon + \epsilon_{sj}^*}{\epsilon} \right] \sigma_{sj}(\epsilon + \epsilon_{sj}^*) v(\epsilon) n(\epsilon) d\epsilon \quad (3-11)$$

Similarly, ionization pumping rate constants are the average rate at which electrons ionize species s while losing energy ϵ_{si}^* and are computed by

$$\langle R_{si} \rangle = \frac{1}{n_e} \int_0^\infty \sigma_{si}(\epsilon) v(\epsilon) n(\epsilon) d\epsilon \quad (3-12)$$

Energy Absorption and Depletion Rates

Energy absorption and depletion rates are the rates at which energy is either gained or lost from the free electron gas due to each of the seven processes described in equation 3-1. NGB computes absorption and depletion rates for each process by

$$EDOT_T = \int_0^\infty \epsilon \left(\frac{dn(\epsilon)}{dt} \right)_T d\epsilon \quad (3-13)$$

where $\left(\frac{dn(\epsilon)}{dt}\right)_T$ is the time rate of change of the electron distribution due to each term in equation 3-1. It should be noted that in true steady state

$$\sum_{T=1}^7 \text{EDOT}_T = 0$$

Drift Velocity

Drift velocity is a parameter used to compare numerical predictions with experimental data and is defined as

$$v_d = \frac{1}{n_e E} (\text{EDOT})_{\substack{\text{Due to Applied} \\ \text{dc Field}}} \quad (3-14)$$

where EDOT is the rate at which electrons gain energy due to an applied dc field, E is the electric field strength, and n_e is the electron density.

Reaction Efficiencies

Reaction efficiencies are the fraction of the total input energy which supports each of the inelastic channels. Excitation efficiencies are computed by NGB in the following manner

$$v_{sj} = \epsilon_{sj} n_e N_s \langle R_{sj} \rangle \left[(\text{EDOT})_{\substack{\text{Due to Applied} \\ \text{dc Field}}} + (\text{EDOT})_{\substack{\text{Due to} \\ \text{E-Beam}}} \right]^{-1} \quad (3-15)$$

where

- ϵ_{sj} = excitation threshold energy for exciting species s to state j
- n_e = number density of electrons
- N_s = number density of species s

$\langle R_{sj} \rangle$ = average rate for exciting species s to state j
 $(\text{EDOT}) + (\text{EDOT})$ = the rate at which energy is supplied to the plasma
 by the applied dc field and the electron beam

Similarly, efficiencies for ionization processes are defined as

$$v_{si} = \epsilon_{si} n_s \langle R_{si} \rangle \left[\begin{array}{c} (\text{EDOT}) \\ \text{Due to Applied} \\ \text{dc Field} \end{array} + \begin{array}{c} (\text{EDOT}) \\ \text{Due to} \\ \text{E-Beam} \end{array} \right]^{-1} \quad (3-16)$$

where

ϵ_{si} = ionization threshold energy for species s
 $\langle R_{si} \rangle$ = average rate for ionizing species s

Again, one should note that in steady state, energy balance requires

$$\sum_{sj} (v_{sj} + v_{si}) = 1 \quad (3-17)$$

Reliability of NGB Numerical Solution

In an attempt to verify the accuracy of results being generated by NGB, a cursory comparison was made between drift velocities generated by Rockwood (Ref 5) and those produced by NGB using similar input parameters. Figure 3-1 illustrates the results.

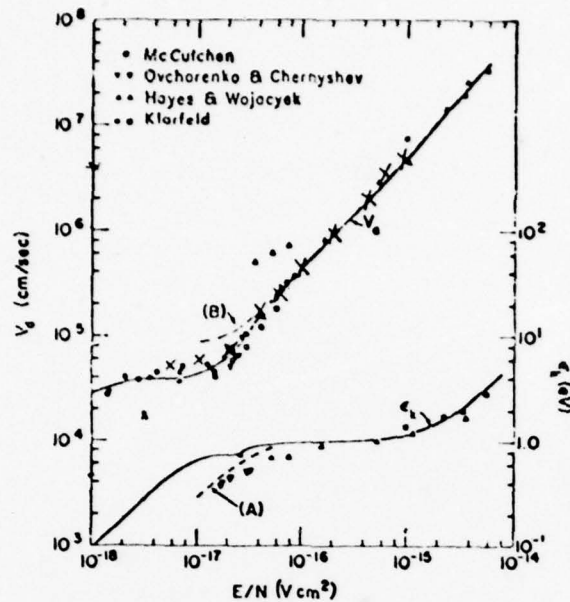


Figure 3-1

Comparison of computed values (solid curve) and experimental data from Refs. 8 and 13-15 for drift velocity v_d (cm/sec) and characteristic energy ϵ_e (eV) as a function of E/N (V cm²).

(Ref 5:2351)

The solid line designates the Rockwood results and the x's represent NGB produced drift velocities using similar input parameters. The drift velocities obtained through NGB appear to be consistent with those obtained by Rockwood. This correlation tends to lend credence to other NGB results.

IV. Analytic Solution

Although computer codes are capable of numerically solving the Boltzmann equation, only a single solution is produced for each set of physical parameters specified. Hence, it is often difficult to determine the effect of each parameter on the distribution function.

Due to the increasing popularity of electron beam sustained lasers, beam effects on the electron distribution function have gained considerable attention. To obtain some insight into the problem, a simple analytic model was derived in which emphasis was placed on the effects of electron beam currents and applied dc fields on the electron distribution function. ~~Details of the derivation and analysis of a number of the approximations~~ required are contained in Appendices C and D.

Assumptions

A number of simplifying assumptions were made in the analytic solution. Among these were

- 1) Steady state
- 2) Single species which exists only in the ground and singly ionized state
- 3) Secondary electrons resulting from non-electron-beam collisions emerge with zero energy
- 4) Momentum transfer cross sections are independent of the electron energy
- 5) Electron attachment occurs only from electrons with zero energy

With these assumptions, the Boltzmann equation discussed in Chapter II (equation 2-11) becomes

$$\frac{(E/N)^2}{3Q} \frac{d}{du} \left[u \frac{df}{du} \right] + cS(u) + \sigma_i(u+I)(u+I)f(u+I) - \sigma_i(u)(u)f(u) - \delta(u)\Psi_a \sigma_a(u)(u)f(u) + \delta(u) \int_I^\infty \sigma_i(u)(u)f(u) du = 0 \quad (4-1)$$

where I is the ionization threshold energy.

Since the significance of many of the above terms varies in different regions of the energy axis, solutions to the Boltzmann equation above and below the ionization threshold energy were considered separately (see Figure 4-1).

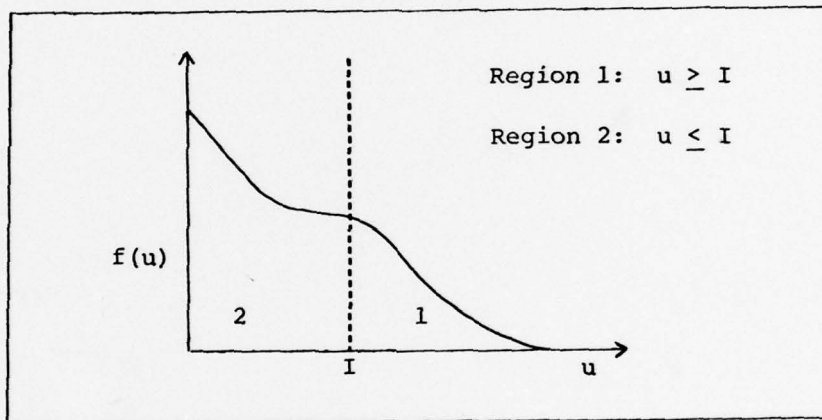


Figure 4-1 Regions of Solution

Constraints

To insure at least minimal validity, the following constraints were imposed on the solution:

- 1) Piecewise continuity

$$f_1(I) = f_2(I) \quad (4-2)$$

- 2) The function and its derivatives must vanish at infinity

$$\lim_{u \rightarrow \infty} f(u) = 0 \quad \lim_{u \rightarrow \infty} \frac{df(u)}{du} = 0 \quad (4-3)$$

- 3) The function must be finite at $u = 0$ (4-4)

4) Electrons must be conserved

$$cS(u) + \delta(u) \int_I^\infty \sigma_i(u)(u)f(u)du = \delta(u) \int_0^\infty \Psi_a \sigma_a(u)(u)f(u)du \quad (4-5)$$

Region 1: ($u \geq I$)

Allowing for attachment only at zero energy and assuming non-electron-beam generated secondary electrons emerge with zero energy, the Boltzmann equation for u greater than the ionization threshold becomes

$$\begin{aligned} \frac{(E/N)^2}{3Q} \frac{d}{du} \left[u \frac{df}{du} \right] + cS(u) + \sigma_i(u+I)(u+I)f(u+I) \\ - \sigma_i(u)(u)f(u) = 0 \end{aligned} \quad (4-6)$$

Approximating the inelastic cross section by (Ref 10)

$$\sigma_i(u) = \sigma_o \left(1 - \frac{I}{u}\right) \quad (4-7)$$

then

$$u \sigma_i(u) = \sigma_o(u - I) \quad (4-8)$$

$$(u + I)\sigma_i(u + I) = \sigma_o u \quad (4-9)$$

where I is the ionization threshold energy and σ_o is a constant dependent upon the species and reaction considered (approximately 10_{-16}cm^2).

If one can also assume that $f(u)$ is not a rapidly varying function for $u \geq I$ then one can further make the approximation

$$[f(u+I) - f(u)] \approx I \frac{df}{du} \quad (4-10)$$

Substituting equations 4-8 through 4-10 into equation 4-6 yields

$$\frac{(E/N)^2}{3Q} \frac{d}{du} \left[u \frac{df}{du} \right] + \sigma_o I \frac{d(uf)}{du} = -cS(u) \quad (4-11)$$

Direct solution of this second order differential equation yielded a form which became prohibitively complicated as the solution in Region 2 was developed. Therefore, a modified solution was sought.

If

$$\frac{(E/N)^2}{3Q} \frac{d}{du} \left[u \frac{df}{du} \right]$$

can be considered small compared to remaining terms in equation 4-11, an iterative technique can be employed to obtain an approximate solution in which the second order term is ignored. Using this approximate solution, the second order term can be solved explicitly and reinserted into equation 4-11 to obtain increasingly accurate solutions.

Using this technique, the analytic solution for $u \geq I$ becomes

$$f_1(u) = \frac{cu_0 S_0}{2\sigma_0 I} \frac{1}{u^2} + \frac{(E/N)^2}{3Q} \frac{cu_0 S_0}{(\sigma_0 I)^2} \frac{1}{u^3} + \frac{c''}{u} \quad (4-12)$$

where c'' is a constant of integration introduced when solving the differential equation and the secondary source spectrum has been approximated by

$$S(u) = \begin{cases} \frac{S_0}{2u_0} & , 0 \leq u \leq u_0 \\ \frac{u_0 S_0}{2u^2} & , u_0 \leq u \end{cases} \quad (4-13)$$

where S_0 is the volumetric production rate of electrons due to ionization from a mono-energetic electron beam

$$S_0 = \int_0^\infty S(u) du \quad (4-14)$$

and u_0 is the ionization threshold energy (Reference Appendix D).

To satisfy the initial condition of normalization

$$\int_0^\infty u^{\frac{1}{2}} f(u) du = 0$$

it is clear that c'' must equal zero. Thus, the form of $f(u)$ for $u \geq I$ is

$$f_1(u) = \frac{cu_0 S_0}{2\sigma_0 I} \frac{1}{u^2} + \frac{(E/N)^2}{3Q} \frac{cu_0 S_0}{(\sigma_0 I)^2} \frac{1}{u^3}$$

(4-15)

It should be noted that

$$\lim_{u \rightarrow \infty} f(u) = 0 \quad \text{and} \quad \lim_{u \rightarrow \infty} \frac{df(u)}{du} = 0$$

as required by the initial constraints on allowed forms for $f(u)$.

Region 2: ($0 \leq u \leq I$)

As in Region 1, if we allow for attachment only at zero energy and assume non-electron-beam generated secondary electrons emerge with zero energy and recall that $\sigma_i(u) = 0$ for $u < I$, the Boltzmann equation for u greater than the ionization threshold energy becomes

$$\frac{(E/N)^2}{3Q} \frac{d}{du} \left[u \frac{df}{du} \right] + c g(u) + \sigma_i(u+I)(u+I)f(u+I) = 0 \quad (4-16)$$

From equation 4-9

$$(u+I)\sigma_i(u+I) = u\sigma_0$$

and from Region 1 (equation 4-15)

$$f(u+I) = \frac{cu_0 S_0}{2\sigma_0 I} \frac{1}{(u+I)^2} + \frac{(E/N)^2}{3Q} \frac{cu_0 S_0}{(\sigma_0 I)^2} \frac{1}{(u+I)^3}$$

Substituting these values for $(u+I)\sigma_i(u+I)$ and $f(u+I)$ into equation 4-16 and solving for the second order term yields

$$\begin{aligned} \frac{d}{du} \left[u \frac{df}{du} \right] &= -\frac{3QC}{(E/N)^2} g(u) - \frac{3QC}{(E/N)^2} \frac{cu_0 S_0}{2I} \frac{u}{(u+I)^2} \\ &\quad - \frac{cu_0 S_0}{\sigma_0 I^2} \frac{u}{(u+I)^3} \end{aligned} \quad (4-17)$$

Again, unfortunately, direct substitution by separation of variables results in an obnoxious form for $f(u)$ which appears to be unbounded at $u = 0$. Therefore, a modified WKB was used to express

$$\frac{d}{du} \left[u \frac{df}{du} \right] = g(u) \quad (4-18)$$

as

$$f(u) = 2 \int g(u) du - u g(u) + \text{const} \quad (4-19)$$

(Reference Appendix D).

Using this approach, equation 4-17 becomes

$$\begin{aligned} f(u) = & - \frac{3Qc}{(E/N)^2} [2 \int g(u) du - u g(u)] \\ & - \frac{3Q}{(E/N)^2} \frac{cu_o S_o}{2I} \left[2 \int \frac{u}{(u+I)^2} du - \frac{u^2}{(u+I)^2} \right] \\ & - \frac{cu_o S_o}{\sigma_o I^2} \left[2 \int \frac{u}{(u+I)^3} du - \frac{u^2}{(u+I)^3} \right] \\ & + c''' \end{aligned} \quad (4-20)$$

Substituting the approximation for this secondary source spectrum (equation 4-13) into equation 4-20 and performing the necessary integrations yields the solution to the Boltzmann equation for $0 < u \leq I$

$$\begin{aligned} f_2(u) = & - \frac{3Q}{(E/N)^2} \frac{cS_o}{2u_o} u \\ & - \frac{3Q}{(E/N)^2} \frac{cu_o S_o}{2I} \left[2 \ln(u+I) + \frac{2I}{(u+I)} - \frac{u^2}{(u+I)^2} \right] \\ & - \frac{cu_o S_o}{\sigma_o I^2} \left[\frac{2}{(u+I)} - \frac{I}{(u+I)^2} + \frac{u^2}{(u+I)^3} \right] \\ & + c''' \end{aligned}$$

(4-21)

To complete the solution for $f(u)$, c''' must be determined and manipulations necessary to meet the initial normalization requirement must be performed.

Apply Piecewise Continuity of $f(u)$ to Compute c'''

c''' is obtained by applying the piecewise continuity boundary condition

$$f_1(I) = f_2(I) \quad (4-22)$$

Substituting equation 4-21 for $f_1(u)$ and 4-15 for $f_2(u)$, evaluating both functions at I and solving for c''' yields

$$c''' = -\frac{3}{8} \frac{c u_o S_o}{\sigma_o I^3} + \frac{(E/N)^2}{3Q} \frac{c u_o S_o}{\sigma_o^2 I^5} + \frac{3Q}{(E/N)^2} \frac{c S_o}{2} \left[\frac{I}{u_o} + \frac{2u_o}{I} \ln(2I) + \frac{3u_o}{4I} \right] \quad (4-23)$$

Normalize

To complete the solution for $f(u)$, the normalization requirement must be fulfilled. An effort was made to utilize the inherent normalization in the definition of $f(u)$. In doing so, it was necessary to obtain the steady state electron density, n_e , which appears in the definition of c (equation 2-11).

To maintain a steady state system, electron sources must be balanced by electron sinks. Therefore, the number of electrons gained through electron beam and field driven ionization must be countered by electron losses through attachment processes. Thus, from equation 4-1

$$c \int_0^{u_{\max}} g(u) du + \int_0^{\infty} \sigma_i(u) (u) f(u) du = \psi \int_0^{\infty} \sigma_a(u) (u) f(u) du \quad (4-24)$$

where Ψ_a is the mole fraction of the species attaching electrons, σ_a is the attachment cross section, and u_{max} is the maximum energy of a secondary electron produced via direct collision with the electron beam.

In solving this equation for the steady state electron density, n_e , it was found that the second integral of equation 4-24 is infinite when evaluated between the limits of zero and infinity. This is due, in part, to the approximation used for the ionization cross section (equation 4-7). Where for a true cross section

$$\lim_{u \rightarrow \infty} \sigma_i(u) = 0 \quad (4-25)$$

the approximated form becomes

$$\lim_{u \rightarrow \infty} \sigma_i(u) = \text{constant} \quad (4-26)$$

Therefore, a finite limit, u^* , was placed on the upper limit of the integral to obtain a finite value for the field driven source term. Unfortunately, this normalization technique proved to be very sensitive to the value selected for this artificial parameter u^* .

Thus, in introducing the various approximations required to obtain $f(u)$ its inherent normalization has been lost. As a consequence of this loss of inherent normalization, the standard normalization procedure was employed in which a normalization constant defined by

$$\int_0^\infty u^{1/2} f(u) du = c_{\text{norm}} \quad (4-27)$$

was determined. The normalized $f(u)$ is thus $1/c_{\text{norm}} f(u)$. It should be noted that this process, though relatively straightforward, is a bit tedious. Evaluating equation 4-27 yields

$$c_{\text{norm}} = \int_0^I u^{1/2} f_2(u) du + \int_I^\infty u^{1/2} f_1(u) du \quad (4-28)$$

Substituting the forms for $f_1(u)$ and $f_2(u)$ (equations 4-15 and 4-21) equation 4-28 becomes

$$\begin{aligned}
 c_{\text{norm}} = & \frac{(E/N)^2}{3Q} \frac{cu_o S_o}{\sigma_o^2} \frac{2}{3} I^{-7/2} \\
 & - \frac{3Q}{(E/N)^2} \frac{cS_o}{2u_o} \frac{2}{5} I^{5/2} \\
 & - \frac{3Q}{(E/N)^2} \frac{cu_o S_o}{2} I^{1/2} \left[\frac{4}{3} \ln 2I - \frac{141}{60} + \frac{3}{2} \tan^{-1}(1) \right] \\
 & + \frac{cu_o S_o}{\sigma_o} I^{-3/2} \left[7 - \frac{55}{8} \tan^{-1}(1) \right] \\
 & + \frac{2}{3} c''' I^{3/2}
 \end{aligned}
 \tag{4-29}$$

where c''' is defined as before (equation 4-23).

In obtaining this solution for c_{norm} , the following approximation was used

$$\int_0^I u^{1/2} \ln(u+1) du \approx \int_0^I u^{1/2} \left[\ln 2I + \frac{u}{2I} - \frac{1}{2} \right] du
 \tag{4-30}$$

Equations 4-15 and 4-21 along with the normalization constant 4-29 form the analytic solution for $f(u)$ for $0 \leq u \leq \infty$.

V. Analysis of Results

Analytic Solution

To verify the accuracy of the analytic solution developed in Chapter IV, the Boltzmann computer code (NGB) was modified to provide numerical solutions consistent with the various analytic assumptions and approximations made in Chapter IV. The Lorentzian secondary electron source spectrum was replaced with the approximate form (equation 4-13)

$$S(u) = \begin{cases} \frac{S_0}{2I} & , \quad 0 \leq u \leq I \\ \frac{S_0 I}{2u^2} & , \quad I \leq u \end{cases}$$

where the volumetric rate of production of electrons due to electron beam-neutral particle collisions, S_0 , was obtained from Appendix D (equation D-15).

Argon was selected as the test species with an ionization threshold energy of 15.7 eV and an energy independent momentum transfer cross section of 10^{-15}cm^2 . Ionization cross sections were replaced with the analytic form (equation 4-7)

$$\sigma_i(u) = \sigma_0 \left(1 - \frac{I}{u}\right)$$

where the value for σ_0 was chosen to be $6.9 \times 10^{-16} \text{cm}^2$ (Ref 10). And finally, excitation and inelastic collision terms were deleted.

By varying the electron beam current density, j_{eb} , and the dc field strength, (E/N) , a number of numerical solutions were obtained and compared with their analytic counterpart. Figure 5-1 illustrates the numerical and analytic solutions obtained for a beam current density of $.001 \text{ amp/cm}^2$ and an E/N value of $10 \times 10^{-17} \text{V-cm}^2$.

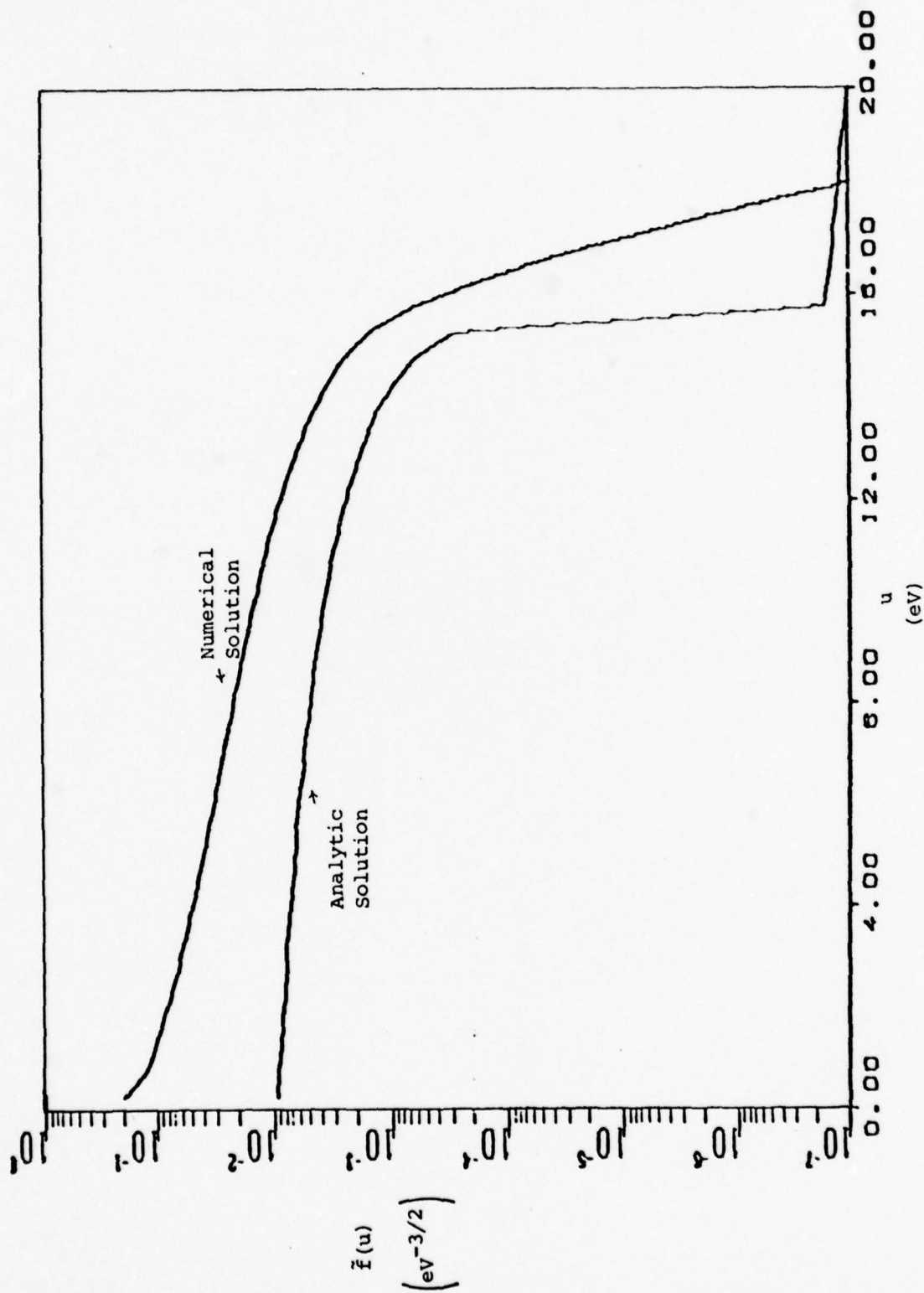


Figure 5-1 Numerical and Analytic Solutions for Argon
 $(E/N = 10 \times 10^{-17} \text{ V-cm}^2 \text{ and } j_{eb} = .001 \text{ amp/cm}^2)$

The most immediate observation is that the procedure used in Chapter IV has failed to yield the desired normalization. The c_{norm} factor appears to be an order of magnitude too large. Unfortunately, this normalization problem could not be resolved in time to be included in this thesis. Hence, a detailed analysis of the validity of the analytic solution could not be performed.

The approximation for the logarithmic integral

$$\int_0^I u^{\frac{1}{2}} \ln(u + I) du \approx \int_0^I u^{\frac{1}{2}} \left[\ln 2I + \frac{u}{2I} - \frac{1}{2} \right] du$$

used in obtaining the normalization constant may partially be responsible for the normalization problem. However, it does not appear that this is the entire problem since the approximation

$$\ln(u + I) \approx \ln 2I + \frac{u}{2I} - \frac{1}{2}$$

has a maximum error of approximately 7% over the range $0 \leq u \leq I$ for $I = 15.7$. Thus, it appears that there may be additional errors in the development of c_{norm} . Due to the considerable algebraic manipulations required to obtain c_{norm} , a simple arithmetic error cannot be completely ruled out.

Ignoring the final magnitude of c_{norm} and considering only its variable dependence, one can see that the analytic solution is independent of the electron beam current density. Since $f(u)$ (equations 4-15, 4-21, and 4-23) depends linearly on S_0 and the normalization factor, c_{norm} (equation 4-29), is also linear on S_0 , $f(u)/c_{\text{norm}}$ is independent of the volumetric production rate of electrons due to the electron beam. This independence is, in part, due to the assumption used in developing the solution in the high energy region.

In applying the WKB method, it was assumed that field effects were much smaller than beam effects. Since the solution in Region 1 ($u \geq I$) was used in developing the solution in Region 2 ($0 \leq u \leq I$), it is not difficult to see how this linear dependence on S_0 could result. As a consequence of the small field, large beam assumption, the analytic solution is not a good approximation in high energy regions for small beams. Figure 5-2 illustrates numerical and analytic solutions for beam current densities of .001, 1, and 10 amps/cm² and a field strength of 10×10^{-17} V-cm². From Figure 5-2, one can see that as the beam current density increases, the analytic solution approaches that of the numerical solution at energies above the ionization threshold energy. The analytic solution, however, does seem to be a reasonable approximation to the numerical solution in the low region of the energy axis where field effects dominate.

Numerical Solution

Using the NGB Boltzmann code to obtain numerical solutions, the effects of beam currents on a more complex system was examined. The system selected was modeled after one used by Stephen Rockwood in the analysis of mercury (Ref 5). The inelastic processes considered were excitation from the Hg ground state to the $6^3P_{0,1,2}$ states, the 6^1P_1 state, a lumped state representative of higher electron levels, and ionization from the ground state. Elastic processes include both electron-electron and electron-heavy particle elastic collisions. The dominant electron loss mechanism was assumed to come from dissociative attachment to Cl₂. The initial electron distribution was assumed to be a Maxwellian with an average electron energy of 1.75 eV.

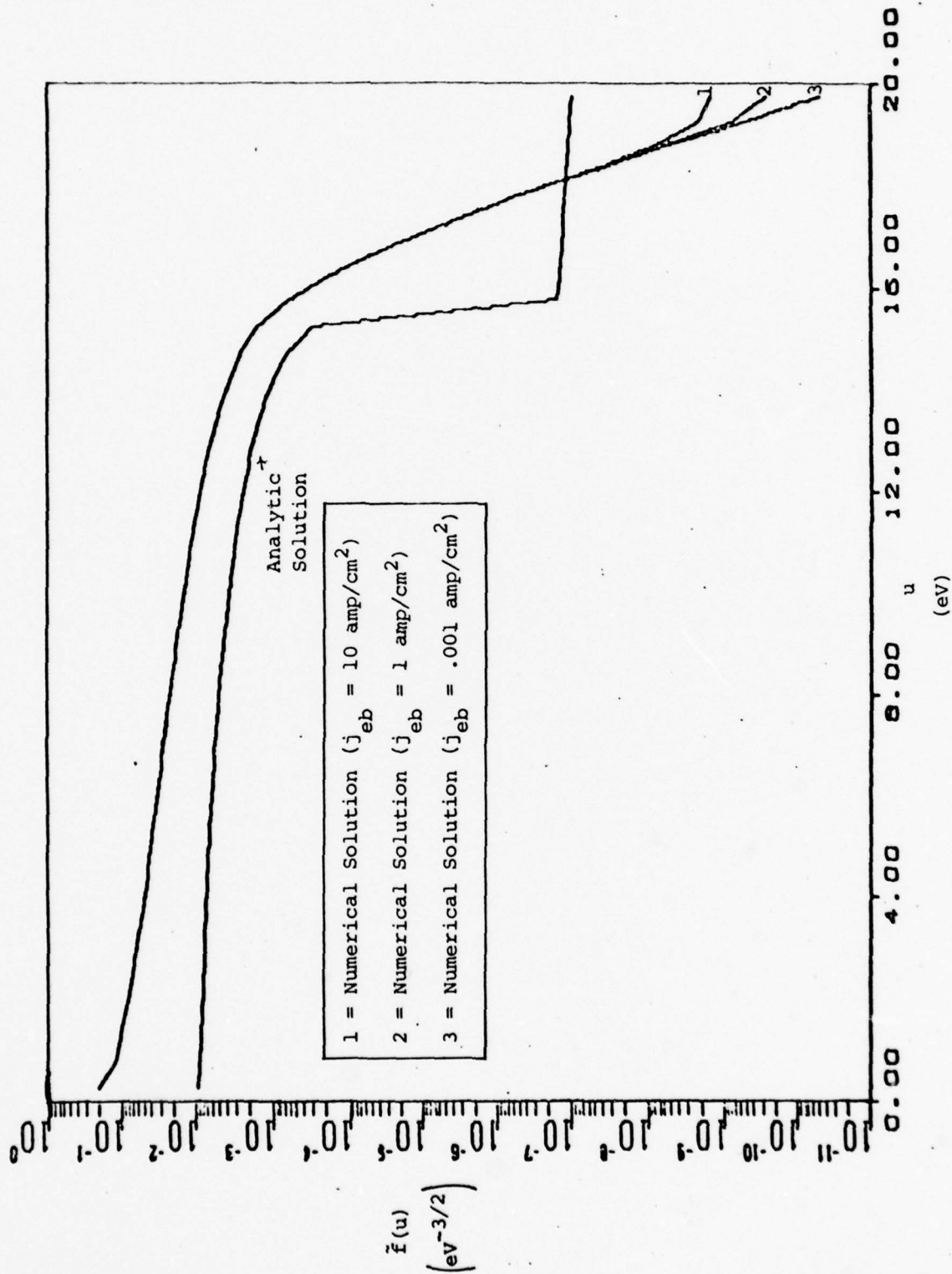


Figure 5-2 Numerical and Analytic Solutions for Argon
 ($E/N = 10 \times 10^{-17} \text{ V-cm}^2$ and $j_{eb} = .001, 1, 10 \text{ amp/cm}^2$)

Solutions were obtained at a variety of values of E/N and j_{eb} . In all cases, however, problems developed in getting NGB to run to a steady state or even a self reproducing solution. After a closer examination of the Boltzmann equation, this failure to arrive at a self reproducing form becomes a bit more obvious.

If one assumes that the effects of electron-electron collisions are small compared to other terms in the Boltzmann equation (a reasonable assumption for electron densities below 10^{12} cm^{-3}) the Boltzmann equation can be written in very general terms as

$$\begin{aligned} \frac{dn(\epsilon)}{dt} = & \left. \frac{dn(\epsilon)}{dt} \right|_{\text{Field}} + \left. \frac{dn(\epsilon)}{dt} \right|_{\text{Inelastic Excitation}} \\ & + \left. \frac{dn(\epsilon)}{dt} \right|_{\text{Ionization}} + \left. \frac{dn(\epsilon)}{dt} \right|_{\text{Momentum Transfer to Heavy Particles}} \\ & + \left. \frac{dn(\epsilon)}{dt} \right|_{\text{Attachment}} + S(\epsilon) \Big|_{\text{Electron Beam}} \end{aligned} \quad (5-1)$$

All terms in this equation are linearly dependent on $n(\epsilon)$ except the source term due to the electron beam.

To obtain a self reproducing form

$$\frac{1}{n_{e,1}} \frac{dn_1(\epsilon)}{dt} = \frac{1}{n_{e,2}} \frac{dn_2(\epsilon)}{dt} \quad (5-2)$$

for all ϵ where $n_{e,1}$ equals the total number density of electrons at time t , $n_{e,2}$ equals the total number density of electrons at time $t + \Delta t$, $n_1(\epsilon)d\epsilon$ equals the number density of electrons with energy ϵ at time t , and $n_2(\epsilon)d\epsilon$ equals the number of electrons with energy ϵ at time $t + \Delta t$. If one defines $n_{e,2} = \gamma n_{e,1}$ and $n_2(\epsilon) = \gamma n_1(\epsilon)$ where γ is some constant depending on Δt then equation 5-2 can be written as

$$\begin{aligned}
& \frac{1}{n_{e,1}} \left[\left. \frac{dn_1(\epsilon)}{dt} \right|_{\text{Field}} + \left. \frac{dn_1(\epsilon)}{dt} \right|_{\text{Inelastic Excitation}} \right. \\
& \quad + \left. \left. \left. \frac{dn_1(\epsilon)}{dt} \right|_{\text{Ionization}} + \left. \frac{dn_1(\epsilon)}{dt} \right|_{\text{Momentum Transfer to Heavy Particles}} \right. \right. \\
& \quad \left. \left. + \left. \frac{dn_1(\epsilon)}{dt} \right|_{\text{Attachment}} + S(\epsilon) \right|_{\text{Electron Beam}} \right] = \\
& \frac{1}{\gamma n_{e,1}} \left[\left. \frac{d\gamma n_1(\epsilon)}{dt} \right|_{\text{Field}} + \left. \frac{d\gamma n_1(\epsilon)}{dt} \right|_{\text{Inelastic Excitation}} \right. \\
& \quad + \left. \left. \left. \frac{d\gamma n_1(\epsilon)}{dt} \right|_{\text{Ionization}} + \left. \frac{d\gamma n_1(\epsilon)}{dt} \right|_{\text{Momentum Transfer to Heavy Particles}} \right. \right. \\
& \quad \left. \left. + \left. \frac{d\gamma n_1(\epsilon)}{dt} \right|_{\text{Attachment}} + S(\epsilon) \right|_{\text{Electron Beam}} \right] \quad (5-3)
\end{aligned}$$

Simplifying yields the result

$$S(\epsilon) = \gamma S(\epsilon) \quad (5-4)$$

Equation 5-4 indicates that a self reproducing form cannot be obtained unless $\gamma = 1$, implying a constant electron number density. This seems to indicate that a steady state solution can be obtained but, due to the non-linearity of the electron beam term, a self reproducing solution in which the electron density is changing, cannot be obtained.

The parameter combinations used in analyzing beam effects unfortunately did not yield a steady state solution. Therefore, in order to compare results for various values of E/N and j_{eb} , all numerical solutions were obtained at a fixed point, 10^{-7} seconds, in the evolution of the distribution function.

Figure 5-3 illustrates the percent of input energy (supplied by the dc field and the electron beam) supporting each of the energy loss mechanisms for a beam current density of $.001 \text{ amp/cm}^2$ and various values of E/N . The results at E/N values below $3 \times 10^{-17} \text{ V-cm}^2$ should be viewed somewhat cautiously. At $t = 10^{-7}$ seconds into the evolution of the distribution function the average electron energy had changed from the initial value of 1.75 eV to a value of $.5 \text{ eV}$ for $j_{eb} = .001 \text{ amp/cm}^2$. Various convergence indicators used by NGB to determine if a steady state or self reproducing solution has been reached indicated that considerable variations were still occurring at $t = 10^{-7}$ seconds into the evolution process for small E/N values. These variations were less pronounced for large beam current densities at similar values of E/N . It appears that 10^{-7} seconds was not sufficient time for the initial distribution function to adjust from an average energy of 1.75 eV to an average energy of approximately $.5 \text{ eV}$ for small field and small beam current densities. This accounts for much of the unusual behavior of the efficiency results at E/N less than $3 \times 10^{-17} \text{ V-cm}^2$.

From Figure 5-3 one can see that the dominant energy loss mechanism at low E/N values is due to momentum transfer (elastic collisions) between electrons and heavy particles. As the magnitude of the applied field is increased, the electrons gain energy and eventually penetrate the excitation threshold energies for the first and second excitation levels (Hg^* and Hg^{**}) of mercury. At this point, the percent of input energy supporting these two inelastic channels begins to increase and the percent of input energy supporting elastic collisions begins to decline. However, as the average electron energy increases as the field strength increases, one would expect the efficiencies for the third and fourth

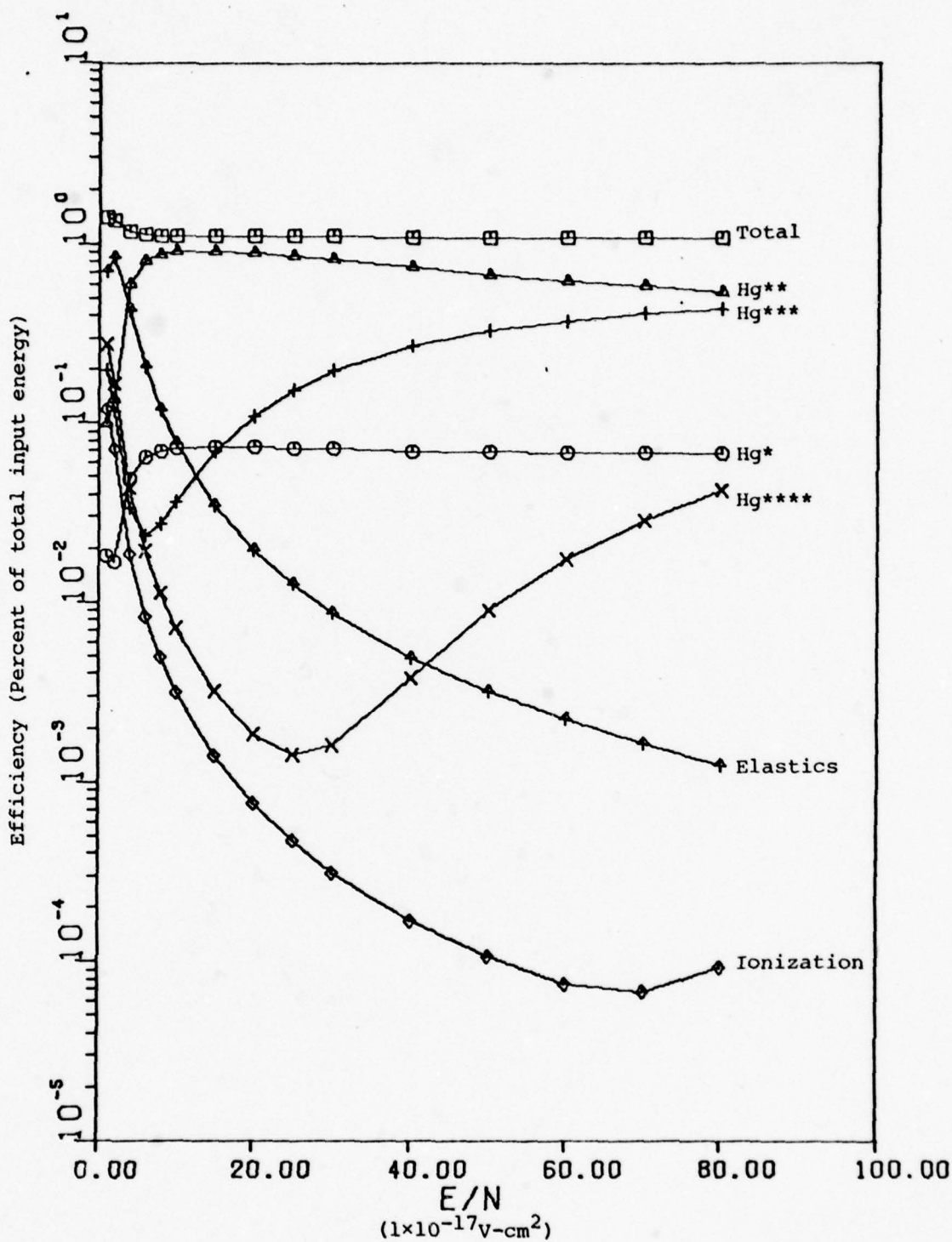


Figure 5-3 Efficiencies for Energy Loss Processes as a Function of Field Strength for Mercury ($j_{eb} = .001 \text{ amp/cm}^2$)

excited states (Hg^{***} and Hg^{****}) and the ionization state to also increase. But from Figure 5-3 one can see that for the Hg^{***} and Hg^{****} excited states and the ionization state, the efficiencies show an initial drop as E/N increases and then an eventual rise.

This drop is a direct consequence of the applied electron beam. The beam maintains a finite number of electrons with energies greater than the Hg^{***} , Hg^{****} , and ionization threshold energies independent of the field strength and tends, at these energies, to mask the effects of increases in the field strength. Thus, for small E/N values, as the field strength increases the amount of energy supporting higher excitation and ionization processes is primarily due to the beam and remains nearly constant. As the field grows, the total energy supplied to the plasma grows while that supporting higher excitation and ionization remains nearly constant; thus, the percent of energy supporting these processes decreases. As the field strength is increased further, the field begins to accelerate more and more electrons to these higher energy states until eventually the field maintains a number of electrons in these higher energy states comparable to the number maintained by the beam. At this point, the efficiency for the higher excitation or ionization process begins to increase with further increases in E/N .

Figures 5-4 through 5-11 illustrate these results. Figures 5-4 through 5-7 show the ratio of field effects to beam effects for the Hg^{**} , Hg^{***} , Hg^{****} , excitation processes and the ground state ionization process. This ratio is defined as

$$R_j = \frac{\int_{\epsilon_j}^{\infty} \sigma_j(\epsilon) v(\epsilon) \frac{dn(\epsilon)}{dt} d\epsilon \Big|_{\text{Field}}}{\int_{\epsilon_j}^{\infty} \sigma_j(\epsilon) v(\epsilon) \frac{dn(\epsilon)}{dt} d\epsilon \Big|_{\text{Electron Beam}}}$$

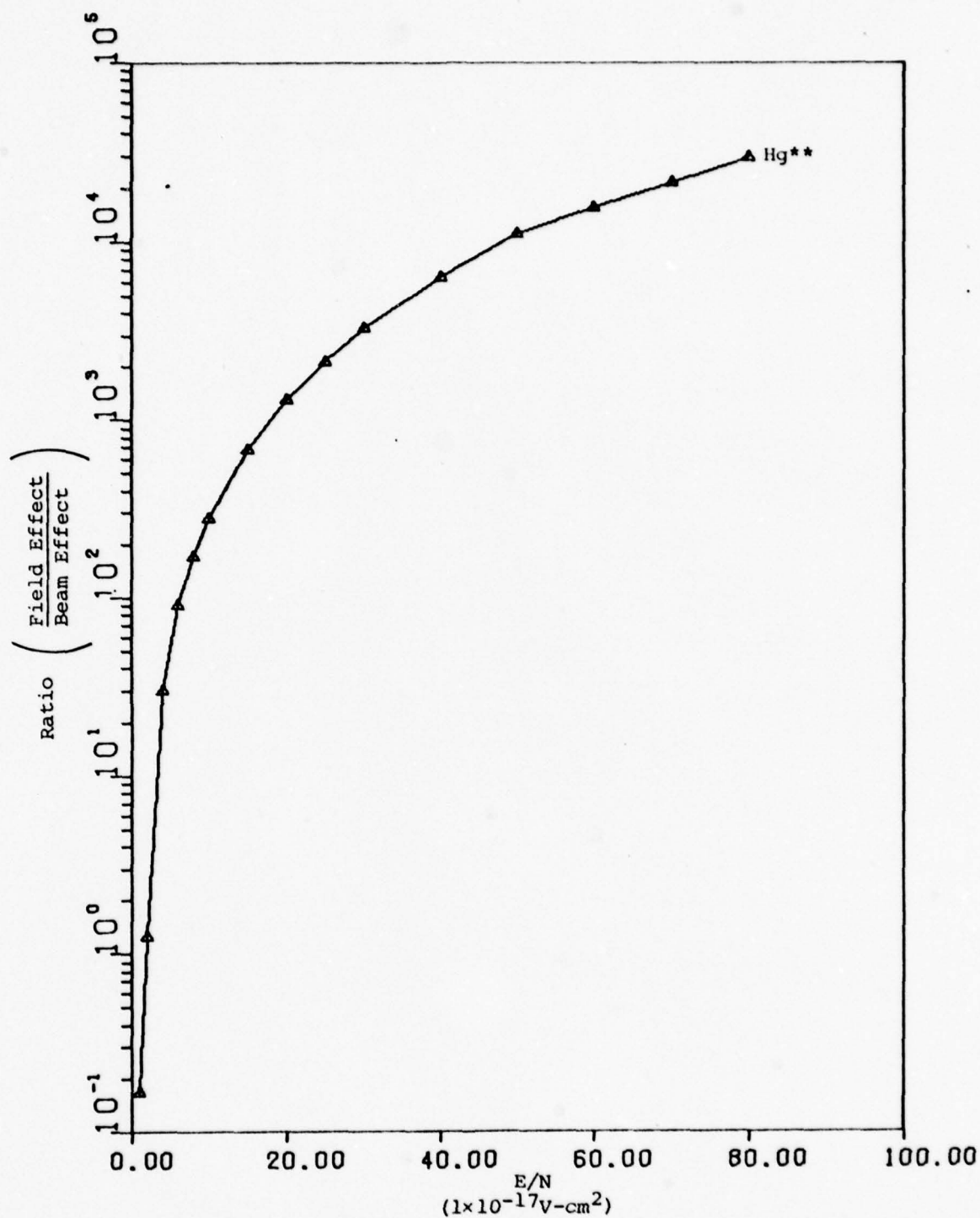


Figure 5-4 Ratio of Field to Beam Effects for the Hg** Excitation Process as a Function of Field Strength ($j_{eb} = .001 \text{ amp/cm}^2$)

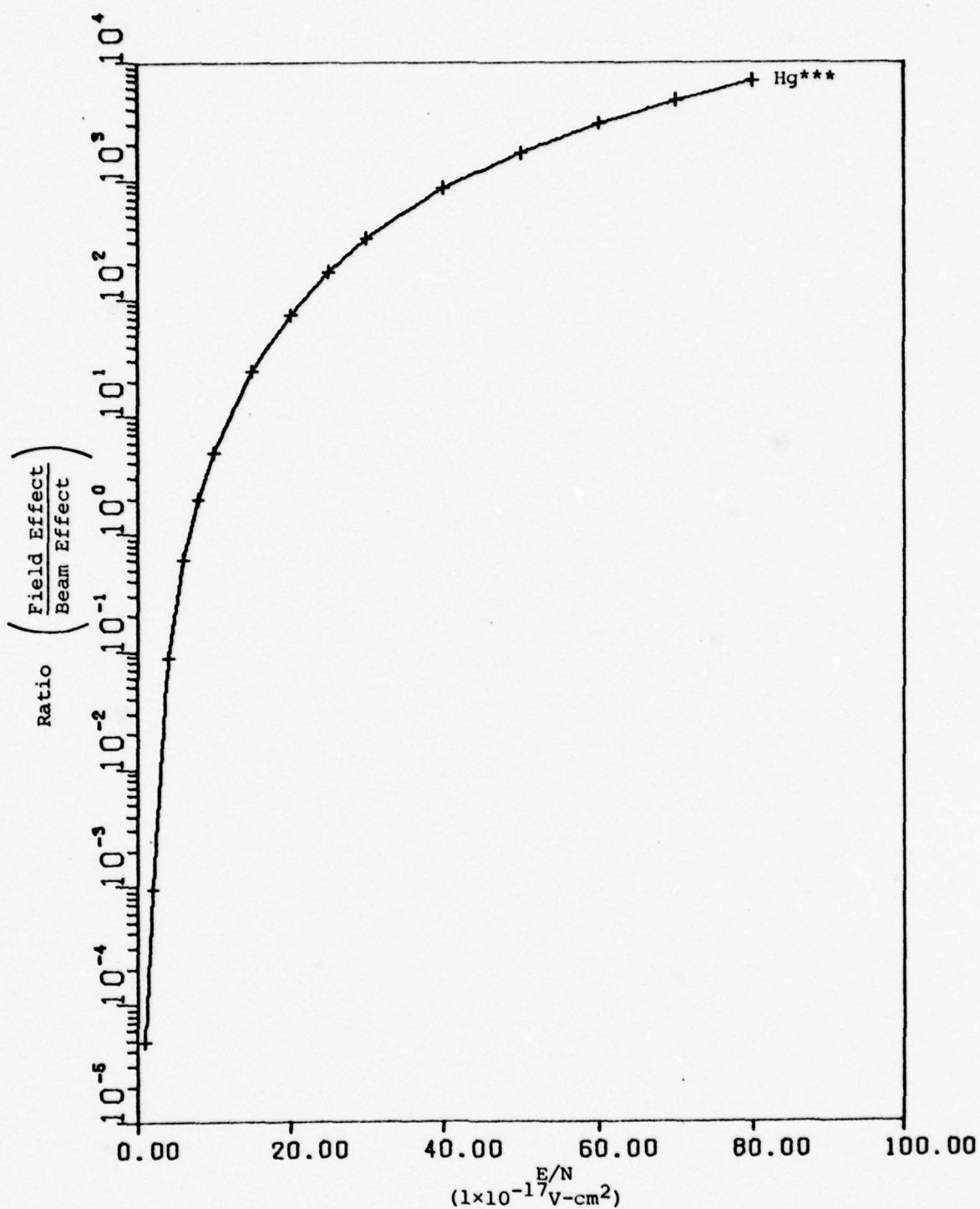


Figure 5-5 Ratio of Field to Beam Effects for the Hg*** Excitation Process as a Function of Field Strength ($j_{eb} = .001 \text{ amp/cm}^2$)

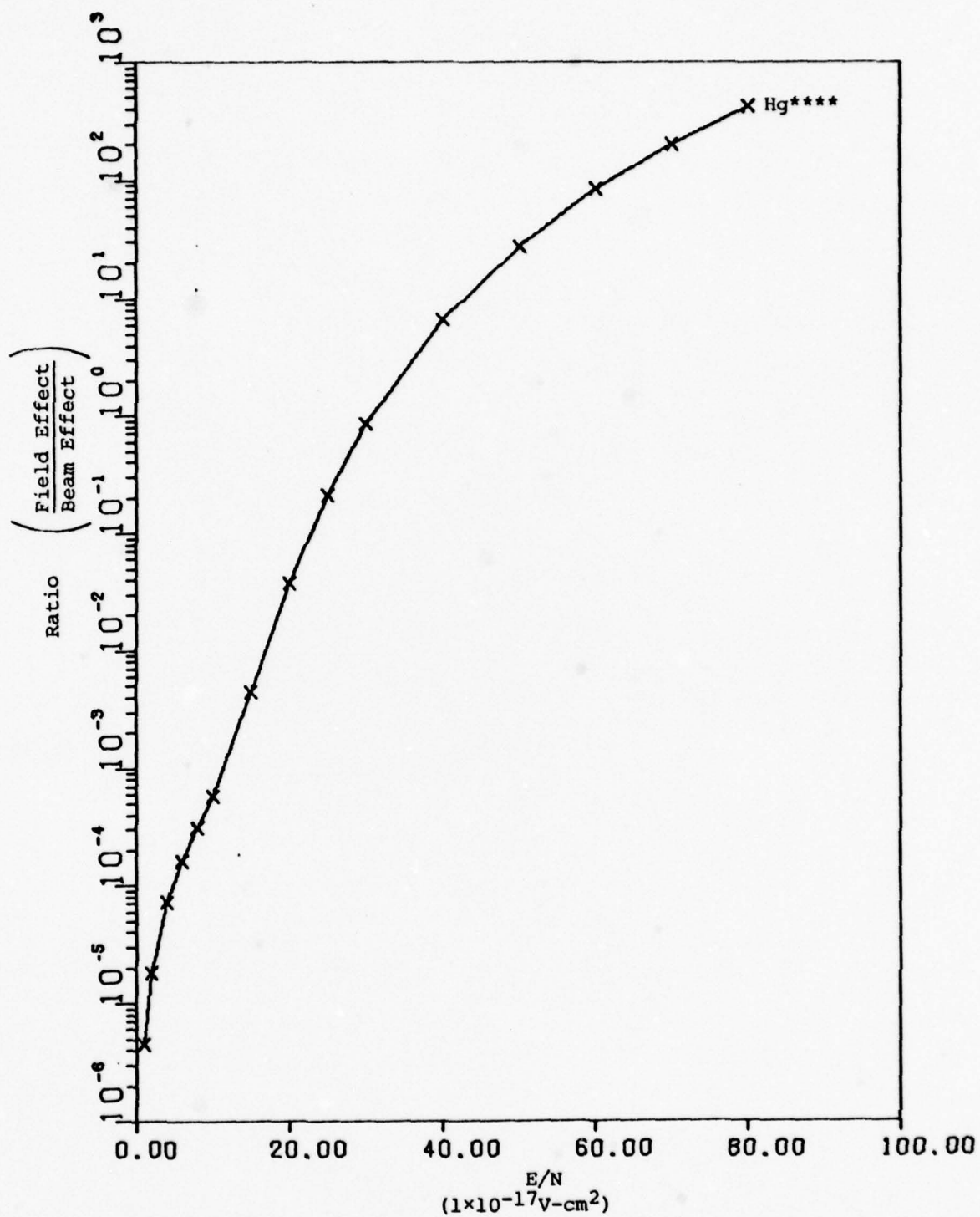


Figure 5-6 Ratio of Field to Beam Effects for the Hg**** Excitation Process as a Function of Field Strength ($j_{eb} = .001 \text{ amp/cm}^2$)

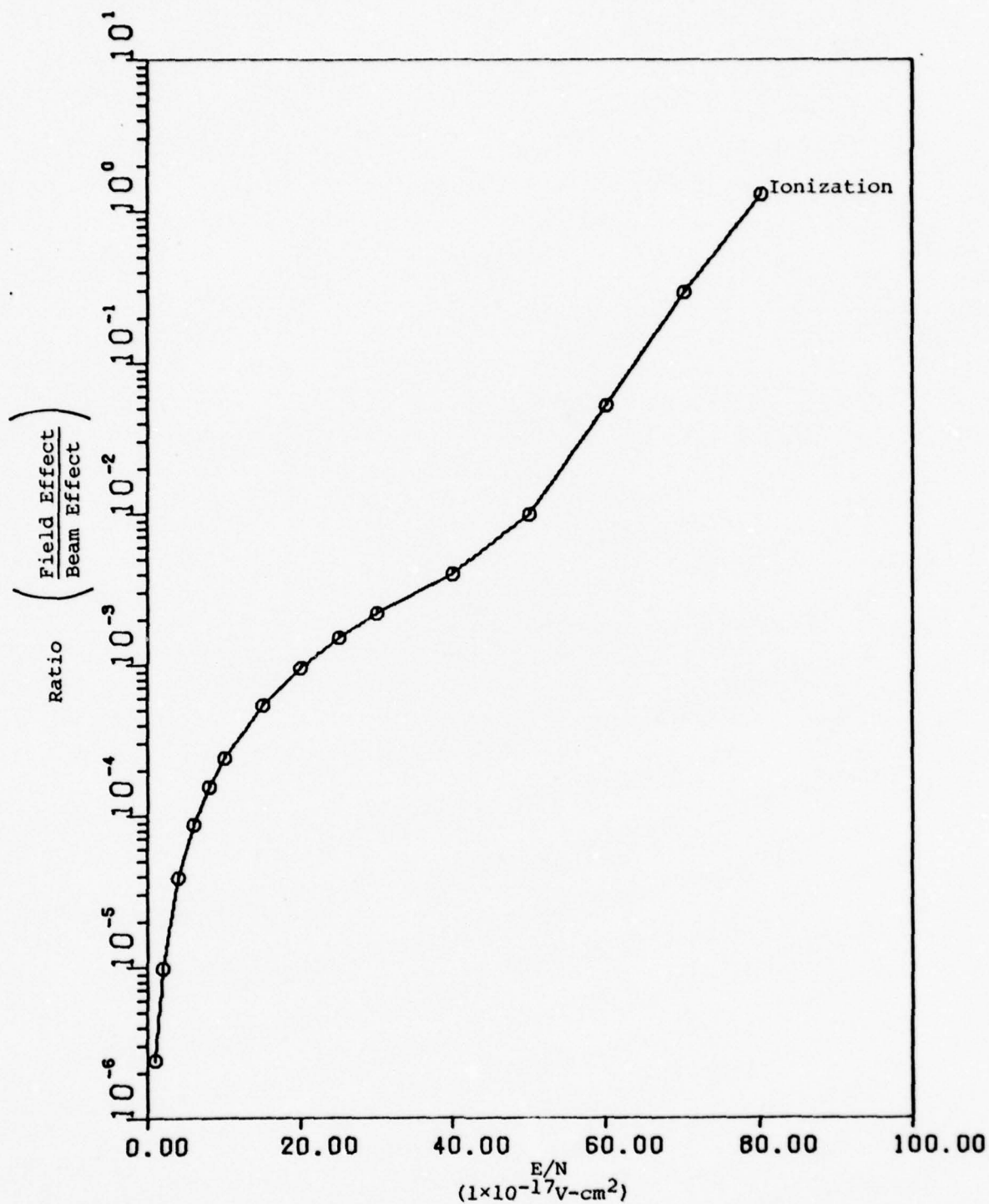


Figure 5-7 Ratio of Field to Beam Effects for the Ground State Ionization of Mercury as a Function of Field Strength ($j_{eb} = .001 \text{ amp/cm}^2$)

where ϵ_j is the excitation or ionization threshold energy and σ_j is the excitation or ionization cross section for process j .

These ratios are plotted as a function of E/N . Figures 5-8 through 5-11 illustrate the efficiencies for the Hg^{**} , Hg^{***} , Hg^{****} excitation and ground state ionization processes as a function of E/N for a $.001 \text{ amp/cm}^2$ beam. As one can see, the point at which the efficiencies for a given process begins to increase corresponds closely to the E/N value at which the field effects for that process begin to be comparable to beam effects (the point at which the field to beam ratio is approximately equal to .1).

Figure 5-12 shows the efficiencies for the Hg^{****} process as a function of E/N for beam current densities of $.001$ and 1 amp/cm^2 . As the beam current density increases, the point at which the field effects become comparable to beam effects also increases. Thus, one can see from Figure 5-12 that the E/N value at which the efficiency for the Hg^{****} excitation process begins to increase is greater for a large beam than for a small beam.

One can also see from Figure 5-12 that at large field strengths (greater than $70 \times 10^{-17} \text{ V-cm}^2$) the field effects begin to dominate beam effects in exciting the Hg^{****} level of mercury and the $.001$ and 1 amp/cm^2 efficiency curves begin to merge.

The field to beam effect ratio also accounts for the strange behavior of the pumping rate constants for the Hg^{**} , Hg^{***} , Hg^{****} excitation processes and the ionization process. Figure 5-13 through 5-16 illustrate the value of various pumping rate constants as a function of E/N for a $.001 \text{ amp/cm}^2$ beam. One can see from Figures 5-13 through 5-16, that the rate constants for a given process remain nearly constant as E/N

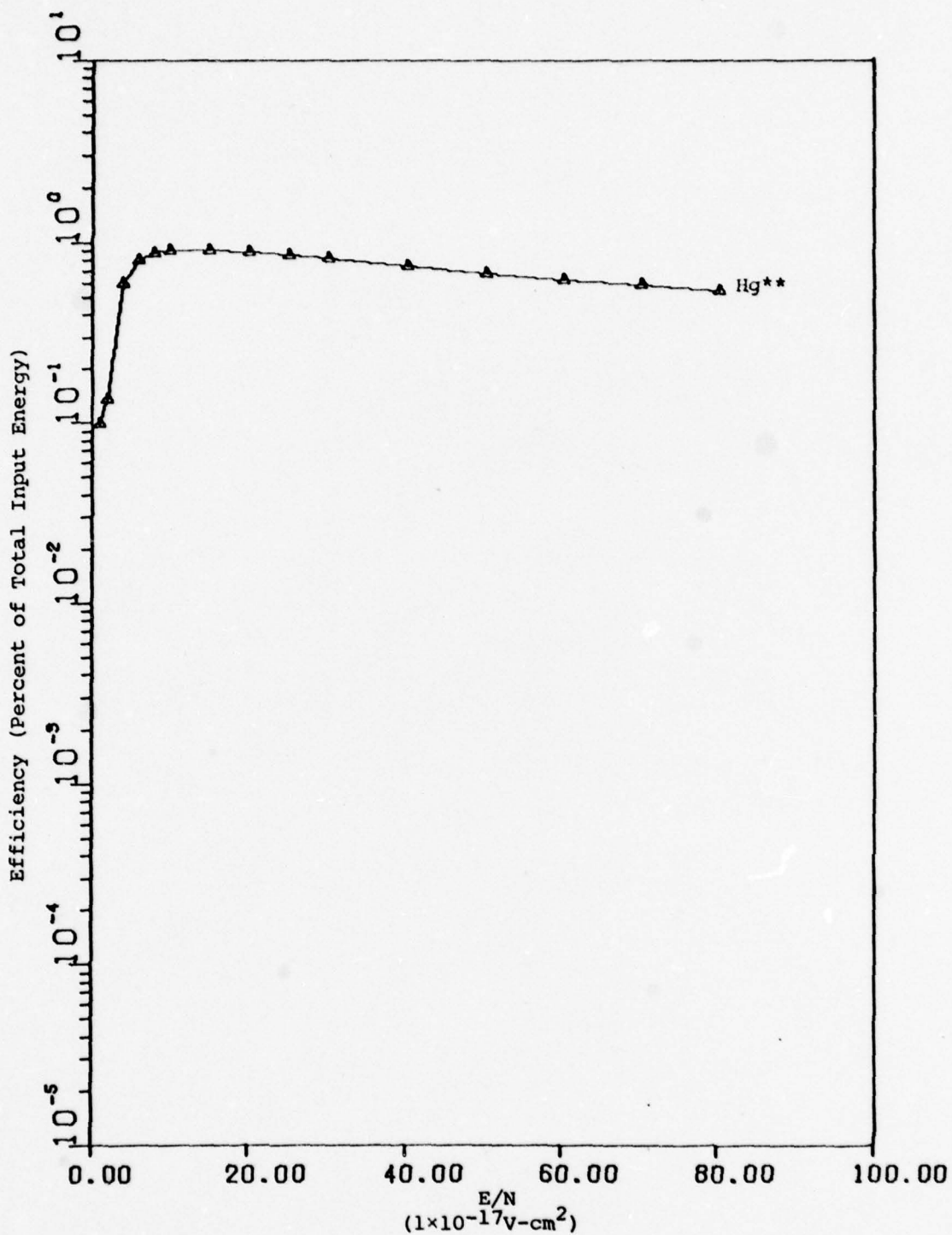


Figure 5-8 Efficiency for the Hg** Excitation Process as a Function of Field Strength ($j_{eb} = .001 \text{ amp/cm}^2$)

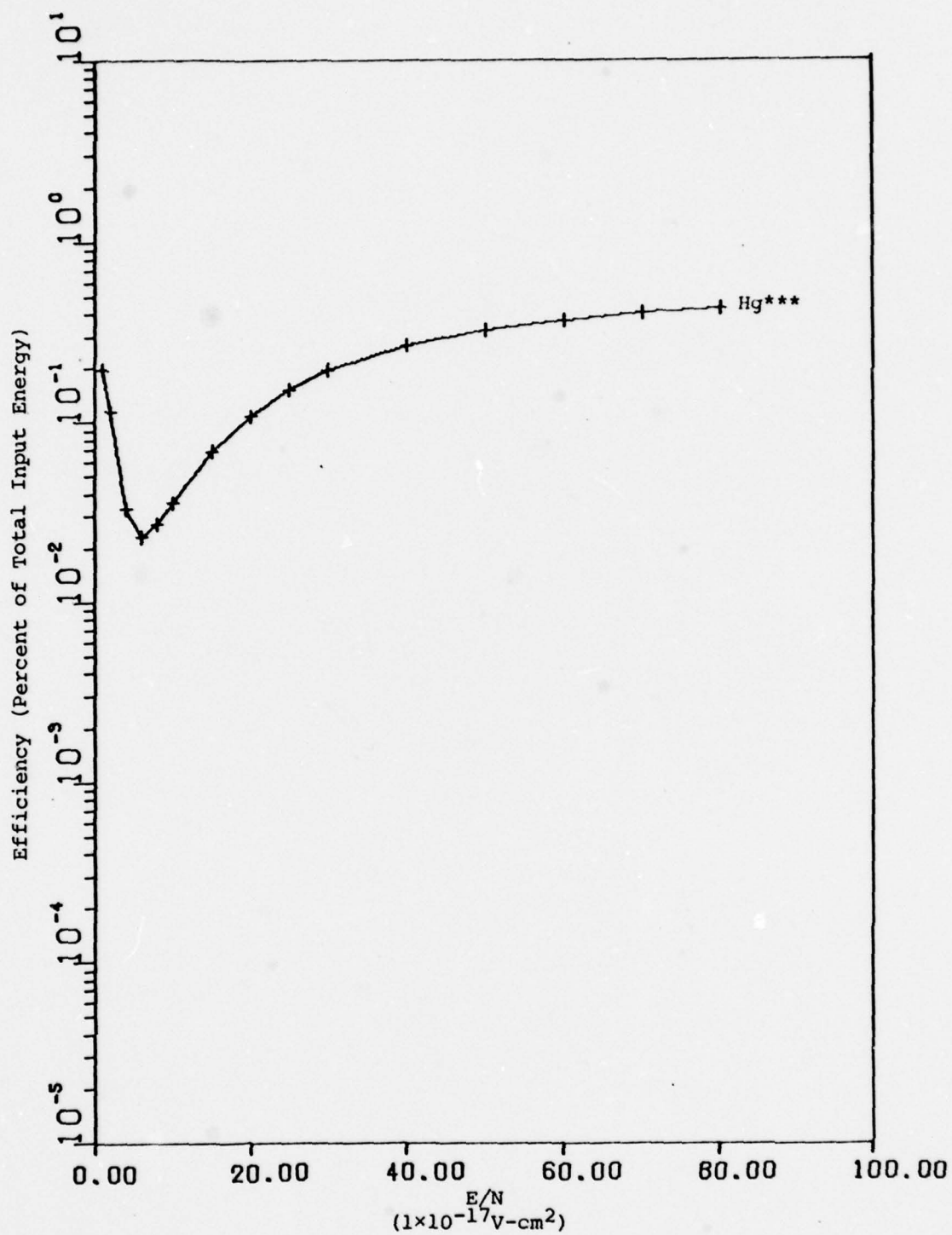


Figure 5-9 Efficiency for the Hg*** Excitation Process as a Function of Field Strength ($j_{eb} = .001 \text{ amp/cm}^2$)

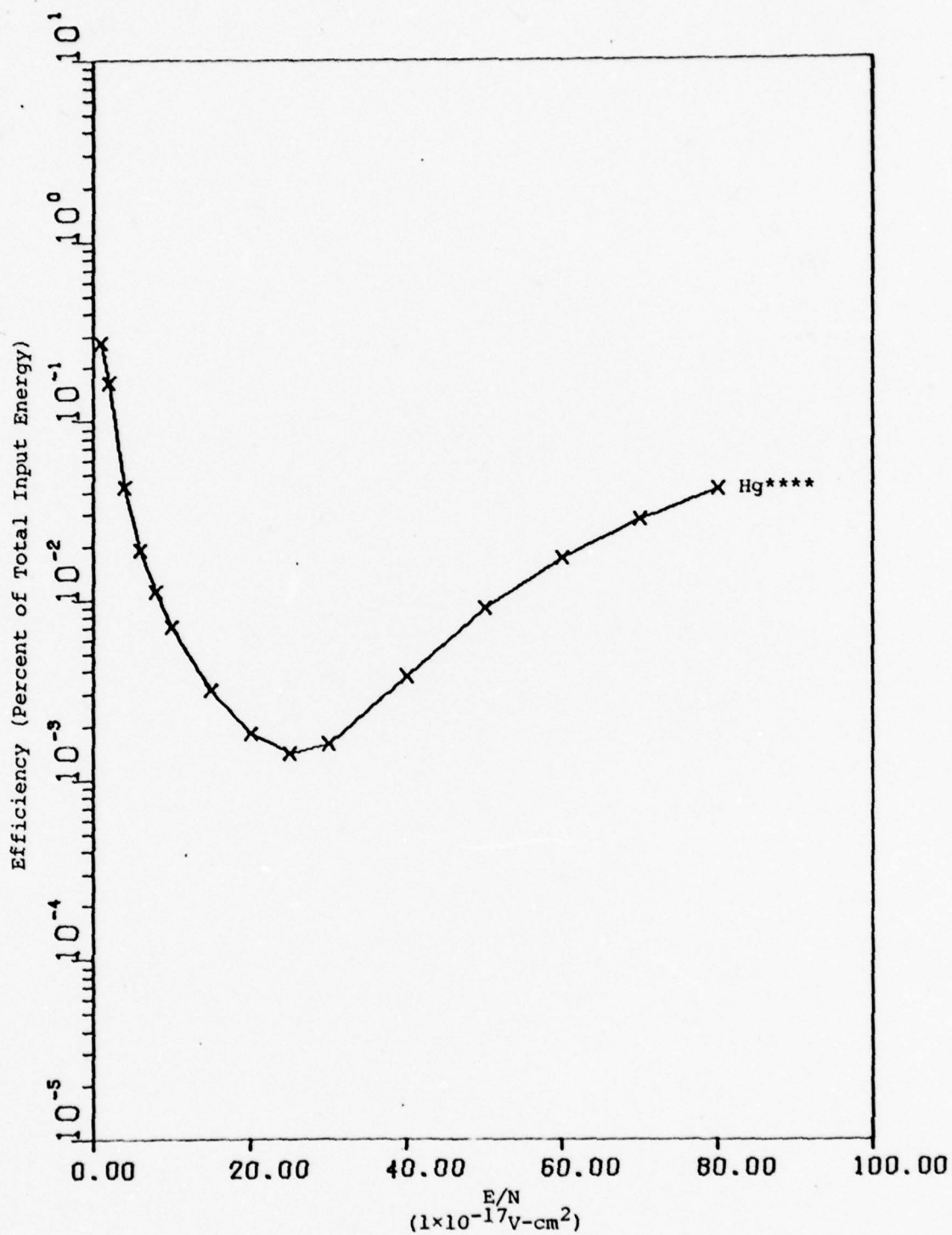


Figure 5-10 Efficiency for the Hg**** Process as a Function of Field Strength ($j_{eb} = .001 \text{ amp/cm}^2$)

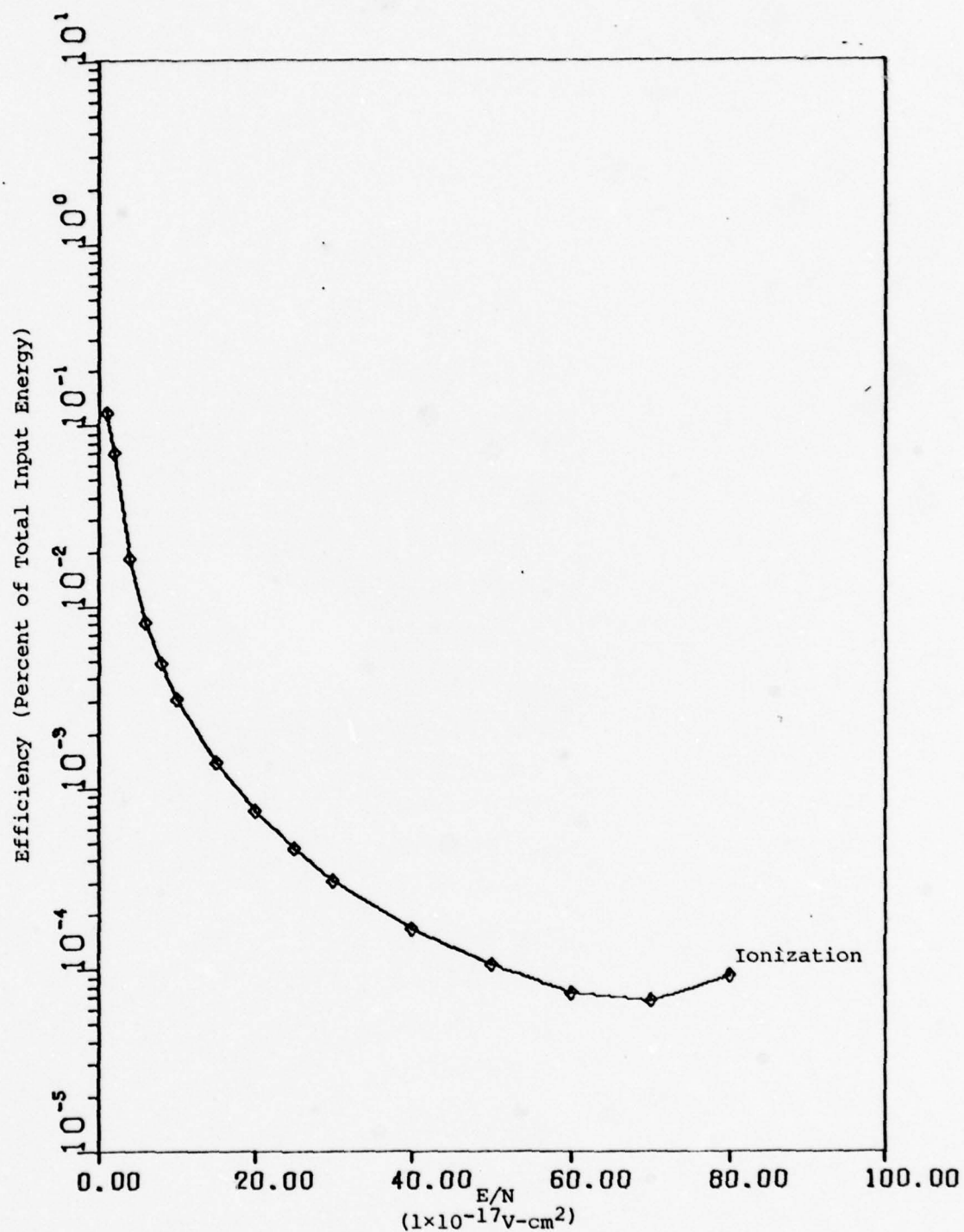


Figure 11 Efficiency for the Ground State Ionization of Mercury as a Function of Field Strength ($j_{eb} = .001 \text{ amp/cm}^2$)

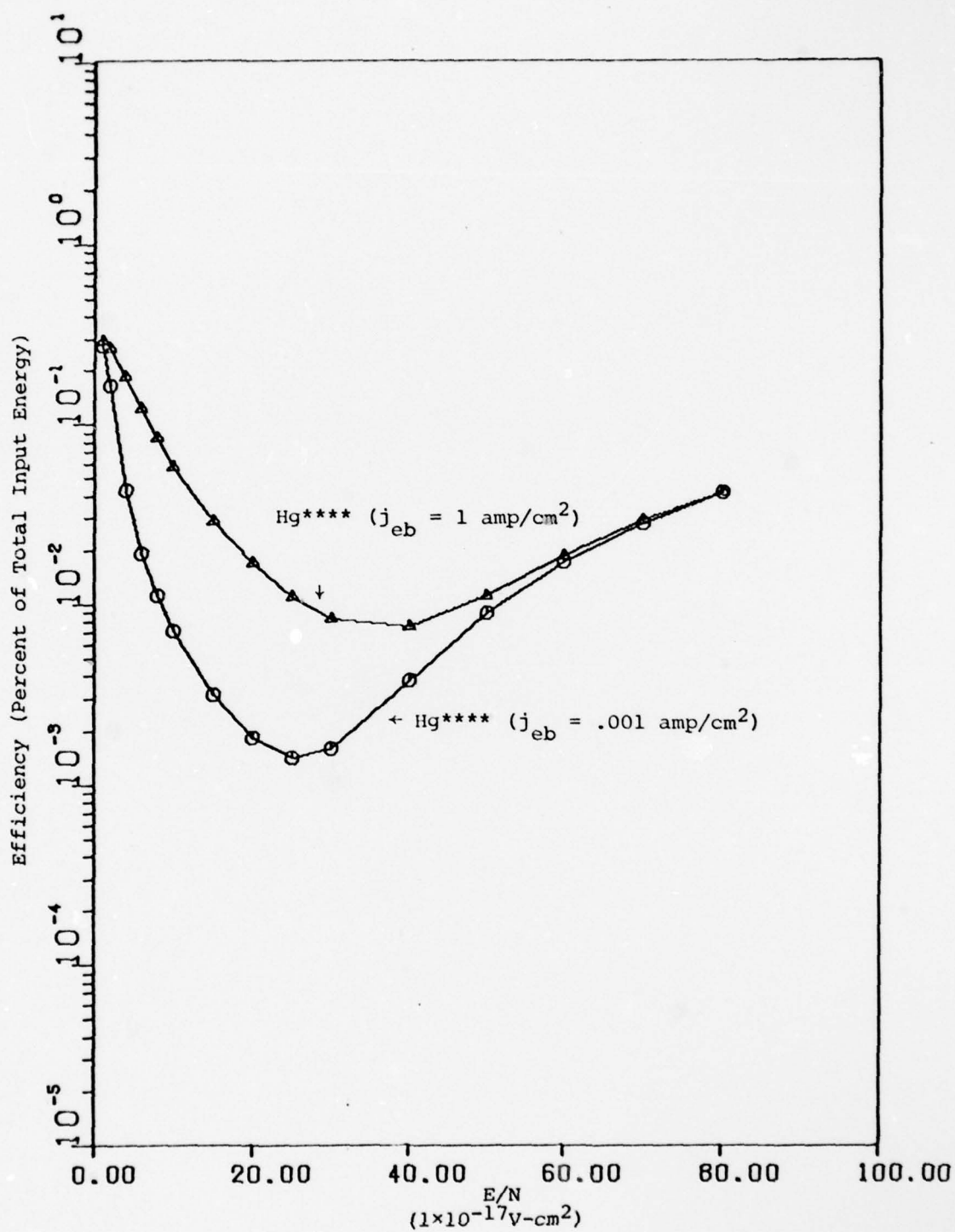


Figure 5-12 Efficiency for the Hg**** Excitation Process as a Function of Field Strength ($j_{eb} = .001$ and 1 amp/cm^2)

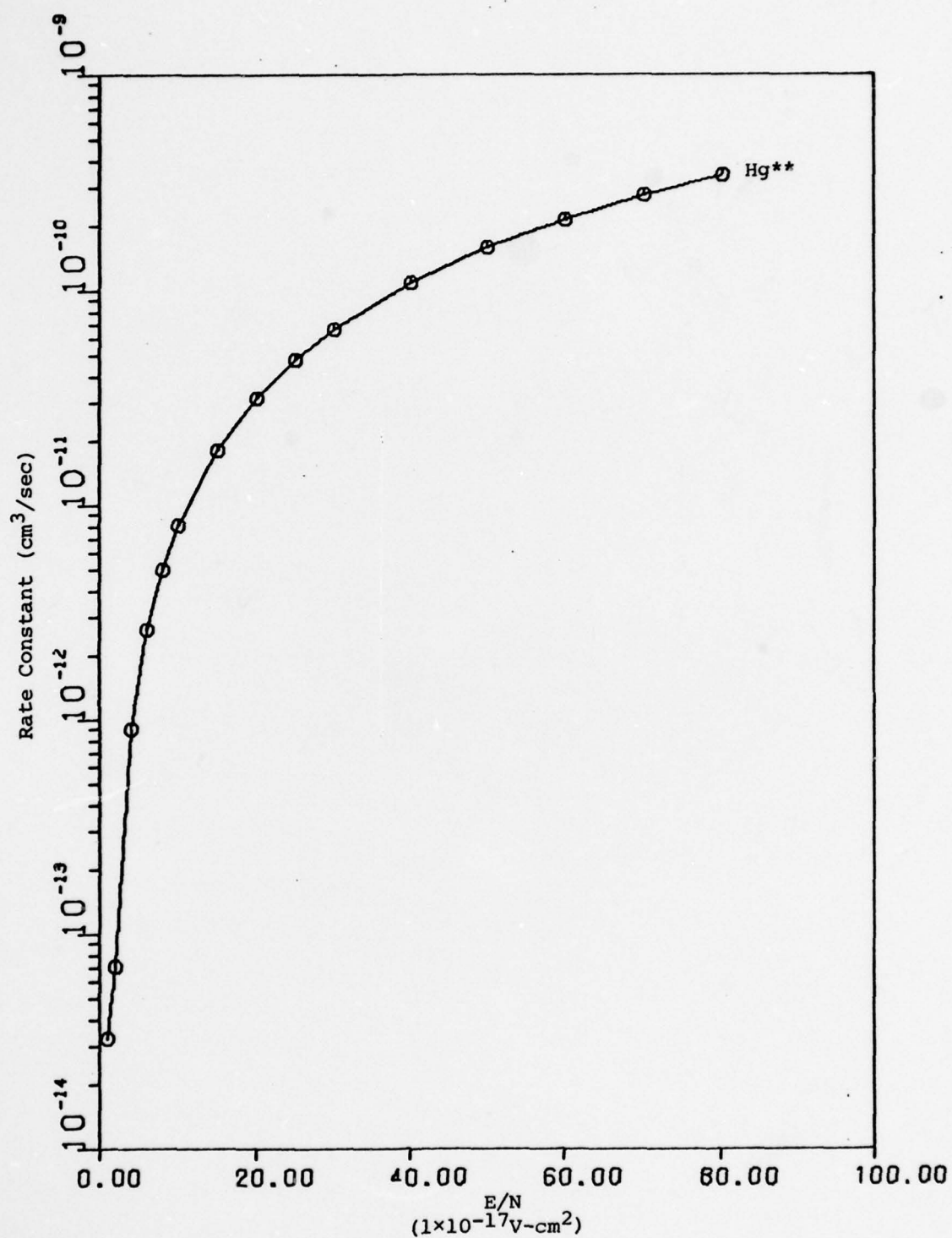


Figure 5-13 Rate Constant for the Hg^{**} Excitation Process as a Function of Field Strength ($j_{\text{eb}} = .001 \text{ amp/cm}^2$)

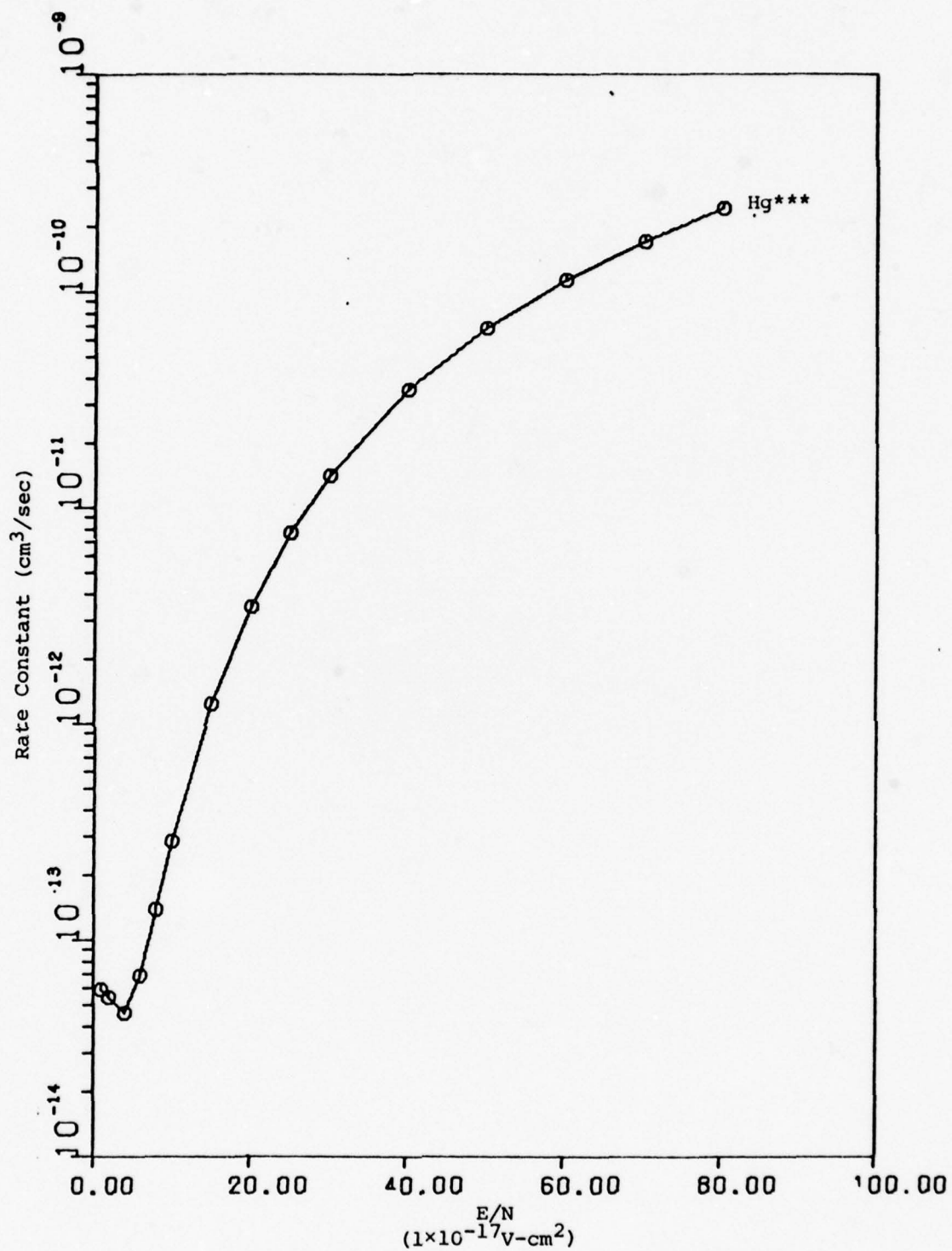


Figure 5-14 Rate Constant for the Hg^{***} Excitation Process as a Function of Field Strength ($j_{\text{eb}} = .001 \text{ amp/cm}^2$)

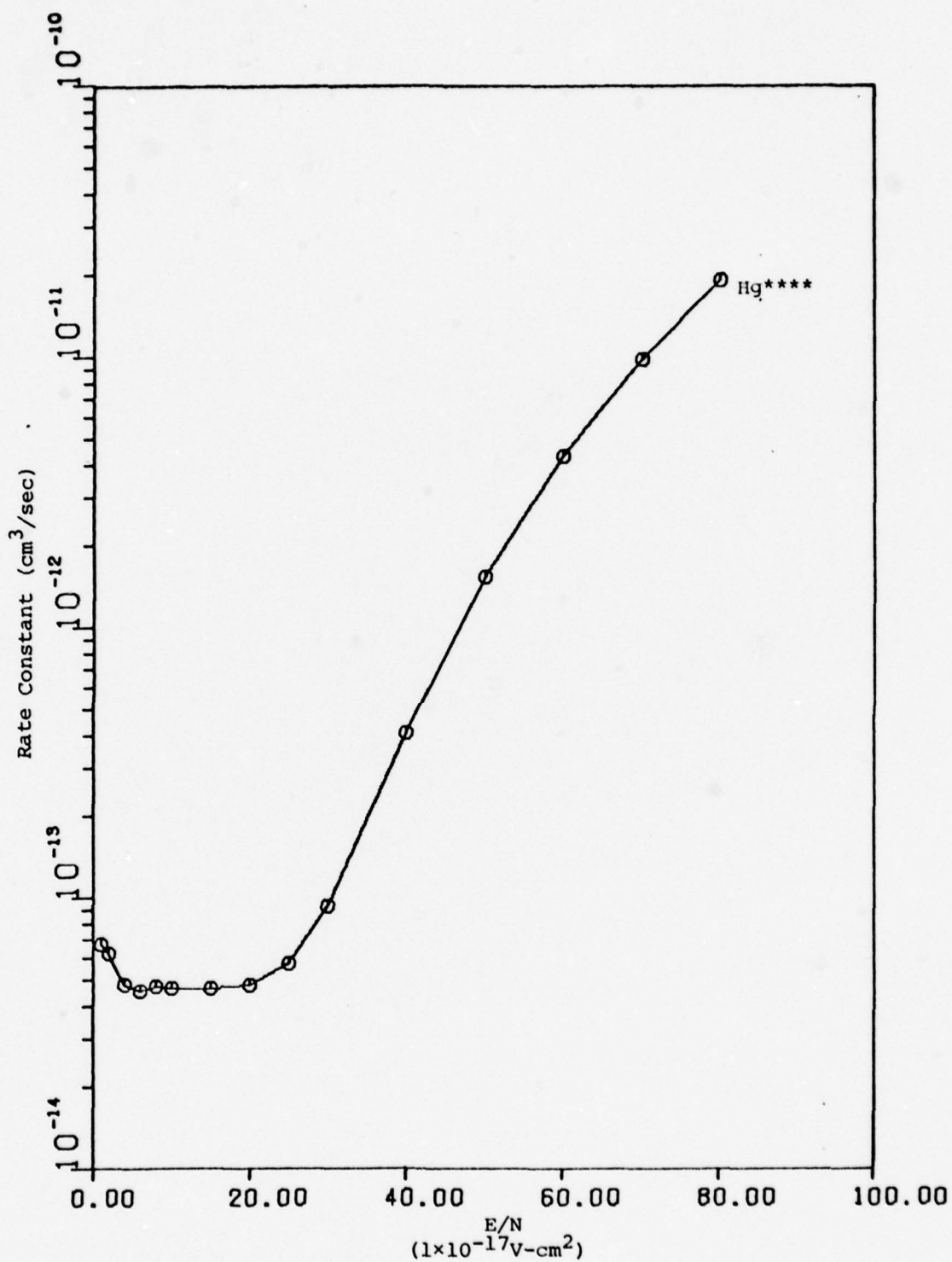


Figure 5-15 Rate Constant for the Hg^{****} Excitation Process as a Function of Field Strength ($j_{\text{eb}} = .001 \text{ amp/cm}^2$)

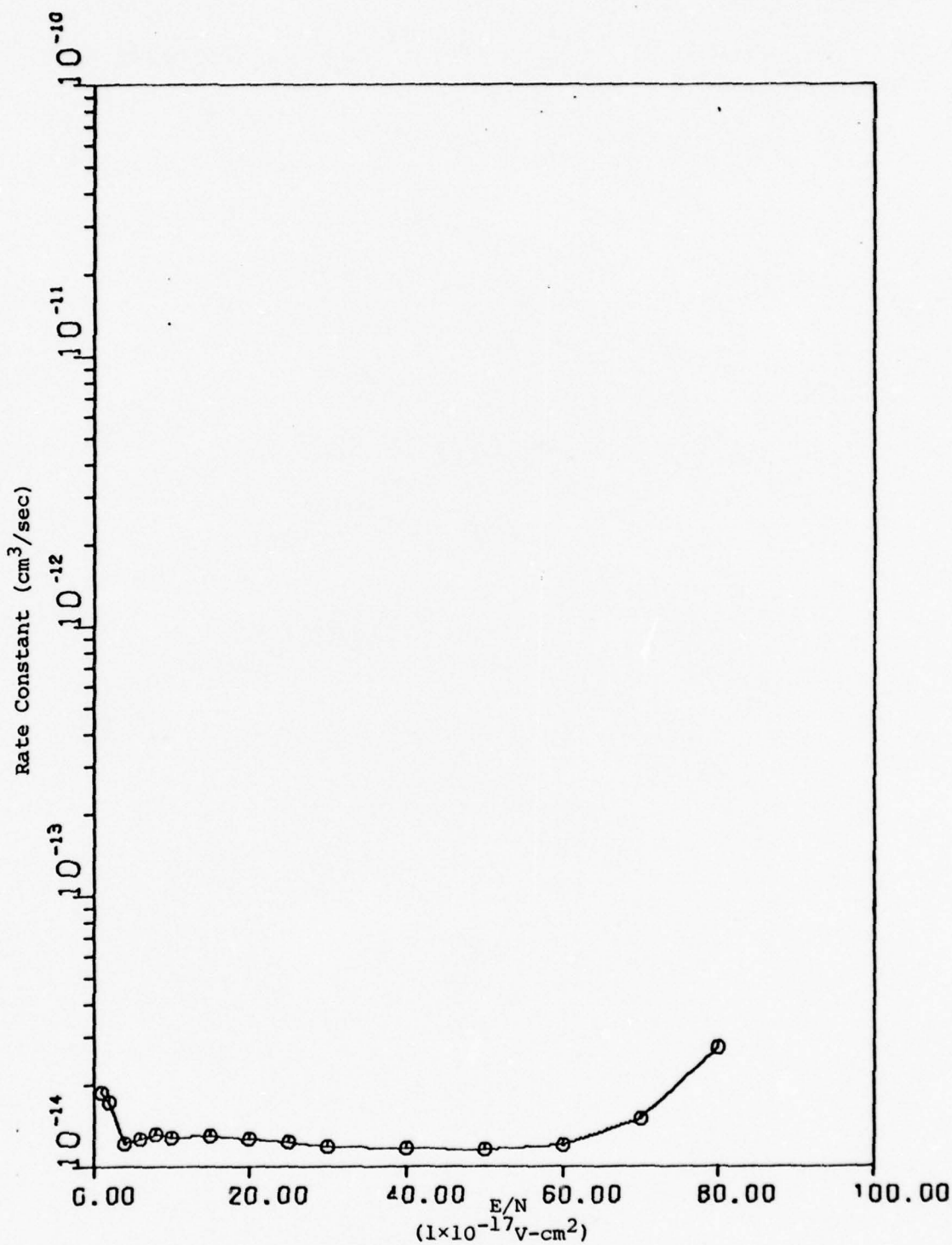


Figure 5-16 Rate Constant for the Ground State Ionization of Mercury as a Function of Field Strength ($j_{eb} = .001 \text{ amp/cm}^2$)

increases until the field effects become comparable to beam effects above the threshold energy for that process. Further increases in E/N then result in increases in the rate constant. If the beam current density is sufficiently large, the field effects over a large range of E/N values can be neglected for processes with large threshold energies. One can see from Figure 5-17 that for a 10 amp/cm^2 beam, E/N values ranging from 1×10^{-17} to $80 \times 10^{-17} \text{ V-cm}^2$ have little effect on the magnitude of the ionization rate constant.

From the analysis of field to beam effects in supporting various excitation and ionization processes, one can conclude that analytic solutions, such as the one derived in Chapter IV, which assume that, at high energies beam effects are much greater than field effects for large beams ($1\text{-}10 \text{ amp/cm}^2$) appear to be valid for a wide range of field strengths. In practice this implies that in determining the optimum field strength for exciting the upper level of an electron beam sustained laser, a wide range of E/N values could be used without significantly affecting the production rate of secondary electrons if a reasonably large beam was used.

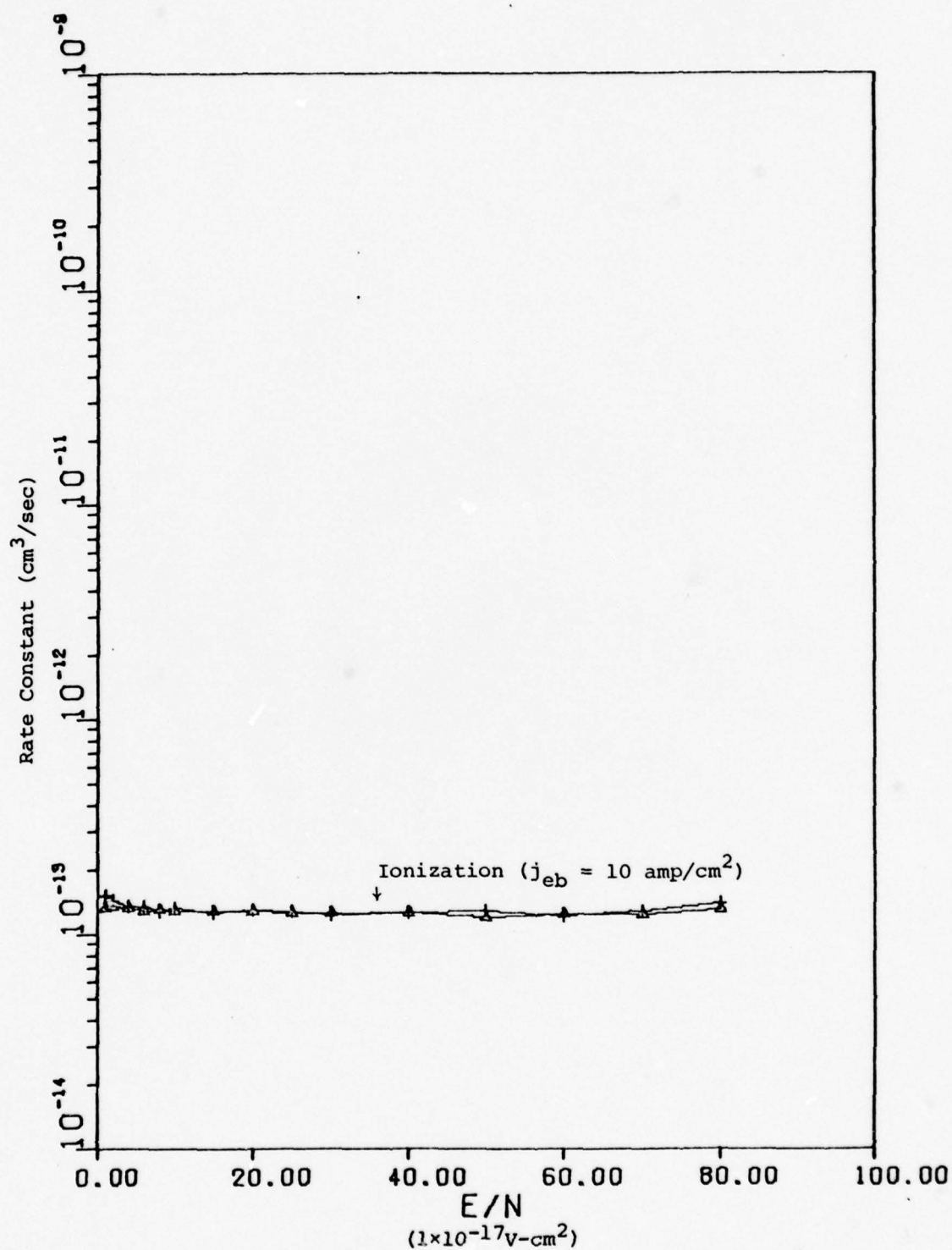


Figure 5-17 Rate Constant for Ground State Ionization of Mercury as a Function of Field Strength (j_{eb} = 10 amp/cm²)

VI. Conclusions and Recommendations

Analytic Solution

The analytic solution derived in Chapter IV displays some major inconsistencies when compared to a numerical solution developed for a similar system. The analytic solution is too small around zero energy, too large at high energies and does not appear to be normalized. Two approaches were used in an attempt to normalize the solution.

The first approach was to use the inherent normalization in the definition of $f(u)$. However, in obtaining the steady state electron density required to complete normalization, it was found that the source of secondary electrons due to the applied dc field was infinite. This may have been a result of the ionization cross section approximation being used. Therefore, the inherent normalization in $f(u)$ was lost in the many approximations required to obtain the analytic solution.

The second normalization approach was a straightforward integration approach where a normalization constant was obtained by integrating $u^{1/2}f(u)$ from $u = 0$ to $u = \infty$. In doing so, some additional approximations were required to evaluate the integrals. In introducing these additional approximations, the normalization may again have been lost; however, the possibility of a simple error in integration has not been completely ruled out.

The analytic solution is independent of the volumetric production rate of electrons due to the electron beam. This is a consequence of the "big beam approximation" used in obtaining the solution. In comparing the analytic solution to a numerical solution for a similar system, it was found that the analytic solution is a poor approximation of the numerical

solution at high energies and small beam current densities. However, as the beam current density increases, the analytic solution more closely resembles the numerical results.

Numerical Solution

Numerical solutions were obtained using a system of parameters modeled after those used by Rockwood (Ref 5) in the analysis of drift velocities and reaction efficiencies for mercury.

Reaction efficiencies and pumping rate constants were obtained for a variety of values of E/N and j_{eb} . Due to the non-linear dependence of the electron beam source term in the Boltzmann equation, self reproducing solutions could not be obtained. However, to compare results at varying values of E/N and j_{eb} , numerical solutions were obtained at a fixed point, 10^{-7} seconds, in the evolution of the electron distribution function.

In analyzing the behavior of reaction efficiencies for the higher excited states and first ionized state of mercury, the efficiencies showed an unexpected drop and then the characteristic rise as the strength of the applied dc field increased. This dip was directly attributed to electron beam effects at high energies. These beam effects at high energies were also responsible for the relative insensitivity of pumping rate constants for processes with high threshold energies to variations in the strength of applied dc fields. It was found that the pumping rate constant for a given process would remain fixed as E/N increases until the effects due to the applied field were comparable to the effects of the electron beam above the threshold energy for that process. Only then did increases in E/N result in increases in the pumping rate constant. This seems to imply that, in determining the optimum field strength for exciting the

upper level of an electron beam sustained laser, a wide range of E/N values could be used without significantly affecting the production rate of secondary electrons if a reasonably large beam was used.

Recommendations

A number of improvements could be made to the analytic solution. To minimize normalization difficulties, a different form of the ionization cross section should be used. Although the cross section used in Chapter IV appears to be a good approximation around the ionization threshold energy, it does not drop off properly at high energies. There are two means by which an improved cross section could be introduced. Either a completely different cross section could be used or a three region solution could be developed in which the form of the cross section in the high energy region could be approximated by a simple function such as σ'_0/u , where σ'_0 is chosen to match cross section boundary conditions. The cross section around threshold could be approximated as in Chapter IV as $\sigma_0(1 - \frac{I}{u})$ and the cross section in the low energy region would be zero. However, the solution developed in Chapter IV is closely tied to the approximation used for the ionization cross section; thus, any drastic changes to this approximation would most likely produce a solution considerably different to the one obtained in this thesis.

Bibliography

1. Beyer, William H. Standard Mathematical Tables (Twenty-fourth Edition). Cleveland: CRC Press, 1976.
2. Mott, Nevill F. and H. S. W. Massey. The Theory of Atomic Collisions (Second Edition). Oxford at the Clarendon Press, 1949.
3. Green, A. E. S. and T. Sawada. "Ionization Cross Sections and Secondary Electron Distributions," Atmospheric and Terrestrial Physics, 34:1719-1728 (1972).
4. Bass, J. N., R. A. Berg, and A. E. S. Green. "Electron Impact Cross Sections for the Element Mercury," Journal of Physics Bulletin,
5. Rockwood, Stephen D. "Elastic and Inelastic Cross Sections for Electron-Hg Scattering from Hg Transport Data," Physical Review A, 8 (5):2343-2358 (1974).
6. Peterson, J. R. and J. E. Allen, Jr. "Electron Impact Cross Sections for Argon," The Journal of Chemical Physics, 56 (12):6068-6076 (15 June 1972).
7. Opal, C. B., E. C. Beaty and W. K. Peterson. JILA Report No. 108, University of Colorado, Boulder, 26 May 1971.
8. IMSL LIB03-0006V1. Houston, Texas: International Mathematical and Statistical Libraries, Inc. (July, 1977).
9. Gear, C. W. Numerical Initial Value Problems in Ordinary Differential Equations. Prentice-Hall, 1971.
10. Hunter, A. M. II. Capt, USAF (private communication). Air Force Institute of Technology, Wright-Patterson AFB, Ohio, 1978.
11. Technical Report for Computer Program NGB. (Publication pending).
12. Hunter, A. M. II. Capt, USAF. "Notes on Atomic and Molecular Excitation Through Collisions With Charged Particles," unpublished, undated.
13. Hunter, A. M. II. Capt, USAF. "Notes on Rockwood Equation," unpublished, undated.
14. Dwight, Herbert B. Tables of Integrals and Other Mathematical Data (Revised Edition). New York: The Macmillan Company.

Appendix A

Differential Ionization Cross Sections

Figures A-1 through A-3 illustrate analytic fits obtained by Green and Sawada (Ref 3) to selected experimental data compiled by Opal et al (Ref 7).

The analytic form for the differential ionization cross sections used is defined as

$$S(\epsilon, T) = A(\epsilon) \left[\frac{\Gamma^2}{(T - T_0)^2 + \Gamma^2} \right]$$

where ϵ is the energy of the primary electron and T is the energy of the secondary electrons being produced. A , Γ , and T_0 are functions of ϵ and are defined as

$$A(\epsilon) = \sigma_0 \frac{K}{\epsilon} \ln \left(\frac{\epsilon}{J} \right)$$

$$\Gamma = \Gamma_s \frac{\epsilon}{\epsilon + \Gamma_b}$$

$$T_0 = T_s - \frac{T_a}{\epsilon + T_b}$$

where σ_0 equals 10^{-16} cm^2 and remaining parameters are adjusted to obtain the desired fit. Parameters used in obtaining the fits illustrated in Figures A-1 through A-3 are contained in Tables A-1 and A-2.

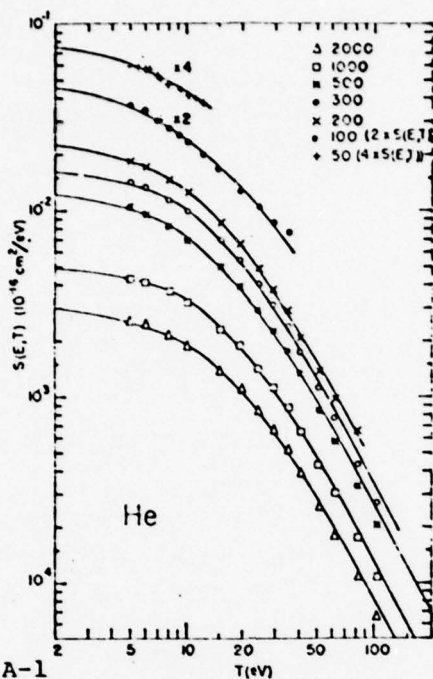


Figure A-1
Differential ionization cross section, $S(E, T)$, for He at various energies as indicated. Data points are selected from the data of Oral *et al.* (1971), and the fits using equation (4) with $\kappa = 1$ are shown by the curves.
(Ref 3:1722)

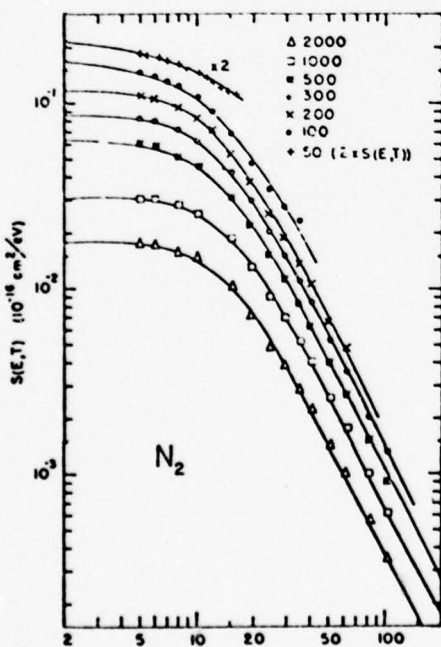


Figure A-2
 $S(E, T)$ for N_2 . See the caption of Fig. 1.
(Ref 3:1723)

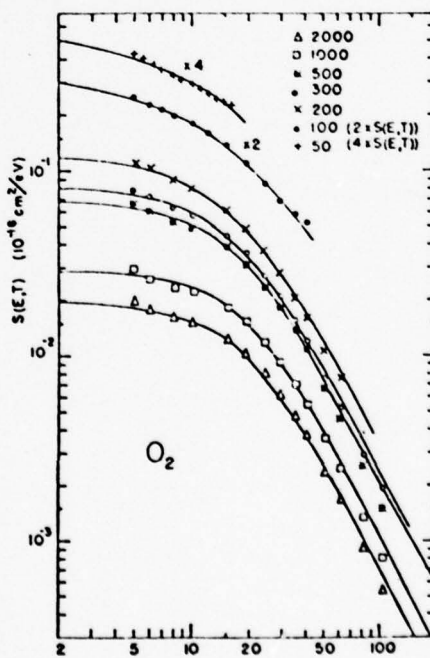


Figure A-3
 $S(E, T)$ for O_2 . See the caption of Fig. 1.
(Ref 3:1723)

Table A-1

 $A(E)$, $\Gamma(E)$ and $T_0(E)$ for He, N₂ and O₂*†

E	A	Γ	T_0
He ($I = 24.5$ eV)			
50	0.0331	14.5	-10.9
100	0.0787	10.1	-13.8
200	0.0275	13.2	-4.30
300	0.0175	14.3	-2.19
500	0.0141	14.2	-3.85
1000	0.00530	16.3	-2.57
2000	0.00355	16.2	-5.11
N ₂ ($I = 15.6$ eV)			
50	0.148	20.6	-10.7
100	0.177	12.8	-0.517
200	0.116	11.9	2.54
300	0.0867	12.5	2.40
500	0.0636	12.6	2.28
1000	0.0312	14.1	3.35
2000	0.0180	13.8	3.03
O ₂ ($I = 12.1$ eV)			
50	0.581	11.9	-20.7
100	0.411	13.9	-16.3
200	0.126	16.7	-2.19
300	0.0836	16.9	-0.519
500	0.0693	17.3	-0.295
1000	0.0259	19.2	0.938
2000	0.0196	19.2	0.460

* $A(E)$ is in units of 10^{-16} cm²/eV, $\Gamma(E)$ and $T_0(E)$ are in eV.

† These values are obtained by fitting OPAL *et al.* (1971) data using equation (4) with $\kappa = 1$.

(Ref 3:1724)

Table A-2

Parameters of He, N₂ and O₂

	T_s (eV)	Γ_s (eV)	K_{cp}	J_{cp} (eV)	K_s	J_s (eV)
He	-2.25	15.5	1.48	6.34	1.30	1.32
N ₂	4.71	13.8	7.12	6.82	6.85	1.74
O ₂	1.86	18.5	7.96	11.1	7.67	3.76

* $T_s = 1000$ eV, $T_b = 2I$, and $\Gamma_b = I$. K_{cp} and J_{cp} are obtained by fitting $S(E, T)$ of OPAL *et al.* (1971), and K_s and J_s are obtained by fitting $\sigma_i(E)$ of KIEFFER and DUNN (1966).

(Ref 3:1726)

Loss Functions and Reaction Efficiencies

Figures A-4 through A-7 illustrate loss functions and reaction efficiencies obtained by Peterson and Allen (Ref 6) for the element argon, and Bass, Berg, and Green (Ref 4) for the element mercury.

The loss function is defined as

$$L(\epsilon) = \sum_j \omega_j \sigma_j(\epsilon) + \sum_i (I_i \sigma_i(\epsilon) + \int_0^{(\epsilon-I)/2} TS_i(\epsilon, T) dT)$$

where

ω_j = excitation energy of the j^{th} excited state

σ_j = excitation cross section for state j

I_i = ionization potential of state i

σ_i = ionization cross section for state i

ϵ = energy of the incident electron

T = energy of ejected secondary electrons

Reaction efficiencies are defined as the fraction of incident energy going into each of the inelastic channels and can be expressed as

$$\eta_j = \frac{\omega_j J}{\epsilon}$$

where J is the number of excitations to state j produced by a primary electron of energy ϵ .

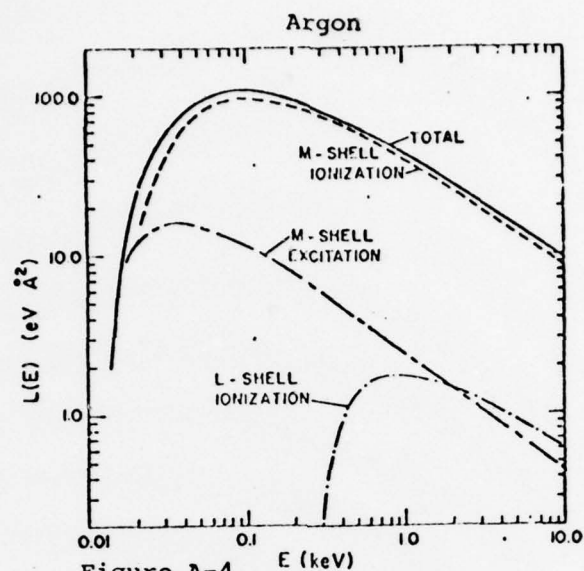


Figure A-4
The loss function and its contributions as computed directly from the cross sections.

(Ref 5:6074)

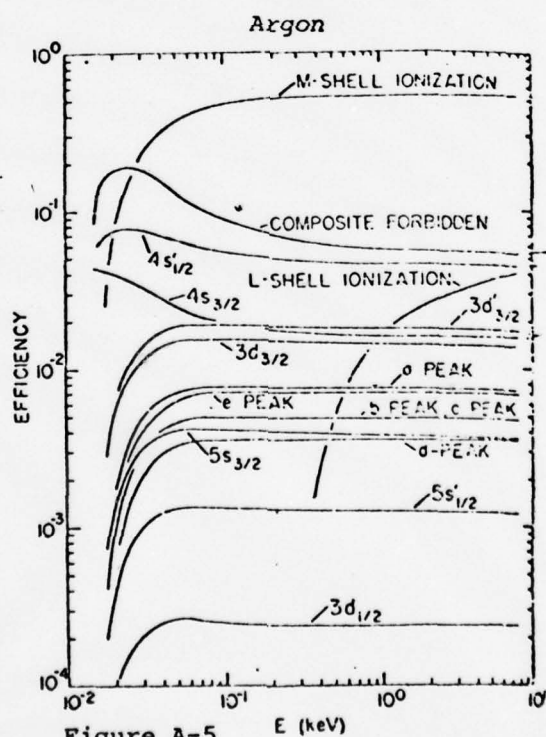


Figure A-5
Efficiency of each state as a fraction of the incident energy

(Ref 5:6074)

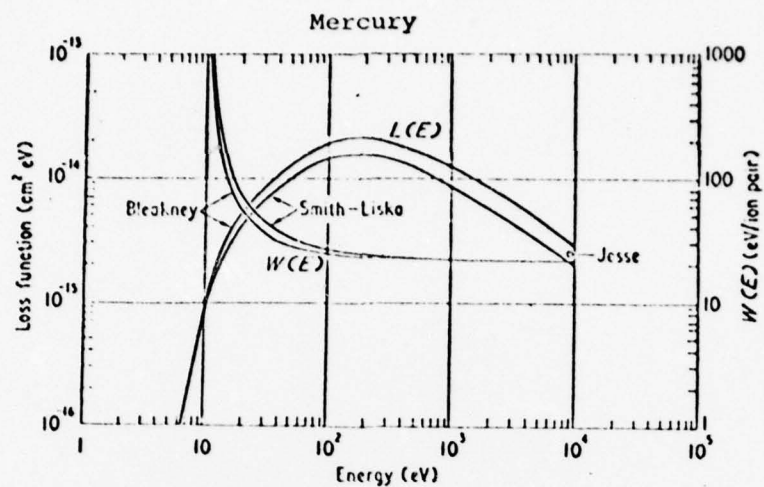


Figure A-6

Loss function and eV/ion pair. The square is the eV/ion pair result of Jesse (1971).

(Ref 4:1863)

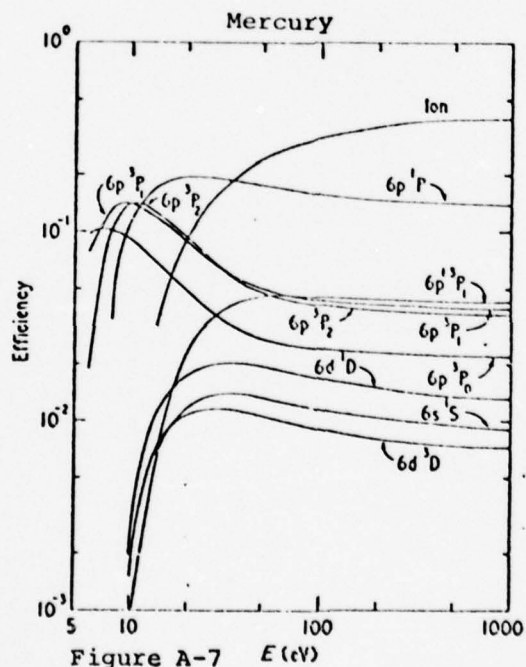


Figure A-7 $E(eV)$

Efficiencies, using Smith-Liska ionization cross section.

(Ref 4:1863)

Appendix B

Justification of Initial Assumptions

Secondary Electrons Produced via a Mono-energetic Electron Beam Emerge Isotropically in Velocity Space

Rigorous analysis of the velocity space isotropy of secondary electrons produced by a mono-energetic electron beam is beyond the scope of this thesis. However, Mott (Ref 2) has performed cursory examination of the phenomena. Using wavefunction for electrons in a given energy state, moving in a specified direction, in a field of charge Ze ; and, a wavefunction dependent equation for differential ionization cross sections, he obtained a relationship between the energy of the incident electron and the angle which secondary electrons are ejected. Figure B-1 illustrates his results.

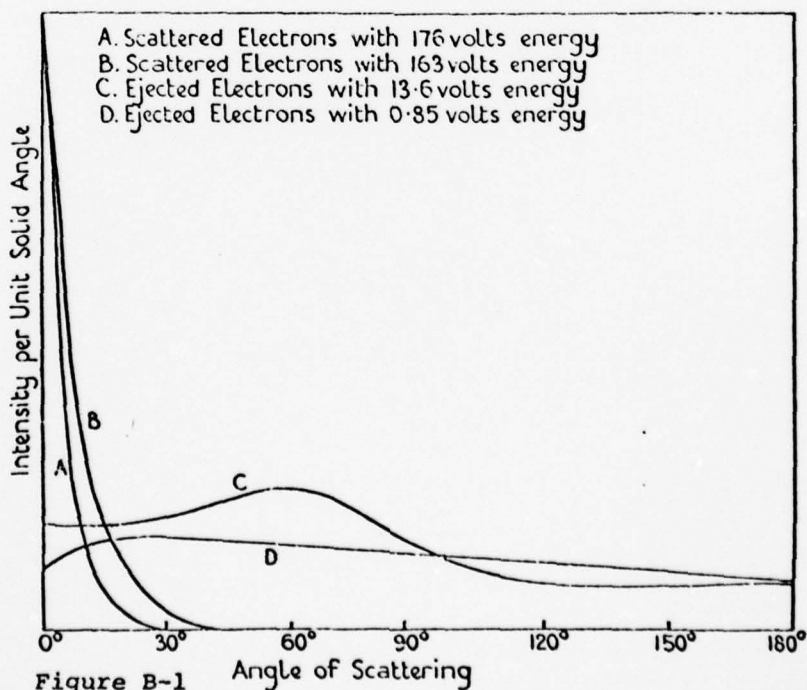


Figure B-1 Angular distributions of scattered and ejected electrons corresponding to electrons of 200 volts incident energy.

(Ref 2:234)

For incident electrons with energy much greater than ejected secondary electrons, it is apparent from Figure B-1 that ejected electrons show no real directional preference and hence, can be considered isotropic in velocity space.

Elastic Collisions Between Electrons
and Heavy Particles Can Be Ignored

Consider the collision in one dimension of an electron of mass m with a heavy particle of mass M (assumed stationary). Conservation of momentum and energy equations require

$$mu = mu_1 + MV \quad (B-1)$$

and

$$\frac{1}{2}mu^2 = \frac{1}{2}mu_1^2 + \frac{1}{2}MV^2 \quad (B-2)$$

where

m = mass of the electron

M = mass of the heavy particle

u = initial velocity of the electron

u_1 = velocity of the electron following the collision

V = velocity of the heavy particle following the collision

From equation B-2

$$m(u^2 - u_1^2) = MV^2 \quad (B-3)$$

or

$$m(u + u_1)(u - u_1) = MV^2 \quad (B-4)$$

But from the conservation of momentum equation (B-1)

$$(u - u_1) = \frac{M}{m} V \quad (B-5)$$

Substituting equation B-5 into equation B-4 and simplifying terms yields

$$(v + v_1) = V \quad (B-6)$$

Adding equation B-5 and B-6 and simplifying yields

$$2v = V \left(1 + \frac{M}{m} \right) = \frac{M}{m} V \quad (B-7)$$

or

$$V = 2 \frac{m}{M} v \quad (B-8)$$

This last result can be used to determine the amount of energy lost by the electron during the collision process (or the amount of energy gained by the heavy particle) as a function of the initial electron energy.

$$\frac{1}{2} M V^2 = 4 \frac{m}{M} \left(\frac{1}{2} m v^2 \right) \quad (B-9)$$

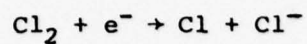
Thus, the energy transferred is proportional to the ratio of the masses of the particles colliding. Therefore, one can conclude that the energy lost from an electron when undergoing a collision with a heavy particle is on the order of 10^{-3} of the electron energy.

Since the energy lost by an electron in an inelastic collision is typically an eV or greater, changes in the electron distribution function due to elastic collisions between electrons and heavy particles will be small compared to changes resulting from inelastic collisions. This, of course, assumes that the average electron energy is large enough for a significant number of electrons to have energy greater than the inelastic threshold energy.

The Dominant Electron Loss Mechanism is Due to Attachment

In many of today's gas laser systems, a significant electron loss mechanism results from chemical reactions in which a molecular species reacts with a free electron to form a neutral atom and an ion. In the

case of a mercury chloride laser this reaction becomes (Ref 10)



If the plasma analysis is limited to early in the gas breakdown process, such that the number density of ionized species is small compared to the number density of neutral species, recombination of electrons and ions can be ignored.

If one also assumes infinite geometry, such that finite boundaries are eliminated, electrons physically leaving the plasma can be neglected. With these restrictions on the solution, the dominant electron loss mechanism comes from dissociative attachment.

Appendix C

Derivation of Analytic Solution

From the modified Boltzmann equation derived in Chapter II and assuming:

- 1) Steady state
- 2) No superelastic collisions
- 3) Attachment only at zero energy
- 4) Secondary electrons resulting from non-electron-beam collisions emerge with zero energy
- 5) Momentum transfer cross sections (Q) are independent of the incident electron energy
- 6) Single species which exist only in the ground and singly ionized state

the Boltzmann equation becomes

$$\begin{aligned} \frac{(E/N)^2}{3Q} \frac{d}{du} \left[u \frac{df}{du} \right] + c\beta(u) + \sigma_i(u+I)(u+I)f(u+I) \\ - \sigma_i(u)(u)f(u) + \delta(u) \int_0^\infty \sigma_i(u)(u)f(u)du - \delta(u) \Psi_a \sigma_a(u)(u)f(u) = 0 \end{aligned} \quad (C-1)$$

Since the significance of many of the above terms varies in different regions of the energy axis, solutions to the Boltzmann equation above and below the ionization threshold energy (I) were considered separately (see Figure C-1).

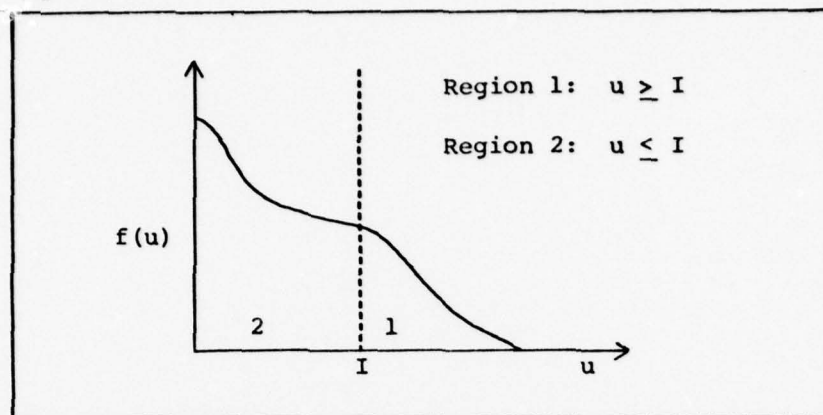


Figure C-1 Regions of Solution

Constraints

Initial constraints imposed on the solution include the following:

- 1) Piecewise continuity

$$f_1(I) = f_2(I)$$

- 2) The function and its derivative must vanish at infinity

$$\lim_{u \rightarrow \infty} f(u) = 0 \quad \lim_{u \rightarrow \infty} \frac{df(u)}{du} = 0$$

- 3) The function must be finite at $u = 0$

- 4) Electrons must be conserved

$$c\beta(u) + \delta(u) \int_0^{\infty} \sigma_i(u)(u)f(u)du = \delta(u) \Psi_a \sigma_a(u)(u)f(u)$$

Region 1: ($u \geq I$)

Allowing for attachment only at zero energy and assuming non-electron-beam generated secondary electrons emerge with zero energy, the Boltzmann equation for u greater than the ionization threshold energy becomes

$$\frac{(E/N)^2}{3Q} \frac{d}{du} \left[u \frac{df}{du} \right] + c\beta(u) + \sigma_i(u+I)(u+I)f(u+I) - \sigma_i(u)(u)f(u) = 0 \quad (C-2)$$

Approximating the inelastic cross section (Ref 10)

$$\sigma_i(u) = \sigma_o \left(1 - \frac{I}{u}\right) \quad (C-3)$$

then

$$u\sigma_i(u) = \sigma_o(u - I) \quad (C-4)$$

$$(u + I)\sigma_i(u + I) = \sigma_o u \quad (C-5)$$

where I is the excitation threshold energy and σ_o is a constant dependent upon the species and reaction considered (approximately 10^{-16} cm^2). Substituting C-4 and C-5 into equation C-2 yields

$$\begin{aligned} \frac{(E/N)^2}{3Q} \frac{d}{du} \left[u \frac{df}{du} \right] + cS(u) + \sigma_o u f(u + I) \\ - \sigma_o u f(u) + \sigma_o I f(u) = 0 \end{aligned} \quad (C-6)$$

or

$$\begin{aligned} \frac{(E/N)^2}{3Q} \frac{d}{du} \left[u \frac{df}{du} \right] + cS(u) + \sigma_o u [f(u + I) - f(u)] \\ + \sigma_o I f(u) = 0 \end{aligned} \quad (C-7)$$

if $f(u)$ is not a rapidly varying function for $u \geq I$ than

$$[f(u + I) - f(u)] \approx I \frac{df}{du} \quad (C-8)$$

Substituting this approximation into equation C-7 yields

$$\frac{(E/N)^2}{3Q} \frac{d}{du} \left[u \frac{df}{du} \right] + cS(u) + \sigma_o u I \frac{df}{du} + \sigma_o I f = 0 \quad (C-9)$$

One is then left with a second order differential equation. However, if

$$\frac{(E/N)^2}{3Q} \frac{d}{du} \left[u \frac{df}{du} \right]$$

can be considered small compared to the remaining terms in equation C-9, an iterative technique can be employed to obtain an approximate solution in which the second order term is ignored. Using this approximate solution, the second order term can be expressed explicitly and reinserted into

equation C-9 to obtain increasingly accurate solutions. This assumption must be checked for self consistency once a final form for $f(u)$ is obtained.

Using this approach and ignoring the second order term, equation C-9 becomes

$$\sigma_o I u \frac{df_o}{du} + \sigma_o I f_o = -c s(u) \quad (C-10)$$

or

$$\frac{d(uf_o)}{du} = \frac{-cs(u)}{\sigma_o I} \quad (C-11)$$

which can be solved to get

$$f_o = \frac{-c}{\sigma_o I} \frac{1}{u} \int s(u) du + \frac{c'}{u} \quad (C-12)$$

Approximating the secondary source spectrum (Reference Appendix D) by

$$s(u) = \begin{cases} \frac{S_o}{2u_o} & , \quad 0 \leq u \leq u_o \\ \frac{u_o S_o}{2u^2} & , \quad u_o \leq u \end{cases} \quad (C-13)$$

where

$$S_o = \int_0^\infty s(u) du$$

$$u_o = \text{excitation threshold energy } I$$

and substituting C-13 into equation C-12 yields

$$f_o = \frac{-c}{\sigma_o I} \frac{1}{u} \int \frac{u_o S_o}{2u^2} du + \frac{c'}{u} \quad (C-14)$$

or

$$\boxed{f_o = \frac{cu_o S_o}{2\sigma_o I} \frac{1}{u^2} + \frac{c'}{u}} \quad (C-15)$$

Using this approximate form for $f(u)$, the second order term in equation C-9 can be written as

$$\frac{(E/N)^2}{3Q} \frac{d}{du} \left[u \frac{df_0}{du} \right] = \frac{(E/N)^2}{3Q} \frac{d}{du} \left[u \frac{d}{du} \left(\frac{cu_0 S_0}{2\sigma_0 I} \frac{1}{u^2} \right) \right] \quad (C-16)$$

or

$$\frac{(E/N)^2}{3Q} \frac{d}{du} \left[u \frac{df_0}{du} \right] = \frac{(E/N)^2}{3Q} \frac{d}{du} \left[- \frac{cu_0 S_0}{\sigma_0 I} \frac{1}{u^2} \right] \quad (C-17)$$

(Note: The c' term has been dropped to prevent introducing two constants of integration when essentially a first order differential equation is being solved.)

Substituting equation C-17 into equation C-9 yields

$$\frac{(E/N)^2}{3Q} \frac{d}{du} \left[- \frac{cu_0 S_0}{\sigma_0 I} \frac{1}{u^2} \right] + cS(u) + \sigma_0 u I \frac{df_1}{du} + \sigma_0 I f_1 = 0 \quad (C-18)$$

which, as before, can be rewritten as

$$\frac{d(uf_1)}{du} = - \frac{cS(u)}{\sigma_0 I} + \frac{(E/N)^2}{3Q} \frac{cu_0 S_0}{(\sigma_0 I)^2} \frac{d}{du} \left[\frac{1}{u^2} \right] \quad (C-19)$$

This is a simple first order equation which can be solved to obtain the form of $f(u)$ for $u \geq I$.

$$f_1(u) = - \frac{1}{u} \frac{cS(u)}{\sigma_0 I} + \frac{(E/N)^2}{3Q} \frac{cu_0 S_0}{(\sigma_0 I)^2} \frac{1}{u^3} + \frac{c''}{u} \quad (C-20)$$

Again, using the approximated form for the secondary source spectrum (equation C-13) equation C-20 becomes

$$f_1(u) = \frac{cu_0 S_0}{2\sigma_0 I} \frac{1}{u^2} + \frac{(E/N)^2}{3Q} \frac{cu_0 S_0}{(\sigma_0 I)^2} \frac{1}{u^3} + \frac{c''}{u} \quad (C-21)$$

To satisfy the initial condition of normalization

$$\int_0^\infty u^{1/2} f(u) du = 0$$

it is clear that c'' must equal zero. Thus, the form of $f(u)$ for $u \geq I$ is

$$f_1(u) = \frac{cu_0 S_0}{2\sigma_0 I} \frac{1}{u^2} + \frac{(E/N)^2}{3Q} \frac{cu_0 S_0}{(\sigma_0 I)^2} \frac{1}{u^3} \quad (C-22)$$

It should be noted that

$$\lim_{u \rightarrow \infty} f(u) = 0 \quad \text{and} \quad \lim_{u \rightarrow \infty} \frac{df(u)}{du} = 0$$

as required by the initial constraints on allowed forms for $f(u)$.

Region 2: ($0 < u \leq I$)

As in Region 1, if we allow for attachment only at zero energy and assume that non-electron-beam generated secondary electrons emerge with zero energy, the Boltzmann equation for u greater than zero, but less than the ionization threshold energy becomes

$$\begin{aligned} \frac{(E/N)^2}{3Q} \frac{d}{du} \left[u \frac{df}{du} \right] + c\beta(u) + \sigma_i(u+I)(u+I)f(u+I) \\ + \sigma_i(u)f(u) = 0 \end{aligned} \quad (C-23)$$

But the ionization cross section for $u < I$ equals zero. Therefore, equation C-23 becomes

$$\frac{(E/N)^2}{3Q} \frac{d}{du} \left[u \frac{df}{du} \right] + c\beta(u) + \sigma_i(u=I)(u+I)f(u+I) = 0 \quad (C-24)$$

From equation C-5

$$(u+I)\sigma_i(u+I) = \sigma_0 u$$

and from Region 1 (equation C-22)

$$f(u+I) = \frac{cu_0 S_0}{2\sigma_0 I} \frac{1}{(u+I)^2} + \frac{(E/N)^2}{3Q} \frac{cu_0 S_0}{(\sigma_0 I)^2} \frac{1}{(u+I)^3}$$

Substituting these values for $f(u+I)$ and $(u+I)\sigma_i(u+I)$ into equation C-24 and solving for the second order term yields

$$\begin{aligned} \frac{(E/N)^2}{3Q} \frac{d}{du} \left[u \frac{df}{du} \right] = -c\beta(u) - \sigma_0 u \left[\frac{cu_0 S_0}{2\sigma_0 I} \frac{1}{(u+I)^2} \right. \\ \left. + \frac{(E/N)^2}{3Q} \frac{cu_0 S_0}{(\sigma_0 I)^2} \frac{1}{(u+I)^3} \right] \end{aligned} \quad (C-25)$$

or

$$\begin{aligned} \frac{d}{du} \left[u \frac{df}{du} \right] = & - \frac{3Qc}{(E/N)^2} S(u) - \frac{3Q}{(E/N)^2} \frac{cu_0 S_0}{2I} \frac{u}{(u+I)^2} \\ & - \frac{cu_0 S_0}{\sigma_0 I^2} \frac{u}{(u+I)^3} \end{aligned} \quad (C-26)$$

Direct solution by separation of variables, unfortunately, results in an obnoxious form for $f(u)$ which appears to be unbounded at $u = 0$. Therefore, a modified WKB method was used to express

$$\frac{d}{du} \left[u \frac{df}{du} \right] = g(u) \quad (C-27)$$

as

$$f(u) = 2 \int g(u) du - u g(u) + \text{const} \quad (C-28)$$

(Reference Appendix D).

Using this approximation, equation C-26 becomes

$$\begin{aligned} f(u) = & - \frac{3Qc}{(E/N)^2} \left[2 \int S(u) du - u S(u) \right] \\ & - \frac{3Q}{(E/N)^2} \frac{cu_0 S_0}{2I} \left[2 \int \frac{u}{(u+I)^2} du - \frac{u^2}{(u+I)^2} \right] \\ & - \frac{cu_0 S_0}{\sigma_0 I^2} \left[2 \int \frac{u}{(u+I)^3} du - \frac{u^2}{(u+I)^3} \right] \\ & + c''' \end{aligned} \quad (C-29)$$

Substituting the approximation for the secondary source spectrum (equation C-13) into equation C-29 and performing the necessary integrations yields the solution to the Boltzmann equation for $0 < u \leq I$

$$\begin{aligned}
 f_2(u) = & - \frac{3Q}{(E/N)^2} \frac{cS_o}{2u_o} u \\
 & - \frac{3Q}{(E/N)^2} \frac{cu_oS_o}{2I} \left[2\ln(u+I) + \frac{2I}{(u+I)} - \frac{u^2}{(u+I)^2} \right] \\
 & - \frac{cu_oS_o}{\sigma_o I^2} \left[\frac{2}{(u+I)} - \frac{I}{(u+I)^2} + \frac{u^2}{(u+I)^3} \right] \\
 & + c'''
 \end{aligned}
 \tag{C-30}$$

To complete the solution for $f(u)$, c''' must be determined and manipulations necessary to meet the initial normalization requirement must be performed.

Apply Boundary Condition to Evaluate c'''

c''' is obtained by insisting that $f(u)$ is piecewise continuous for all u .

$$f_1(u) = f_2(u) \tag{C-31}$$

From equation C-22

$$f_1(u) = \frac{cu_oS_o}{2\sigma_o I} \frac{1}{u^2} + \frac{(E/N)^2}{3Q} \frac{cu_oS_o}{(\sigma_o I)^2} \frac{1}{u^3}$$

Evaluating $f_1(u)$ at $u = I$ yields

$$f_1(I) = \frac{cu_oS_o}{2\sigma_o I^3} + \frac{(E/N)^2}{3Q} \frac{cu_oS_o}{\sigma_o^2 I^5} \tag{C-32}$$

From equation C-30

AD-A064 680

AIR FORCE INST OF TECH WRIGHT-PATTERSON AFB OHIO SCH--ETC F/G 20/8
THE EFFECTS OF BEAM CURRENTS ON ELECTRON ENERGY DISTRIBUTIONS.(U)
DEC 78 E D SEWARD

UNCLASSIFIED

AFIT/GEP/PH/78D-12

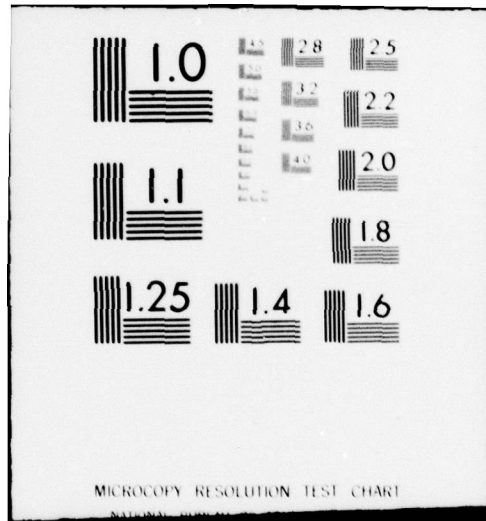
NL

20F2
AD
A064680



END
DATE
FILMED
4-79
DDC





$$\begin{aligned}
f_2(u) = & - \frac{3Q}{(E/N)^2} \frac{cS_o}{2u_o} u \\
& - \frac{3Q}{(E/N)^2} \frac{cu_o S_o}{2I} \left[2 \ln(u + I) + \frac{2I}{(u + I)} - \frac{u^2}{(u + I)^2} \right] \\
& + \frac{cu_o S_o}{\sigma_o I^2} \left[\frac{2}{(u + I)} - \frac{I}{(u + I)^2} + \frac{u^2}{(u + I)^3} \right] \\
& + c'''
\end{aligned}$$

Evaluating $f_2(u)$ at $u = I$, equation C-30 becomes

$$\begin{aligned}
f_2(I) = & - \frac{3Q}{(E/N)^2} \frac{cS_o}{2u_o} I \\
& - \frac{3Q}{(E/N)^2} \frac{cu_o S_o}{2I} \left[2 \ln(2I) + \frac{3}{4} \right] \\
& + \frac{7}{8} \frac{cu_o S_o}{\sigma_o I^3} \\
& + c'''
\end{aligned} \tag{C-33}$$

Substituting C-32 and C-33 into equation $f_1(I) = f_2(I)$ and solving for c''' yields

$$\begin{aligned}
c''' = & - \frac{3}{8} \frac{cu_o S_o}{\sigma_o I^3} + \frac{(E/N)^2}{3Q} \frac{cu_o S_o}{\sigma_o^2 I^5} \\
& + \frac{3Q}{(E/N)^2} \frac{cS_o}{2} \left[\frac{I}{u_o} + \frac{2u_o}{I} \ln(2I) + \frac{3u_o}{4I} \right]
\end{aligned} \tag{C-34}$$

Normalization

To complete the solution for $f(u)$, the normalization requirement must be fulfilled. An effort was made to utilize the inherent normalization

in the definition of $f(u)$. In doing so, it was necessary to obtain the steady state electron density, n_e , which appears in the definition of c (equation 2-11). By employing conservation of electrons, one obtains the following expression which can be solved for n_e .

$$c \int_0^\infty S(u) du + \int_0^\infty \sigma_i(u) (u) f(u) du = \psi_a \int_0^\infty \sigma_a u f(u) du \quad (C-35)$$

Unfortunately, the second integral, representing electron sources resulting from indirect electron beam and field driven ionization, becomes infinite when evaluated between the limits of zero to infinity. This is due in part to the approximation made for the ionization cross section. Where for a true cross section

$$\lim_{u \rightarrow \infty} \sigma_i(u) = 0$$

the approximation becomes

$$\lim_{u \rightarrow \infty} \sigma_i(u) = \text{constant}$$

Thus, in introducing the various approximations required to obtain $f(u)$ its inherent normalization has been lost.

As a consequence of this, the standard normalization procedure was employed in which a constant defined by

$$\int_0^\infty u^2 f(u) du = c_{\text{norm}} \quad (C-36)$$

was determined. The normalized $f(u)$ is thus $1/c_{\text{norm}} f(u)$. It should be noted that this process, though straightforward, is a bit tedious. Evaluating equation C-36 yields

$$c_{\text{norm}} = \int_0^I u^2 f_2(u) du + \int_I^\infty u^2 f_1(u) du \quad (C-37)$$

Substituting the forms for $f_1(u)$ and $f_2(u)$ (equations C-22 and C-33) equation C-37 becomes

$$\begin{aligned}
c_{\text{norm}} = & - \frac{3Q}{(E/N)^2} \frac{cs_o}{2u_o} \int_0^I u^{3/2} du \\
& - \frac{3Q}{(E/N)^2} \frac{cu_o s_o}{2I} \left[2 \int_0^I u^{1/2} \ln(u+I) du + 2I \int_0^I \frac{u^{1/2}}{(u+I)} du - \int_0^I \frac{u^{5/2}}{(u+I)^2} du \right] \\
& + \frac{cu_o s_o}{\sigma_o I^2} \left[2 \int_0^I \frac{u^{1/2}}{(u+I)} du - I \int_0^I \frac{u^{1/2}}{(u+I)^2} du + \int_0^I \frac{u^{5/2}}{(u+I)^3} du \right] \\
& + c'''' \int_0^I u^{1/2} du \\
& + \frac{cu_o s_o}{2\sigma_o I} \int_I^\infty u^{-3/2} du \\
& + \frac{(E/N)^2}{3Q} \frac{cu_o s_o}{(\sigma_o I)^2} \int_I^\infty u^{-5/2} du
\end{aligned} \tag{C-38}$$

Using the following approximation for the logarithmic term and equation C-40 to solve the more difficult integrals

$$\ln(u+I) \approx \ln 2I + \frac{u}{2I} - \frac{1}{2} \tag{C-39}$$

$$\begin{aligned}
\int \frac{\chi^m}{\chi^n} &= - \frac{\chi^{m-1}}{(2n-m-1)a\chi^{n-1}} \\
&+ \frac{(m-1)c}{(2n-m-1)a} \int \frac{\chi^{m-2}}{\chi^n} d\chi \\
&- \frac{(n-m)b}{(2n-m-1)a} \int \frac{\chi^{m-1}}{\chi^n} d\chi
\end{aligned} \tag{C-40}$$

where $\chi = ax^2 + bx + c$ (Ref 14) one obtains the following expression for c_{norm}

$$\begin{aligned}
c_{\text{norm}} = & \frac{(E/N)^2}{3Q} \frac{cu_0 S_0}{\sigma_0^2} \frac{2}{3} I^{-7/2} \\
& - \frac{3Q}{(E/N)^2} \frac{c S_0}{2u_0} \frac{2}{5} I^{5/2} \\
& - \frac{3Q}{(E/N)^2} \frac{cu_0 S_0}{2} I^{1/2} \left[\frac{4}{3} \ln 2I - \frac{141}{60} + \frac{3}{2} \tan^{-1}(1) \right] \\
& + \frac{cu_0 S_0}{\sigma_0} I^{-3/2} \left[7 - \frac{55}{8} \tan^{-1}(1) \right] \\
& + \frac{2}{3} c''' I^{3/2}
\end{aligned}$$

(C-41)

Equations C-22 and C-30 along with the normalization factor C-41, yields the final solution for $f(u)$ for $0 \leq u \leq \infty$.

Appendix D

Analysis of Approximations Used in Analytic

Solution Derivation

Approximation for: $\frac{d}{du} \left[u \frac{df}{du} \right] = g(u)$

For a differential equation of the form

$$\frac{d}{du} \left[u \frac{df}{du} \right] = g(u)$$

or

$$u \frac{d^2 f}{du^2} + \frac{df}{du} = g(u) \quad (D-1)$$

it should be possible to express $f(u)$ as a polynomial series near $u = 0$

for a non-singular $f(u)$

$$f = a_0 + a_1 u + a_2 u^2 \dots$$

where

$$uf'' \rightarrow 0 \quad \text{as} \quad u \rightarrow 0$$

and

$$f' \rightarrow a_1 \quad \text{as} \quad u \rightarrow 0$$

If uf'' vanishes at zero, $f(u)$ can be obtained through successive approximation (Ref 9). Therefore, using the iterative technique

$$\frac{df}{du} \approx g(u) \quad (D-2)$$

and

$$u \frac{d^2 f}{du^2} = u \frac{d}{du} \left[\frac{df}{du} \right] \approx u \frac{dg}{du} \quad (D-3)$$

Substituting equations D-2 and D-3 into equation D-1 and solving for $f(u)$ yields

$$f(u) \approx 2 \int g(u) du - u g(u) + \text{constant}$$

Note: One should check for self-consistency by verifying that

$$u \frac{d^2 f}{du^2} \ll \frac{df}{du}$$

over the range of u for which the approximation is used.

Approximation: $S(u)$

A reasonably accurate analytic model for the secondary source spectrum generated by a mono-energetic electron beam has been developed by Green and Sawada (Ref 3) and is defined as

$$g(u) = \frac{N j_{eb}}{e} A(\epsilon) \left[\frac{\Gamma^2}{(u - T_O)^2 + \Gamma^2} \right]^K \quad (D-4)$$

where

$$A(E) = \sigma_O \frac{K}{E} \ln \frac{E}{J} \quad (D-5)$$

$$T_O = T_S - \frac{T_a}{E - T_b} \quad (D-6)$$

$$\Gamma = \Gamma_S \frac{E}{E + \Gamma_b} \quad (D-7)$$

and

$$\sigma_O = 10^{-16} \text{ cm}^2$$

u = energy of secondary electrons being produced

N = number density of the species being ionized

j_{eb} = current density of the electron beam

e = electron charge

E = energy of the incident electrons (electron beam)

$T_S, \Gamma_S, \Gamma_b, K, J$ = constants dependent on the species being ionized

$$\begin{aligned} T_a &= 1000 \\ T_b &= 2I \\ \kappa &= 1 \end{aligned}$$

where I is the ionization threshold energy.

Unfortunately, this form proves cumbersome when doing the integrations necessary to obtain a partial solution to the Boltzmann equation. Therefore, the above Lorentzian form for $S(u)$ is approximated by

$$g(u) = \begin{cases} c_1 & , 0 \leq u \leq u_0 \\ \frac{c_2}{u^2} & , u_0 \leq u \end{cases} \quad (D-8)$$

With this approximation, the volumetric increase in electrons per unit time produced by the electron beam can be obtained by integrating $S(u)$ over all u . Let the volumetric increase per unit time be defined as

$$\begin{aligned} S_0 &= \int_0^\infty g(u) du \\ &= c_1 \int_0^{u_0} du + c_2 \int_{u_0}^\infty \frac{1}{u^2} du \end{aligned}$$

or

$$S_0 = c_1 u_0 + \frac{c_2}{u_0} \quad (D-9)$$

If one insists that the approximated form for the secondary source spectrum be piecewise continuous

$$\lim_{u \rightarrow u_0^-} g(u) = \lim_{u \rightarrow u_0^+} g(u)$$

then

$$c_1 u_0 = \frac{c_2}{u_0} + c_1 = \frac{c_2}{u_0^2} \quad (D-10)$$

Substituting equation D-10 into D-9 and solving for c_2 yields

$$c_2 = \frac{u_0 S_0}{2} \quad (D-11)$$

Then substituting D-11 into equation D-10 to obtain c_1 yields

$$c_1 = \frac{u_0 S_0}{2u^2} \quad (D-12)$$

Therefore, the approximation for the secondary electron source spectrum becomes

$$S(u) = \begin{cases} \frac{S_0}{2u_0} & , \quad 0 \leq u \leq u_0 \\ \frac{u_0 S_0}{2u^2} & , \quad u_0 \leq u \end{cases} \quad (D-13)$$

To simplify boundary conditions, let u_0 equal the ionization threshold energy I .

S_0 was determined rather heuristically by analyzing the source spectrum resulting from the Lorentzian form of $S(u)$ developed by Green and Sawada and choosing S_0 such that

$$\int_0^{u_0} S_L(u) du = \int_0^{u_0} S_A(u) du \quad (D-14)$$

where $S_L(u)$ is the Lorentzian form and $S_A(u)$ is the approximation.

Table D-1
Parameters for various gases*

	I	T_s	Γ_s	Γ_b	K_s	J_s
N ₂	21.6	-6.49	24.3	21.6	2.19	13.8
Ar†	15.7	6.87	6.92	-7.85	9.30	3.75
Kr†	14.0	3.90	7.95	-13.5	18.7	8.43
Xe†	12.1	3.81	7.93	-11.5	22.8	5.95
H ₂ †	15.4	1.87	7.07	-7.7	2.07	0.0589
CH ₄ †	13.0	3.45	7.06	-12.5	18.7	7.59
H ₂ O	12.6	1.28	12.8	12.6	2.78	0.0309
CO	14.0	2.03	13.3	14.0	5.39	0.568
C ₂ H ₂ †	11.6	1.37	9.28	-5.8	11.9	0.503
NO	9.5	-4.30	10.4	9.5	11.8	0.168
CO ₂	13.8	-2.46	12.3	13.8	10.6	0.530

* Fitted to $S(E, T)$ of OREL *et al.* at $E = 500$ eV and to $\sigma_i(E)$ of the compilation of EIFFER and DUNN (1966).

† Fits improved if $\Gamma_b \neq I$.

(Ref 3:1726)

Figure D-1 illustrates the Lorentzian source spectrum (equation D-4) produced using parameters obtained from Table D-1 for the element argon. Overlaid on Figure D-1 is the approximation to the source spectrum defined by equation D-13 with u_0 equal to the ionization threshold energy and S_0 chosen such that equation D-14 is satisfied.

From Figure D-4, S_0 then becomes

$$S_0 = Au_0 N \frac{j_{eb}}{e} \left[\begin{matrix} 2.0 \\ -20 \end{matrix} \right] \quad (D-15)$$

where A is chosen to be 2.2 .

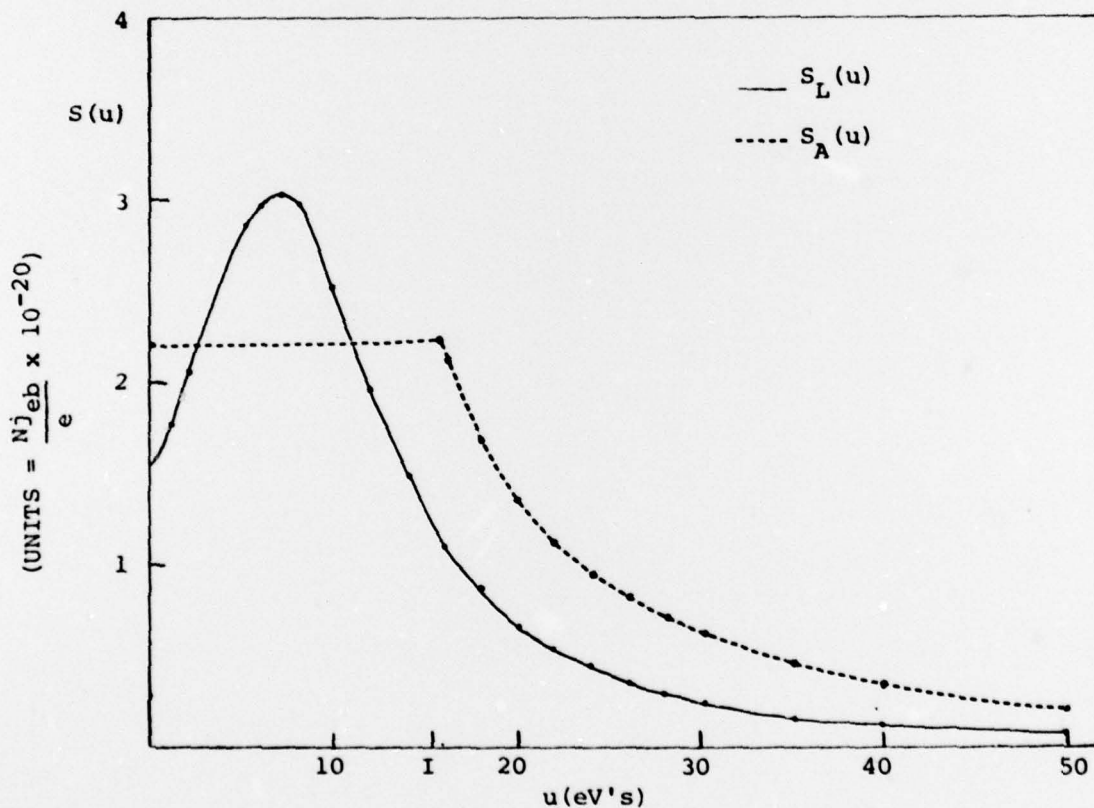


Figure D-1 Lorentzian Form of $S(u)$ and its Approximation $S_A(u)$

$$S_L(u) = \frac{N_j}{e} A(\epsilon_p) \left[\frac{\Gamma^2}{(u - T_O)^2 + \Gamma^2} \right] \quad (D-16)$$

$$\Gamma = 6.92$$

$$T_O = 6.87$$

$$A(\epsilon_p) = 3.04_{-20} \text{ cm}^2/\text{eV}$$

$$S_A(u) = \begin{cases} \frac{S_O}{2u_O} & 0 \leq u \leq u_O \\ \frac{u_O S_O}{2u^2} & u_O \leq u \end{cases} \quad (D-17)$$

$$u_O = I = 15.7 \text{ eV}$$

$$S_O = (2.2)(2u_O) = 69$$

Vita

Edwin D. Seward was born on 21 March 1950 in Greeley, Colorado. He graduated from Greeley Central High School in 1968 and attended the University of Northern Colorado from which he received the degree of Bachelor of Arts in physics and mathematics in May 1972. Upon graduation, he was commissioned as a Second Lieutenant in the USAF. Upon entering active duty in September 1972, he served as a computer systems analyst with the First Aerospace Control Squadron, ENT AFB, Colorado. He was later assigned to similar duties with the Space Object Identification Branch of Norad Intelligence, Norad Cheyenne Mountain Complex, Colorado until entering the School of Engineering, Air Force Institute of Technology, in June 1977.

Permanent address: 1605 8 Street

Greeley, Colorado 80631

UNCLASSIFIED

SECURITY CLASSIFICATION OF THIS PAGE (When Data Entered)

REPORT DOCUMENTATION PAGE		READ INSTRUCTIONS BEFORE COMPLETING FORM
1. REPORT NUMBER AFIT/GEP/PH/78D-12	2. GOVT ACCESSION NO.	3. RECIPIENT'S CATALOG NUMBER
4. TITLE (and Subtitle) THE EFFECTS OF BEAM CURRENTS ON ELECTRON ENERGY DISTRIBUTIONS		5. TYPE OF REPORT & PERIOD COVERED MS Thesis
		6. PERFORMING ORG. REPORT NUMBER
7. AUTHOR(s) Edwin D. Seward Capt USAF		8. CONTRACT OR GRANT NUMBER(s)
9. PERFORMING ORGANIZATION NAME AND ADDRESS Air Force Institute of Technology (AFIT-EN) Wright-Patterson AFB, Ohio 45433		10. PROGRAM ELEMENT, PROJECT, TASK AREA & WORK UNIT NUMBERS
11. CONTROLLING OFFICE NAME AND ADDRESS Defense Advanced Research Projects Agency Washington DC		12. REPORT DATE December 1978
		13. NUMBER OF PAGES 106
14. MONITORING AGENCY NAME & ADDRESS (if different from Controlling Office)		15. SECURITY CLASS. (of this report) Unclassified
		15a. DECLASSIFICATION/DOWNGRADING SCHEDULE
16. DISTRIBUTION STATEMENT (of this Report) Approved for public release; distribution unlimited		
17. DISTRIBUTION STATEMENT (of the abstract entered in Block 20, if different from Report)		
18. SUPPLEMENTARY NOTES Approved for public release; IAW AFR 190-17 JOSEPH P. HIPPS, Major, USAF 19 Jan 79 Director of Information		
19. KEY WORDS (Continue on reverse side if necessary and identify by block number) Electron Beam Secondary Electron Energy Deposition		
20. ABSTRACT (Continue on reverse side if necessary and identify by block number) An attempt is made at determining the effects of an external flux of high energy electrons on the electron energy distribution function. An analytic model is developed for a simple system and compared against numerical results. Normalization problems precluded detailed investigation of the analytic solution. Numerical solutions were obtained for a more complex system using a Boltzmann computer code developed for this and three related theses. It was found that an electron beam tends to "mask" the effects of an applied dc field		

UNCLASSIFIED

SECURITY CLASSIFICATION OF THIS PAGE(When Data Entered)

20.

in the high energy region of the electron distribution function. This accounts for an uncharacteristic dip in efficiency curves for processes with high threshold energies as the magnitude of the applied field increases. The beam also accounts for an insensitivity of pumping rate constants to variations in applied field strength for processes with high threshold energies.

UNCLASSIFIED

SECURITY CLASSIFICATION OF THIS PAGE(When Data Entered)